2016-01-01

Manufacturing and Characterization of Energetic Materials

Carlos Alberto Catzin
University of Texas at El Paso, cacatzin@miners.utep.edu

MANUFACTURING AND CHARACTERIZATION OF ENERGETIC MATERIALS

CARLOS ALBERTO CATZIN

Master's Program in Mechanical Engineering

APPROVED:

Calvin M. Stewart, Ph.D., Chair

John F. Chessa, Ph.D.

Cesar Carrasco, Ph.D.

Charles Ambler, Ph.D.
Dean of the Graduate School

Dedicado a mi familia

MANUFACTURING AND CHARACTERIZATION OF ENERGETIC MATERIALS

by

CARLOS ALBERTO CATZIN, B.S.M.E.

THESIS

Presented to the Faculty of the Graduate School of

The University of Texas at El Paso

in Partial Fulfillment

of the Requirements

for the Degree of

MASTER OF SCIENCE

Department of Mechanical Engineering

THE UNIVERSITY OF TEXAS AT EL PASO

May 2016

ACKNOWLEDGEMENTS

I would like to thank my advisor Dr. Calvin M. Stewart, whose leadership, guidance, and knowledge was fundamental to complete my master degree. It has been a privilege and an honor to work and learn by your side. I want to state my gratitude to the Mechanical Engineering Department for everything that was and was not provided which impacted my professional development greatly. Finally but not least, I would like to thank my family for being my inspiration and support during my education. I especially would like to thank my wife, Jana, whose patience and love make me the man that I am today. Thank you my one true love. Я тебя люблю навсегда.

ABSTRACT

Few products take several years of research effort to be synthesize yet disintegrate in scarcely millionths of a second when used. Despite their short lifespan energetic materials, particularly high explosives, are in demand as never before by the Aerospace, Defense, Energy, Gas, Mining, and Oil Industry for their unique properties. One class of high explosives known as polymer bonded explosives (PBXs) are popularly used in a wide variety of applications ranging from solid rocket propellants to the main explosive charge in conventional ammunitions. A key characteristic behind the popularity of PBXs in comparison to other high explosives is their handling safety. This characteristic of the PBXs has its root in its composition. Polymer bonded explosives are comprised of two different constituent materials: micron size energetic crystals and polymer binder material. The polymer binder material cohere the energetic crystal together into a single mass. In addition, the polymer binder material prevents friction between the energetic crystals and allows deformation. This characteristic of PBXs makes them safer to handle than any other class of high explosive. Is important to keep in mind that the particular behavior of the constituent materials will dictate the mechanical properties of the PBX. Polymer bonded explosives have a high demand for research development among industry due to the unexplained phenomena that occurs on the mechanical response regime. Interest in the mechanical response of PBXs continues to rise as applications for these continue to evolve. Characterizing the mechanical properties of a PBX is not an easy task in terms of security. This is due to user and equipment safety. Despite the fact the PBXs are safer to handle than any other high explosive, it is not advised to conduct mechanical testing on a real PBX. In order to characterize the mechanical properties of a PBX safely is imperative to adapt a "mock" PBX. A mock PBX has the ability to reproduce the mechanical behavior of a PBX closely without the risk of detonation. In this thesis, a new manufacturing method for a mock PBX named Miner mock will be covered. Quasi-static uniaxial compression, indirect tensile test, and semi-circular bending were carried out to extract the compressive, tensile, and fracture properties of the Miner mock. This mechanical properties will be compared to a real

PBX formulation in order to provide validation to the new manufacturing method and the Miner mock formulation.

TABLE OF CONTENTS

LIST OF TABLES

LIST OF FIGURES

CHAPTER 1: INTRODUCTION

1.1 Motivation

Few products take several years of research effort to be synthesize yet disintegrate in scarcely millionths of a second when used. Despite their short lifespan energetic materials, particularly high explosives, are in demand as never before by the Aerospace, Defense, Energy, Gas, Mining, and Oil Industry for their unique properties. Explosives have been around since the invention of the black powder or more commonly known as the gun powder developed in China during the 11th century. The development of new explosives like dynamite impulse a new generation of applications for explosives. The expansion in the knowledge of explosives impulse humanity to explore new horizons and reach new challenges. Still certain research areas of explosives like their mechanical characterization remained under mystery for several years. The need to figure out the unexplained phenomena generated by explosives lead to a major breakthroughs during the 1950s. Since then research of explosives has continue to evolve, however explosives remain unexplained in certain areas. Recently their development has been characterized by combining computer simulation codes and experimental diagnosis to explain the physical phenomena of explosives. One class of high explosives known as polymer bonded explosives (PBXs) possess a wide variety of applications ranging from solid rocket propellants to the main explosive charge in conventional ammunitions. However, there is still many unexplained phenomena in the mechanical characterization of these explosives. Explaining this phenomena will lead to breakthroughs in space exploration and national defense which are the main industries that will benefit from it. What is more appealing is that by having total knowledge of the explosive regime will enable our nation to lead the market in space exploration and remain as the most powerful military force in the world. Opening roads to a bright new future.

1.2 Background

Polymer bonded explosives (PBXs) are a complex class of particulate composite materials that are formed by two constituent materials: micron size energetic crystals in a polymer binder [1].

These complex particulate composites may also consist of a small percent of additives like plasticizers, oxidizers, and antioxidants that are added to the ratio composition to improve the explosive output and decrease the effects of aging [2]. The content of energetic crystals to polymer differs greatly. The energetic crystals typically comprises about 50 to 98% of the total mass of the composite, depending on the desired explosive output, similarly to pressed explosives [3]. There are many differences between PBXs and pressed explosives including the composition, application, and cost [4-5]. However, PBXs are preferred over pressed explosives mainly because of handling safety. PBXs are safer than pressed explosives because of their composition where the polymer binder prevents friction between crystals and allows deformation [2]. This deformation is the result of the polymer binder absorbing mechanical energy and preventing friction between crystals that leads to detonation. Despite this fact, it is not advised to handle and conduct mechanical testing on real PBX due to user and equipment safety. Nonetheless, a wide variety of investigations on the explosive output, deformation, and fracture of real PBXs have been performed with the necessary safety precautions [7-12]. One key feature in the characterization of PBX, seen in literature, is the need to apply a measurement technique during testing in order to have a quantitative data of the deformation process.

In order to characterize the mechanical properties of a PBX with a relative low cost and minimum safety requirements it is imperative to adapt a “mock” PBX. A mock PBX has the ability to reproduce the mechanical behaviour of a real PBX closely without the risk of detonation [13]. This feature allows the safe study of the mechanical behavior of PBXs and provide reliable data for constituent model development. One issue that keeps arising in literature is the lack of a detailed description of the manufacturing process of mocks and their composition. Also, the fact that not many research articles have validated the usage of their mock composition. This issue has not been address in several research articles due to the distinct combinations for PBX compositions. Since there is many different compositions for PBXs, different mock PBXs compositions have been derived. However just a few compositions have strictly follow a mock that simulates the particular behavior of a preferred PBX formulation. The continuous usage, an

inventory of the formulation, and the desire to utilize the aging inventory is what makes that particular formulation more desirable to characterize, ergo preferred. These preferred formulations were validated by comparing the mechanical response of the mock to their real counterpart or to an existent PBX composition used in industry [14]. Validated mock PBX formulations have been used in literature. Liu and colleagues conducted two approaches in measuring the fracture toughness on Mock 900-21, a mechanical simulant of the PBX 9501 [15]. One approach was through the global measurement according to ASTM 1820-06 and the other through local measurement approach using DIC. The study concluded that the ASTM 1820-06, which is a well establish method for metallic materials, is applicable to obtain a homogenized description of the fracture process in heterogeneous materials. Also, the study concluded that DIC can be used to extract quantitative information regarding the location and extent of the macroscopic cracks. Hoffman and colleagues conducted several mechanical and thermal test including uniaxial compression to determine the replacement for a current mock RM-03-AC, a mock substitute for LX-17 and PBX 9502. The study concluded that it is possible to formulate mock explosives that have similar mechanical responses without using the same binder [14]. Several of the validated mocks manufacturing processes have disadvantages such as difficulty gathering the constituent materials, high cost of equipment, expensive mock powders, and difficulty in replicating the manufacturing process. A new formulation of mock PBX that provides a low cost, easy manufacturability, step by step manufacturing process , and validated to a real PBX formulation is required to promote scientific effort and research. A new mock PBX formulation called Miner mock provides low cost, easy manufacturability, and step by step manufacturing process, but lacks the validation of its mechanical response [18].

CHAPTER 2: MANUFACTURING METHOD FOR MOCK POLYMER BONDED EXPLOSIVE

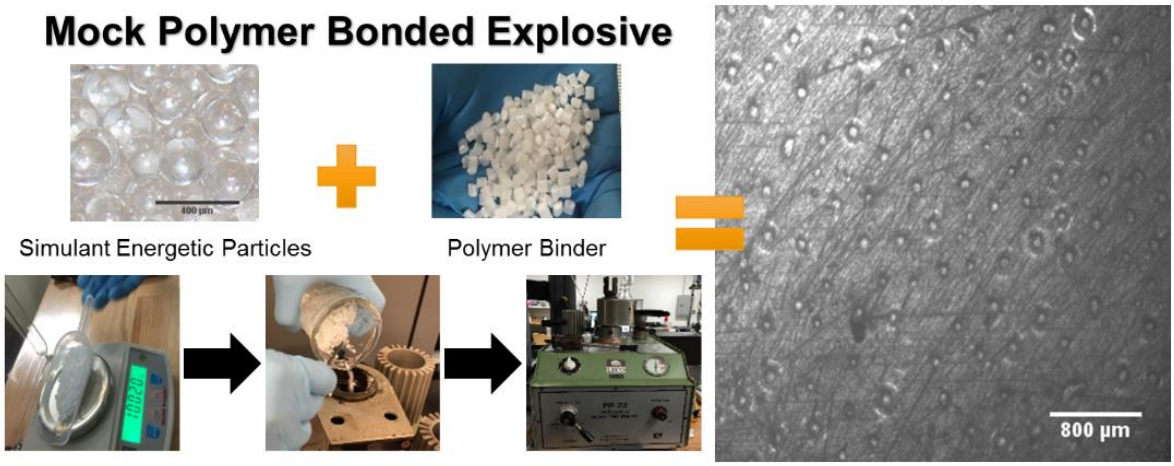

Figure 2.1 Visual representation of Manufacturing Process

The mechanical testing and characterization of polymer bonded explosives (PBXs) is a difficult field of study. The high cost of the constituent materials, expensive testing setups, and the arduous task of following safe handling procedures slows down research progress in the mechanical behaviour of PBXs. Often a PBX simulant or "mock" PBX is used as a safe and mechanically similar surrogate for PBX. This paper will describe a precise and well developed method for manufacturing a mock PBX that closely resembles the mechanical behavior of PBX. Several methods of manufacturing mock PBXs have been proposed in literature; however, many of the proposed methods lack a clear description of the manufacturing method or details concerning the required equipment and mixing process. This new method has several advantages:

- A clear and detailed description that enables repeatability and reproduction
- The simple mixing and fusion process allows for dispersion and agglomeration of the simulant energetic particles.
- The mass percent composition of simulant energetic particles and polymer binder can be adjusted to accommodate several types of PBX.

2.1 Method Details

Although PBXs are safer to handle than pressed explosives, the safety controls required to handle them properly makes them unsuitable for mechanical testing in most laboratory settings. In order to characterize the mechanical properties of PBX safely, it is necessary to manufacture a “mock” PBX that has the capability to reproduce very closely the mechanical behaviour of a PBX without the risk of detonation. The method to produce a mock PBX remains very similar to the actual manufacturing process for PBXs with obvious changes such as the substitution of energetic crystals for an appropriate substitute like sugar or soda lime glass beads. Innovating methods such as the precision coating of high explosives have left their mark in the manufacturing of mock PBX [19]. The following method will not only describe the steps to manufacture a mock PBX, but will be the most economical option to reproduce the mechanical behavior of a PBX. The Pressure molding of mock PBX using agglomeration effect Method.

2.2 Required equipment and materials

Material selection is a crucial factor in the manufacturing process of a mock PBX. The specific mechanical behavior of each constituent material will define the mechanical behavior of the resulting mock PBX. Hence, the constituent materials of the mock PBX must maintain a similar mechanical behavior to the constituent materials of a typical PBX.

(a) (b)

Figure 2.2 Mock PBX constituent materials

(a) High impact polystyrene polymer pellets (b) soda lime glass spheres

Constituent Materials

- **Polymer:** High Impact Polystyrene (HIPS) in pellet form. The HIPS pellets used in this method were produced in a typical process of the polymerization of styrene in the presence of butadiene rubber. The HIPS pellets were selected as the polymer binder material because of their excellent adhesive properties, relatively low melting temperature, and continuous selection as binder material among typical PBX composites [20].
- **Simulant Energetic Particle:** 150 – 250 micron size soda lime glass beads. The soda lime glass beads used in this study are sold by Jaygo Incorporated as Dragonite® soda lime glass beads [21]. The soda lime glass beads were selected as the simulant energetic particles because of their similarity to real energetic materials including: mechanical behavior (Young's Modulus), size, particle size distribution, and their common selection as a simulant energetic particle in literature [22].

Equipment

- **Scale:** BE1188 Bald Eagle powder scale or a powder scale with the capability of measuring mass with an accuracy of 0.001 g.
- **Mounting Pneumatic Press:** Leco PR-22 pneumatic mounting press with a 1.5 in. diameter cylindrical mold capable of applying a maximum pressure of 4000 psi with a heating element that possess a maximum temperature above the melting point of the polymer binder material.
- Urethane and styrene silicone release spray.
- **Multimeter:** Fluke 175 True-RMS digital multimeter or any temperature measuring device with thermocouple probe.
- **Containers and tools:**
    - Beakers will be used as containers in the mixing process.
    - Flasks will be used to hold the weighted constituent materials.
    - Forceps will be used to handheld the pellets during the weight in process.

- Stirring rod will be used during the mixing process
- Plastic scoops will be used to transfer the materials between containers.

- **Cleaning accessories:** Acetone to clean the equipment properly.

Note: This list does not include laboratory safety equipment, which are assumed to be available.

Any equipment with similar capabilities as those mentioned above can be used to accomplish the manufacturing process of mock PBX.

2.3 Manufacturing Method

The manufacturing method in this study was established to achieve a full coat of the polymer binder about the simulant energetic particles [22]. This will prevent the segregation of the constituent materials during machining and ensure that the resulting product closely resembles the mechanical properties of a PBX [23, 24]. The proposed manufacturing method can be tuned to a desired constituent composition. The following method will manufacture a 50-50 composition mock PBX.

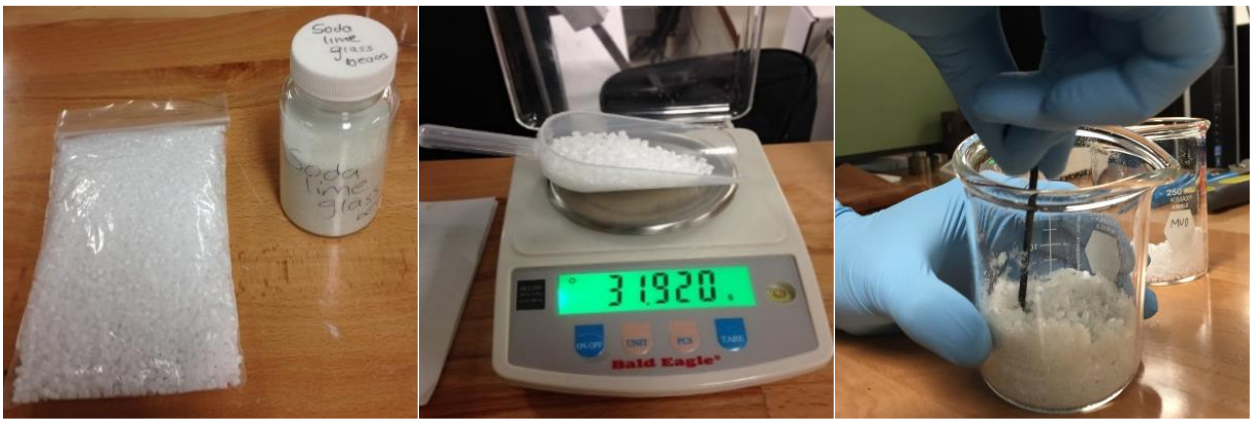

(a) (b) (c)

Figure 2.3 Manufacturing Method Stage 1

(a) Constituent materials (b) Weigh-in (c) Mixing

Stage 1: Weigh-In and Mixing of Constituent Materials

1. Make sure all equipment is clean and ready for operation.
2. Turn on the heating element and heat until the temperature exceeds the melting temperature of the polymer binder material (HIPS pellets). Note: The melting temperature of the HIPS pellets used in this study is 132.22°C.
3. The powder scale must be turned on and calibrated for the desired accuracy.
4. Collect beakers, flask, and scoops capable of retrieving and storing the measured constituent materials.
5. Collect constituent materials as depicted in Figure 2.3(a).
6. Measure 40 grams of each constituent material and place them in individual flasks as depicted in Figure 2.3(b).
7. Reserve 5 grams out of the previously weighted 40 grams of HIPS pellets in an additional flask. Note: These HIPS pellets will be used to create a foundation for the mock PBX specimen.
8. Measure half a gram of water and place it in a relative large beaker that will be used for mixing the constituent materials.
9. Place the remaining 35 grams of HIPS pellets into the mixing beaker making sure that the pellets become completely covered by a small layer of water.
10. Add the 40 grams of soda lime glass beads into the mixing beaker.
11. Mix the constituent materials for 10 minutes making sure that each polymer pellet is completely covered in soda lime glass beads by agglomeration. This step is demonstrated in Figure 2.3(c). Note: this step is crucial in the making of the mock PBX.

(a) (b) (c)

Figure 2.4 Manufacturing Method Stage 2

(a) Applying the silicone release spray to the cylindrical mold (b) Secure the cylindrical mold into the press safely (c) Pressure applying die in the lock position

Stage 2: Press Preparation

12. Apply a thick layer of urethane and styrene silicone release spray to the cylindrical mold, the pressure applying die, and the upper locking die as depicted in Figure 2.4(a). Note: A thick layer of the urethane and styrene silicone release spray agent should be applied to any surface that will come into contact with the constituent materials during the densification process.
13. Place the cylindrical mold into the press making sure that it fits snugly and is properly attached as depicted in Figure 2.4(b).
14. Place the pressure applying die into the lock position as depicted in Figure 2.4(c).The lock position is located at the point where the cylindrical mold and the pressure applying die have no gap between them.
15. Place the heating element around the cylindrical mold in order to start heating the mold.
16. Constantly measure the temperature of the mold using the thermocouple probe of the fluke meter until reaching 140°C at the center of the pressure applying die. This is done in order to melt the polymer pellets as soon as they come in contact with the surface of the cylindrical mold and/or pressure applying die.

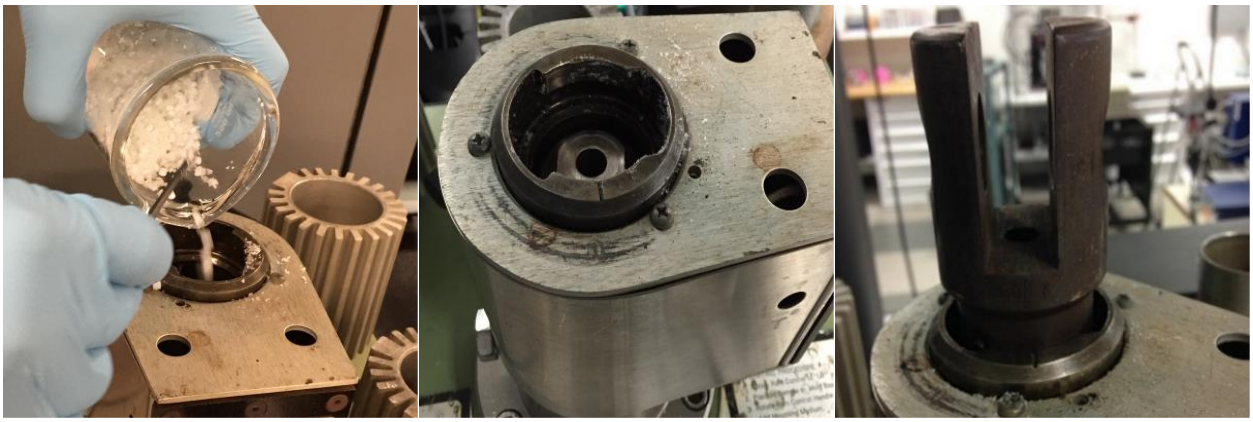

(a) (b) (c)

Figure 2.5 Manufacturing Method Stage 3

(a) Pour the constituent materials into the cylindrical mold (b) Place the upper locking die in to the cylindrical mold (c) Secure lock in the lock position

Stage 3: Press Operation

17. Once a temperature above the melting point of the polymer has been reached (140°C), carefully pour 2.5 grams of the HIPS pellets that were set aside in step 6, then proceed to pour the mixed constituent materials into the mold as depicted in Figure 2.5(a). The mold will be hot. It is recommended to use safety equipment that will reduce the risk of burn during this step.
18. Pour the remaining 2.5 grams saved in step 6 to the top of the mixture inside the cylindrical mold. During this process the heating element must remain in contact with the mold at all time (constant heat).
19. Place the upper locking die into the cylindrical mold as depicted in Figure 2.5(b). Make sure to place the die in a way that the surfaces with the urethane and styrene silicone release spray make contact with the constituent materials inside the mold.
20. Mount the secure lock on top of the upper locking die and set it to lock by twisting the secure lock 90° in order to ensure that once the pressure is applied the constituent materials remain inside the mold. It is possible to verify that the secure lock is in lock position by trying to gently take it out. The secure lock should not be able to move. This is shown in Figure 2.5(c).

21. Allow the heat generated by the heating element to reach the pellets located at the center of the cylindrical mold by waiting 30 minutes. This soaked time was determined by the soda lime glass beads which have a very low coefficient of heat transfer.
22. Move the RAM lever in an upward position in order to increase the pressure to a maximum of 4000 psi. A gentle crushing sound will be heard initially during the densification stage.
23. Apply constant heat and pressure for 150 minutes.

(a) (b) (c)

Figure 2.6 Manufacturing Method Stage 4

(a) Cylindrical mold in cool down state (b) Cylindrical mold remove from the press (c) Retrieve mock PBX.

Stage 4: Solidification and Retrieval of Mock PBX

24. Turn off the heating element and remove it from the cylindrical mold. Configure the cylindrical mold into its cool down state as depicted in Figure 2.6 (a)
25. Maintain constant pressure until the outer surface of the cylindrical mold reaches 45°C.
26. Remove all applied pressure by lowering the RAM lever.
27. Remove the secure lock by twisting 90° and gently remove it from the cylindrical mold.
28. Remove the still hot cylindrical mold from the press using heat resistant gloves as depicted in Figure 2.6 (b). Use proper safety equipment to avoid any burns.
29. Place an impact absorbent material below the hot cylindrical mold. Note: this material is used to catch the specimen.

30. Gently strike the upper locking die with a hammer in order to retrieve the specimen safely. The cylindrical mold should remain between 30-45°C. This will ease the retrieval of the mock PBX. The extracted specimen is shown in Figure 2.6(c).
31. Place specimen in a proper storage place with the date and specimen composition.
32. Clean mold with the acetone and a shop towel.

2.4 Additional information

Polymer bonded explosives are heterogeneous particulate composites where each energetic particle should be completely coated by the polymer binder in a disorderly fashion throughout the material. This new manufacturing method for mock PBX initially faced challenges in achieving this outcome. The main issues that this method faced was the mixture and pouring stages. These stages are critical for the formation of a good specimen. Several mixing procedures were assessed during the first trials until the optimal procedure was achieved. One method consisted of mixing the constituent materials in a beaker without adding water. This proved to be inefficient and left large areas of pure polymer and loosely fused glass beads dispersed throughout the specimen. Another procedure was to partially pour each constituent material directly into the cylindrical mold alternating constituents and then proceed to mix the materials. This procedure also proved to be ineffective. The optimal process involved adding a precise amount of water to the pellets placed in a flask and then adding the glass beads to create an agglomeration effect that proved to be an effective procedure to mix the materials. The precise amount of water, a quarter of a gram per each 40 grams of the soda lime glass beads, was discovered by experimentation. Several trials proved that the above ratio is the most ideal to generate the agglomeration effect while developing desirable small air voids (Hot spots) within the particulate composite material.

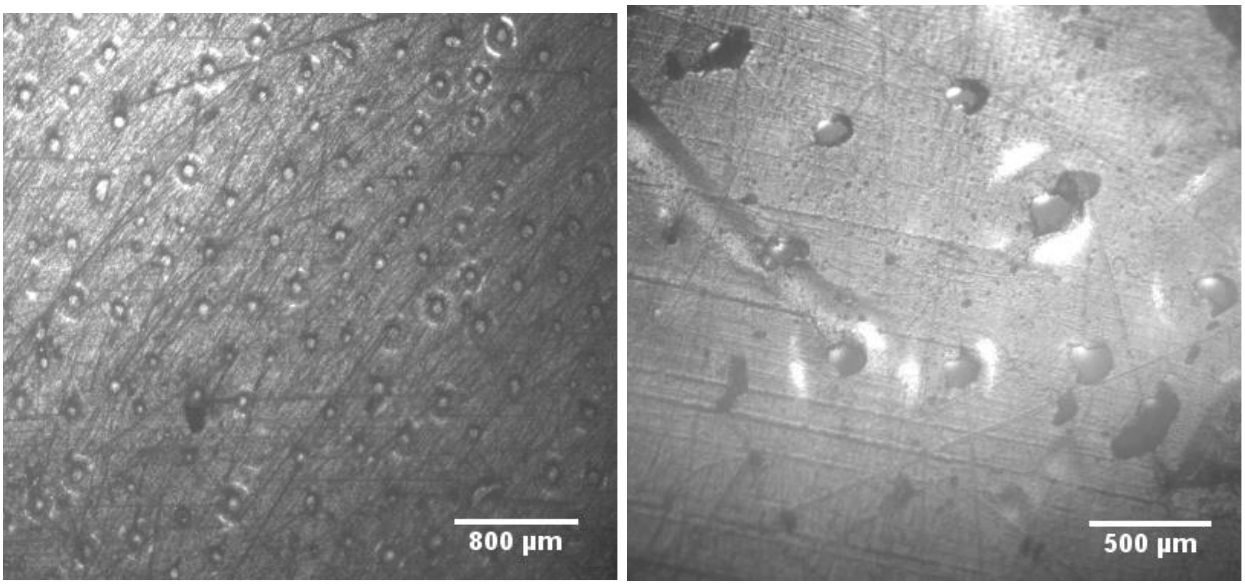

(a) (b)

Figure 2.7 Optical microscopy of the product

(a) Microstructure at 800 micrometers (b) Microstructure at 500 micrometers.

Product

The product was evaluated in order to assess its similarity to a standard PBX specimen. A typical PBX specimen has a heterogeneous distribution of polymer coated energetic crystals with small air voids that enhance detonation. These characteristics are observed in the product mock PBX specimen as depicted in Figure 2.7. The bright white rings around the glass beads indicate a halo effect created by the reflection of the microscope light and the glass beads. The micrographs show a heterogeneous arrangement of glass beads in a polymer matrix. The glass beads are full and individually coated. All conclusions are established by the fact that the piece of specimen used in the microscopy was selected at random. The product has the characteristics necessary to accurately simulate the mechanical properties of a real PBX specimen.

CHAPTER 3: COMPRESSIVE, TENSILE, AND FRACTURE PROPERTIES OF MOCK POLYMER BONDED EXPLOSIVE USING DIGITAL IMAGE CORRELATION

The mechanical behavior of a mock polymer bonded explosive (PBX) called "Miner mock" was experimentally studied using the three-dimensional digital image correlation (3D-DIC) method in order to characterize its mechanical response. Uniaxial compression, Brazilian, and semi-circular bending tests were performed in order to validate the mechanical response of the Miner mock to a real PBX composition at room temperature. The displacement and strain fields on the surface of the specimen were recorded using a 3D DIC system. Based on the contour plots produced, key features of each loading conditions were identified and recorded such as surface topology, prediction of failure modes, crack initiation and crack path.

Digital image correlation (DIC) provides high resolution measurements of displacement and strain fields. The DIC method is a non-contact displacement measurement technique that has been proven to be an effective measuring tool for real and mock PBXs formulations [25]. This non-contact measuring method records the surface displacement of objects up to the magnification limit of the given optics [26]. In addition, an unlimited number of virtual strain gauges and extensometers can be placed on the specimen after testing. Cunningham and colleagues applied DIC to perform a variety of strain measurements on PBXs specimens at low strain rate [27]. The study also discuss the use of DIC to obtain measurements of thermal expansion, Poisson's ratio, and tensile creep. The study concluded that DIC provides significant improvements in the ability of acquiring mechanical property data, even with the disadvantage of the DIC of only measuring the strain at the surface of the specimen. Zhou and Colleagues applied DIC to an SCB test in order to quantify the deformation and damage of a simulation material of PBX [6]. The study concluded that the DIC provided strain fields that are effective in predicting the micro-crack growth path and that the dominant fracture mode is inter-granular cracking. Furthermore, the DIC method has been used to study the mechanical properties of PBX at different strain rates [25-27]. However the above studies require expensive testing set ups and strict safety requirements for the equipment and the experimentalist. In this study a series of quasi-static test including uniaxial compression, Brazilian

test, and semi-circular bending (SCB) test are executed along DIC at room temperature to characterize the mechanical behavior of the Miner mock formulation in order to validate its mechanical response.

3.1 Materials and Equipment

3.1.1 Material

The Miner mock is a complex particulate composite of soda lime glass beads in a high impact polystyrene (HIPS) polymer matrix. The Miner mock specimens were manufactured using a pneumatic press with a heating element. The agglomeration effect of micron(or smaller) particles was exploited during the mixing of the constituent materials, followed by the application of constant heat and pressure (beyond the melting point of the HIPS) to fully coat the simulant energetic crystals. The Miner mock has a formulation containing approximately 50 wt% micron size soda lime glass beads in a bimodal size distribution and 50 wt% high impact polystyrene polymer binder. The output of manufacturing was a right circular cylinder of 1.5 inches in diameter and 2 inches in length. The contact surfaces were polished on each of the specimen using a PoliMet 1000 Grinder/ Polisher and a 200 silicon carbide grid to ensure proper contact.

TABLE 3.1 EXPECTED FAILURE MODE OF RIGHT CYLINDRICAL SPECIMEN BY GEOMETRY CONFIGURATION

$\frac{l}{d}$	***Expected Failure Mode***	***Frictional Effects***
≤ 1.5	*Barreling*	*High*
1.5-2	*Barreling*	*High*
2-2.5	*Double Barreling*	*Above Minimal*
2.5-5	*Shear*	*Minimal*
$5 \leq$	*Buckling*	*Minimal*

It is very important to understand the relationship between the specimen geometry and the failure mode for each testing method. For cylindrical specimen, the length to diameter ratio has an impact on the dominant failure mode under compression for pure polymer materials. The expected failure mode and frictional effects of a cylindrical geometry of polymers are depicted in Table 3.1[28].

Equipment

All testing was conducted on an INSTRON 5969 Universal Testing Machine with $\pm$ 50 KN load cell and synchronized with Vic 3D DIC system. All testing was carried out at a temperature of 25°C. Three specimen of uniaxial compression, Brazilian, and SCB were tested along 3D DIC. The data captured from the INSTRON machine during the tests included time, load, displacement. The three-dimensional digital image correlation (3D DIC) equipment used in this study is a Correlated Solutions VIC-3D DIC system which performs in-situ measurement of the surface displacement and strain fields of specimen during mechanical testing. Before correlation, the specimen is primed with a randomly applied speckle pattern. An example of the applied speckle patterns are shown in

(a) (b) (c)

Figure. The speckle pattern was applied using flat/matte general purpose spray paint. A white layer of paint is deposited as a background and topped with black speckles to generate a high contrast speckle pattern. These speckles act as reference points. The 3D DIC software, VIC 3D, tracks the displacement of reference points, compares the displacements to a physical reference, and calculates strain using continuum mechanics. Tunable LED lights where focused on the specimen to increase the contrast of captured photographs. A 3 mm calibration pad was used to calibrate the Vic 3D for each specimen.

(a) (b) (c)

Figure 3.1 Speckle Pattern Examples

a) Quasistatic Uniaxial Compression specimen b) Brazilian specimen c) SBC specimen.

3.2 Test Methods

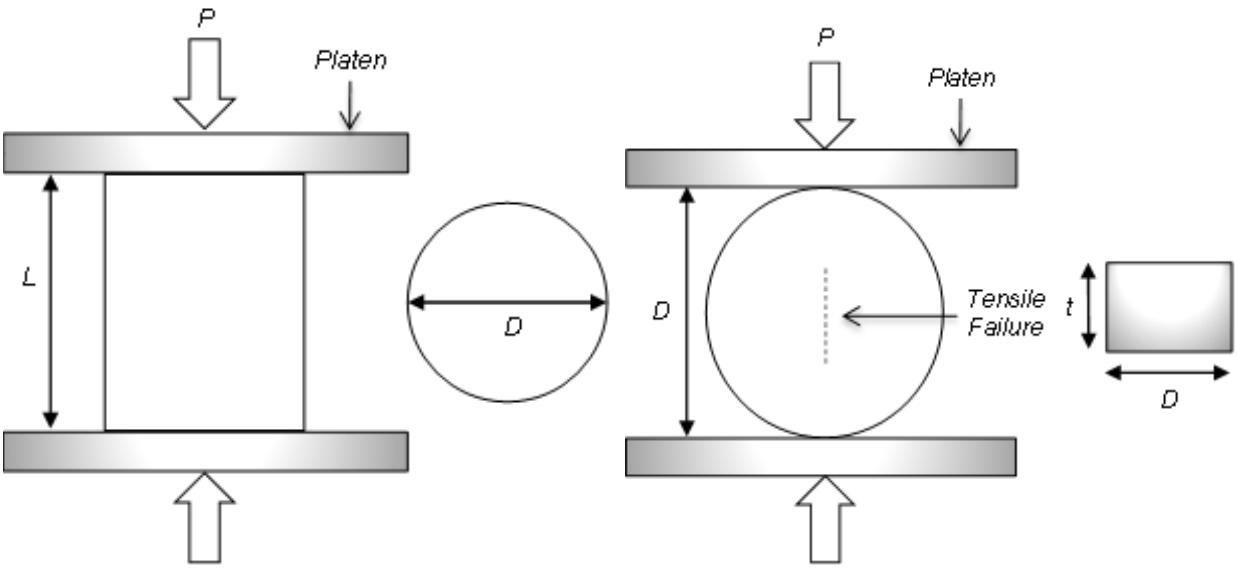

(a) (b)

Figure 3.2. Uniaxial Compression and Brazilian Test methods configuration

(a) Quasistatic Uniaxial Compression with a specimen diameter (D) and a length (l) (b) Brazilian disk with a specimen with diameter (D) and a thickness (t)

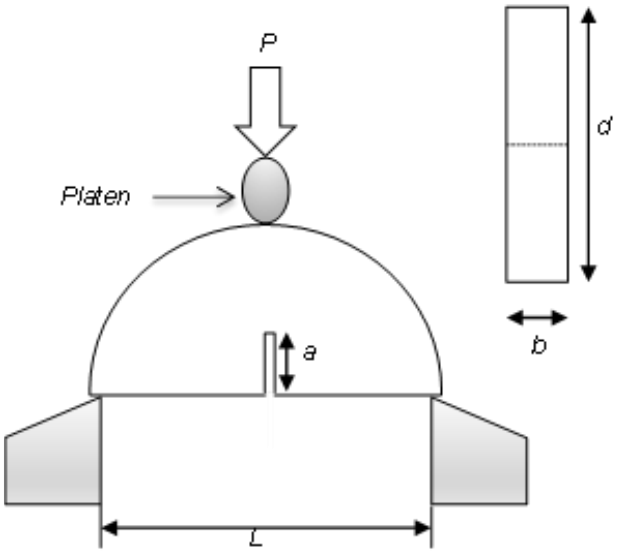

Figure 3.3 SCB Test method Configuration

Semicircular Bending with a pre-notch (a), diameter (d), and thickness (b)

Uniaxial Compression (UC) Test

The uniaxial compression specimens are right circular cylinders of 1.5 inches of diameter and 1.8 inches in length. The uniaxial compression test configuration consists of two 6 inches diameter compression platens with a capacity of $\pm$ 100 KN load bearing mounted to the Instron frame as illustrated in Figure 3.2(a)**.** It is important to avoid misalignment by placing the specimen at the center of the compression platens right under the loading axis as indicated in the schematic. Friction can develop at the contact surface leading to a multiaxial state of stress and undesired failure mode. The adaptation of PTFE (poly-tetrafluoro-ethylene) lubricant or tape to reduce friction during testing has been proven successful [28]. The PTFE provides a smooth low coefficient of friction surface between the compression platen and the specimen. Compression testing procedures act in accordance with ASTM D695-10. The cylindrical specimens were compressed under displacement controlled at a constant crosshead displacement rate of 1.3 ± 0.3 mm/ min. The first procedure indicated by the standard is to calculate the minimum value of the cross-sectional area. In order to do this is necessary to measure all along the length of the specimen the width and thickness to the nearest 0.01 mm. This calculation is one of the most crucial one as

it will affect the calculations. The compressive strength can be calculated by dividing the maximum compressive load carried by the original minimum cross-sectional area:

$$\sigma_{compressive} = \frac{P_{Max}}{A} \quad (1)$$

The compressive yield point can be calculated by dividing the load carried by the specimen at the yield point by the original minimum cross-sectional area:

$$\sigma_{yield} = \frac{P_{yield}}{A} \quad (2)$$

The compressive modulus of elasticity can be calculated by drawing a tangent line to the initial linear portion of the stress vs strain curve, selecting any point at this line, and dividing the stress by its corresponding strain.

Brazilian Disk Test

The Brazilian disk test is an alternative method to determining the tensile strength of materials that possess very low tensile strength and are brittle [29]. The Brazilian specimen were trimmed from the as-manufactured cylinder to a disk shape. The Brazilian disk specimens are circular disks of 1.5 inches of diameter and 0.875 inches of thickness. The Brazilian disk test configuration consists of two 6 inches diameter compression platens with a capacity of $\pm$ 100 KN load bearing mounted to the Instron frame. The specimen is placed such as the compressive force acts across the diameter as illustrated in Figure 3.2(b). The Brazilian test requires a smooth contact surface between the compression platens and the surface of the specimen. PTFE tape and lubricant were applied to the compression platens in order to marginally reduce frictional effects. The specimen was loaded at a constant crosshead displacement rate of 0.5 mm/min [30]. Compression testing procedures act in accordance with ASTM D6931-12. In order to calculate the indirect tensile force of the specimen is necessary to perform the following calculation:

$$\sigma_{IDT} = \frac{2000P}{\pi tD} \quad (3)$$

Where P is the maximum load, t is the specimen height, and D is the diameter of the specimen.

Semi-Circular Bend (SCB) Test

The SCB test configuration consist in using a three-point bending structure under compressive displacement. The SCB specimens were trimmed from the as-manufactured cylinder to a half disk shape with a notch located at the center of the specimen. The SCB specimens are a half-disk with 1.5 inches diameter and 0.62 inches thick with a prefabricated notch of 0.3 inches of depth located at the center of the specimen. The three point bend fixture consists of a top loading anvil and two support anvils under the specimen as illustrated in Figure 3.3**.** The diameter of the load and support anvils were 3 mm with a distance of 36 mm between the supports. The loading anvil was place such that it only makes contact with the top surface of the SCB specimen. The tests were executed under displacement control at a constant crosshead displacement rate of 0.05 mm/min as in accordance to literature [31].The fracture energy G_f of the specimen is calculated by dividing the work of fracture W_f (the area under the curve of the load vs displacement) by the ligament area A_{lig}.

$$G_f = \frac{W_f}{A_{lig}} \tag{4}$$

Where A_{lig} can be calculated by multiplying the difference of the specimen radius and the notch length by the specimen thickness.

$$A_{lig} = (r - a)t \tag{5}$$

3.3 Results and Discussion

Three Dimensional DIC was performed on each test type. During calibration, the VIC-3D software computed an average error of 0.021, 0.019 and 0.029 for the quasistatic uniaxial compression, Brazilian disk, and SCB specimen respectively. The calibration error was calculated as the average error (in pixels) between the position where the target point was found in the image and the theoretical position where the mathematical calibration model places the point. The allowable error ranges from 0 (the ideal case) to an average error of 0.039 which is the maximum error allowed

by the system. After testing, during post processing, an average estimated analysis error of 0.023, 0.029 and 0.036 was recorded for the quasistatic uniaxial compression, Brazilian disk, and SCB specimens respectively. The analysis error is a measure of correlation accuracy that represents the epipolar projection error carried out during the correlation. Similar to the average error, the analysis error should be kept at a minimum. The optimal range for the analysis error starts at 0 to about 0.1 maximum. The post processing scores obtained in this study are within the limits. Variability is expected due to the heterogeneity of the specimen and the different loading configurations.

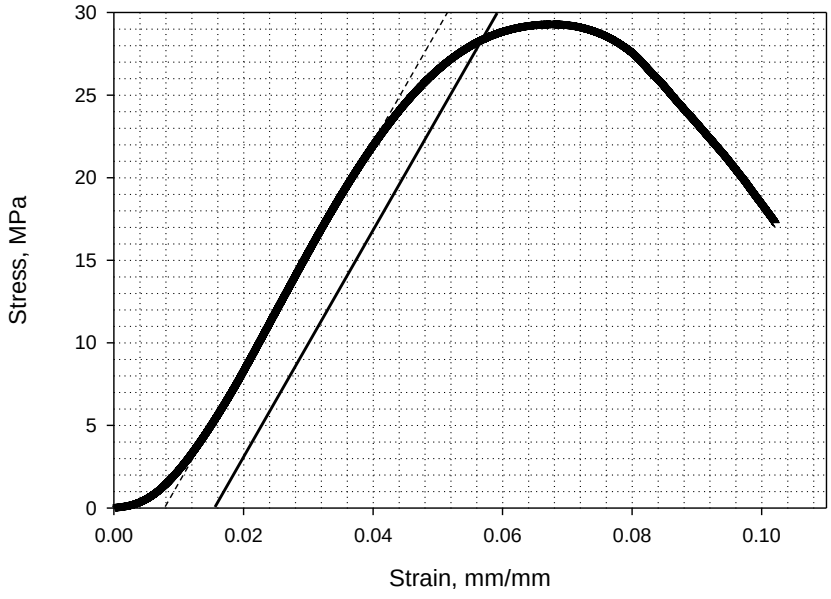

Figure 3.4 Uniaxial compression stress vs strain curve

Uniaxial Compression (UC) Test

The stress-strain curve for uniaxial compression is depicted in Figure 3.4. One feature of the graph that grabs the attention is the softening region at the beginning of the curve. However, this region is known as the toe region and does not represents a property or behavior of the material. This region is caused by the slack and alignment of the specimen. The compressive strength of the Miner mock are listed in Table 3.2. Comparing the elastic modulus obtained in this study to literature, the Miner mock behaves similar to the X0242 PBX simulant [32].

TABLE 3.2 COMPRESSIVE STRENGTH AND MODULUS OF MINER MOCK

E_c *MPa*	σ_{yield} *MPa*	ε_{yield}	σ_{UCS} *MPa*	σ_{break} *MPa*	ε_{break}
655.3	*26.2*	*0.04*	*29*	*29*	*0.06*

With the help of the surface measurements provided by the DIC, the Poisson's ratio of the Miner mock specimen was calculated an obtained. As indicated by the Figure 3.5, the Poisson's ratio of the Miner mock is 0.35.This can be seen as the majority of the specimen is colored at the indicated calculation of the Poisson's ratio.

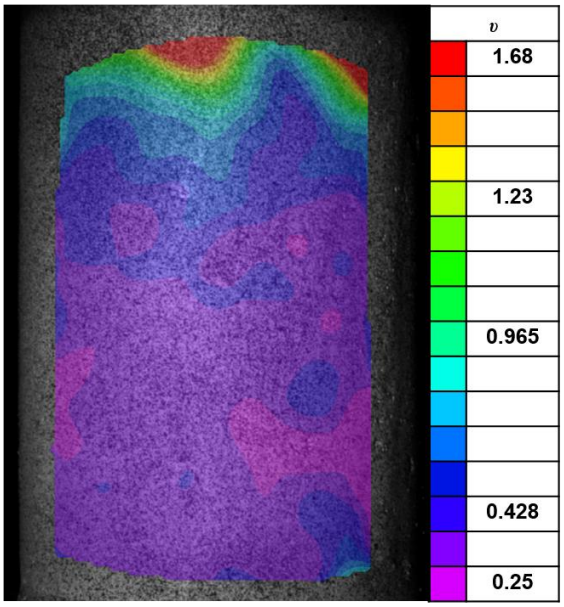

Figure 3.5 Poisson's ratio calculated by the DIC system

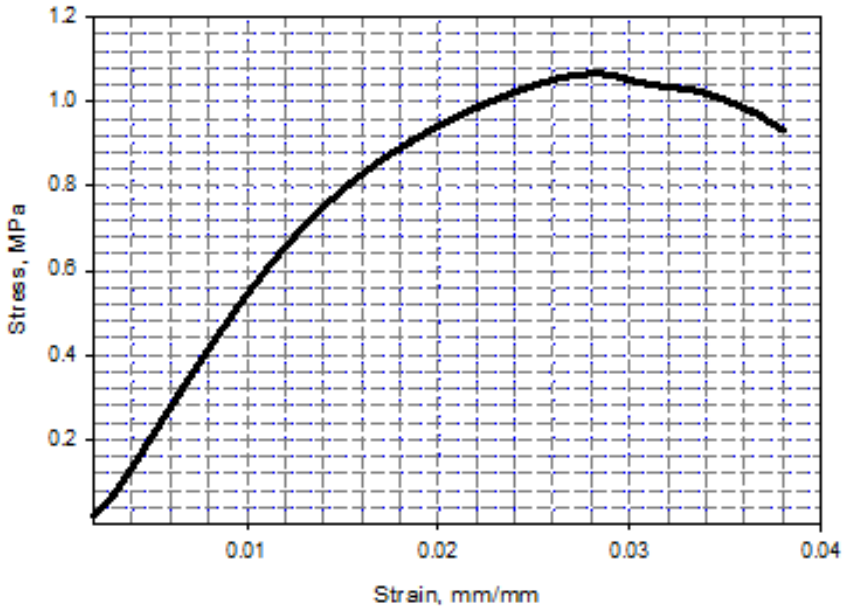

Figure 3.6 Brazilian Disk stress vs strain curve

Brazilian Disk Test

The stress-strain curve for the Brazilian disk is depicted in Figure 3.6. The tensile strength of the Miner mock are listed in Table 3.3.

TABLE 3.3 TENSILE STRENGTH AND MODULUS OF MINER MOCK

E_T *MPa*	σ_{yield} *MPa*	ε_{yield}	σ_{IDT} *GPa*	σ_{break} *MPa*	ε_{break}
56	*0.9*	*0.016*	*6.18*	*1.1*	*0.028*

The magnitude of the properties of the Miner mock show that the material has weak tensile properties. The weakness of the tensile properties is mainly because of debonding and micro cracking of the polymer binder material during tension. The debonding of the polymer binder material is expected as the tensile load is applied. This eventually leads to microcracks at the interface of the polymer and the soda lime glass beads. This is expected mainly at the center where most of the tensile force will be applied. DIC technique was applied along testing in order to capture the surface effects leading to the main crack development or the fusion of the center crack with the surface.

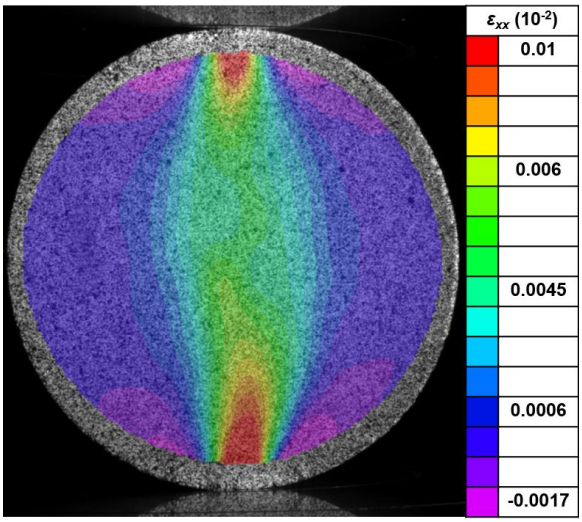

Figure 3.7 Strain in the x direction of Brazilian specimen

The Figure 3.7 shows strain concentrations at the location of the anvils. The figure shows that the specimen is suffering compression all along its diameter with the exception of the center where the specimen is under tension.

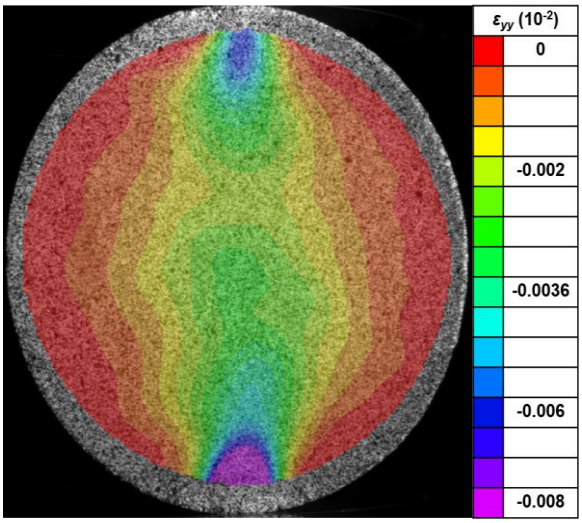

Figure 3.8 Strain in the y direction of Brazilian specimen

Likewise, Figure 3.8 shows stress concentrations near the anvils. However, the figure also shows that the specimen is compacting at the center or suffering a negative strain in the y direction along its center. Both of this figures shows that at the center is where fracture will occur however none of them predict the possible crack path. The equivalent strain shows a possible crack path for the surface of the specimen. This is shown in Figure 3.9.

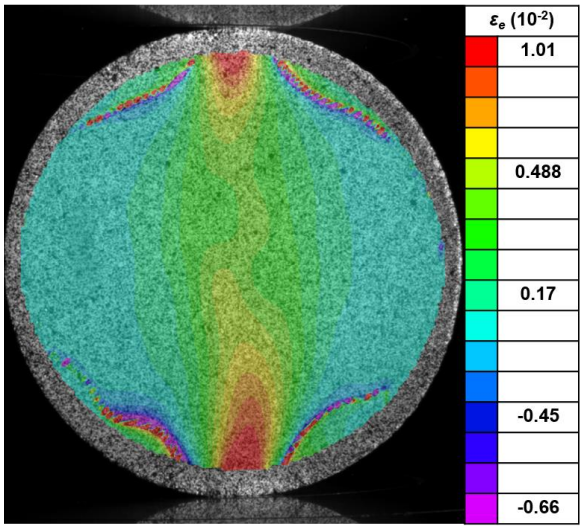

Figure 3.9 Equivalent Strain of Brazilian specimen

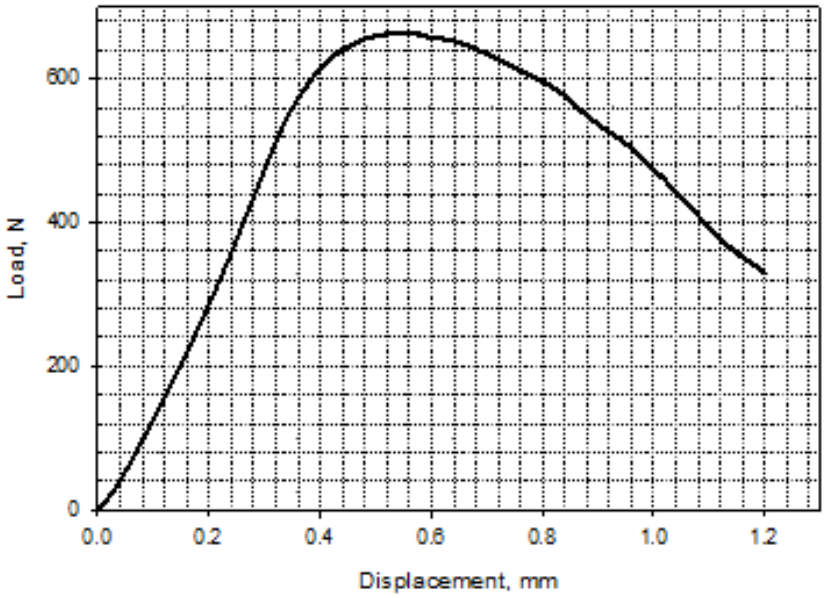

Figure 3.10 Load vs displacement curve for SCB specimen

Semi-Circular Bending (SCB) Test

The load with respect to the displacement for the miner mock SCB specimen is depicted in Figure 3.10. This plot is analyzed to obtain the fracture energy of the specimen. The transition point from the elastic region to the plastic region was determine to be at 0.381 mm of displacement. The maximum load reached was 783N. After 0.4 mm of displacement, a hardening effect is observed. The hardening effect was caused by micro cracking at the particle-binder interfaces and the

viscoelastic behavior of the polymer. The total fracture energy of the SCB miner mock specimen was calculated to be $0.289\frac{\text{kJ}}{\text{m}^2}$.

Conclusions

This study was performed to evaluate the mechanical properties of the Miner mock specimen at different loading conditions. Additionally, the DIC technique was implemented to surrogate the results obtained from the experimental data. The analysis performed using DIC technique satisfactorily showed the Poisson's ratio and equivalent strain on of the testing configurations, the prediction of the initiation and propagation of the crack by using the strain fields from DIC postproceesing. The DIC technique has a high impact, as a tool, in the analysis of heterogeneous particulate composites. The mechanical properties at each testing configurations where extracted and analyzed. When comparing the results to different PBX and mock PBX formulations, the properties vary in magnitude. The potential source of variability for the miner mock formulation can be categorized as the composition, material, and test related. To conclude, the following potential sources of variability were identified:

- PBXs are complex composite materials with high heterogeneity and anisotropy behavior. Alternative data analysis methods must be implemented to properly characterize the heterogeneous and anisotropy behavior of PBX.

CHAPTER 4: CONCLUSION & FUTURE WORK

4.1 Conclusion

The following conclusions can be formulated from the manufacturing and characterization of the Miner mock formulation:

- The manufacturing method does provide a specimen that can be machine and tested under different loading configurations.
- The manufacturing method can be improved in order to increase the energetic material simulant weight percentage.
- The material characterization provided a starting point for constitutive model development and simulations.
- The Miner mock formulation at a 50-50 weight percentage cannot be properly compared to real PBX data.
- Material characterization for a mock PBX was develop successfully.

4.2 Future Work

The following future work is suggested:

- Evaluate alternative formulations and procedures.
- Dynamic testing such as SHPB
- Evaluate the mechanical behavior of the Miner mock at different loading conditions and different temperatures such as near the glass transition temperature of the polymer binder material.
- Development of a Bridgman notch for the Miner Mock or mock PBX in order to induce a triaxial state of stress.
- Use of current data for constitutive model development.

REFERENCES

[1] Cooper, P. W., and Kurowski, S. R., 1996, "Introduction to the Technology of Explosives". New York: Wiley-VCH.

[2] Siviour, C. R., Laity, P. R., Proud, W. G., Field, J. E., Porter, D., Church, P. D., Gould, P., and Huntingdon-Thresher, W., 2008, "High strain rate properties of a polymer-bonded sugar: their dependence on applied and internal constraints," *Proc. R. Soc. A Math. Phys. Eng. Sci.*, **464**(2093), pp. 1229–1255.

[3] Cady, C. M., Liu, C., Rae, P.J., and Lovato, M. L., 2009, "Thermal and Loading Dynamics of Energetic Materials," *Proc. of the SEM Annual Conference*, Albuquerque, NM.

[4] Ramsay, J.B., and Popolato, A., 1965," *ANALYSIS OF SHOCK WAVE AND INITIATION DATA FOR SOLID EXPLOSIVES*." United States: N. p., Web. Doi: 10.2172/4618401.

[5] Skidmore, C.B. et al., 1998, "The Evolution of Microstructural Changes in Pressed HMX Explosives." United States: N. p., Web. Doi: 10.2172/334323.

[6] Zhou, Z., Chen, P., Huang, F., and Liu, S., 2010,"Experimental study on the micromechanical behavior of a PBX simulant using SEM and digital image correlation method." *Optics and Lasers in Engineering,* **49**(3), pp. 366-370.

[7] Li, M., Zhang, J., Xiong, C. Y. et al., 2005, "Damage and fracture prediction of plastic-bonded explosive by digital image correlation processing." *Optics and Lasers in Engineering*, **43**(8), pp. 856-868.

[8] Liu, Z. W., Xie, H. M., Li, K. X. et al., 2009, "Fracture behavior of PBX simulation subject to combined thermal and mechanical loads." *Polymer Testing*, **28**(6), pp. 627-635.

[9] Rae, P. J., Palmer, S. P., Goldrein, H. T. et al., 2004, "White-light digital image cross-correlation (DICC) analysis of the deformation of composite materials with random microstructure." *Optics and Lasers in Engineering*, **41**(4), pp. 635-648.

[10] Rae, P. J., Goldrein, H. T., Palmer, S. J. P. et al., 2001, "Moire interferometry studies of PBX 9501." *Shock Compression of Condensed Matter*, pp. 825-828.

[11] Chen, P. W., Xie, H. M., Huang, F. L. et al., 2006, "Deformation and failure of polymer bonded explosives under diametric compression test." *Polymer Testing*, **3**(25), pp. 333-341.

[12] Chen, P. W., Huang, F. L., Ding, Y. S., 2007, "Microstructure, deformation and failure of polymer bonded explosives." *J. Mater. Sci.*, **42**(13), pp. 5272-5280.

[13] Banerjee, B., Cady, C. M., and Adams, D. O., 2003, "Micromechanics simulations of glass-estane mock polymer bonded explosives," *Modelling and Simulation in Materials Science and Engineering,* **11**(4), pp. 457–475.

[14] D. M. HOFFMAN, BRUCE J. CUNNINGHAM & TRI D. TRAN (2003) "Mechanical Mocks for Insensitive High Explosives," *Journal of energetic Materials*, 21:4, pp. 201-222.

[15] C. Liu, C.M. Cady, P.J. Rae, M.L. Lovato, On the Quantitative Measurement of Fracture Toughness in High Explosive and Mock Materials, in: 14th Int. Detonation Symp, 2010: pp. 425–434.

[16] Xu, X., Mares, J., Groven, L. J., Son, S. F., Reifenberger, R. G., and Raman, A., 2014, "Nanoscale Characterization of Mock Explosive Materials Using Advanced Atomic Force Microscopy Methods," *J. Energ. Mater,* **33**(1), pp. 51–65.

[17] Ferranti Jr, L., Gagliardi, F. J., Cunningham, B. J., and Vandersall, K. S., 2010, "Measure of Quasi-Static Toughness and Fracture Parameters for Mock Explosive and Insensitive High Explosive LX-17," *14th Int. Detonation Symp,* pp. 522–529.

[18] Catzin, C.A., Reyes, J.G., Stewart, C.M., 2016,"Manufacturing Method for Mock Polymer Bonded Explosives", MethodsX. (Submitted)

[19] Hunt, E. M., and Jackson, M., 2012, "Coating and characterization of mock and explosive materials," *Advances in Material Science and Engineering*, **2012**, pp. 1-5.

[20] Cooper, P. W., and Kurowski, S. R., 1996, "Introduction to the Technology of Explosives". New York: Wiley-VCH.

[21] Jayco Inc., 2012, *Dragonite® soda lime glass beads sizes,* Randolph, New Jersey.

[22] Banerjee, B., Cady, C. M., and Adams, D. O., 2003, "Micromechanics simulations of glass-estane mock polymer bonded explosives," *Modelling and Simulation in Materials Science and Engineering,* **11**(4), pp. 457–475.

[23] Yeager, J. D., Ramos, K. J., Hooks, D. E., Majewski, J., and Singh, S., 2014, "Formulation-Derived Interface Characteristics Contributing to Failure in Plastic-Bonded Explosive Materials," LA-UR-14-24860, *Proc. 15th International Detonation Symposium*, San Francisco, CA.

[24] Cady, C. M., Liu, C., Rae, P.J., and Lovato, M. L., 2009, "Thermal and Loading Dynamics of Energetic Materials," *SEM 2009 Annual Conference and Exposition on Experimental and Applied Mechanics*, Albuquerque, NM.

25] Chen, P., Zhou, Z. and Huang, F., 2011, "Macro-Micro Mechanical Behavior of a Highly-Particle-Filled Composite Using Digital Image Correlation Method," InTech, pp. 437-460, Chap. 18.

26] Zhou, Z., et al., 2012, "Study on Fracture Behaviour of a Polymer-Bonded Explosive Simulant Subjected to Uniaxial Compression Using Digital Image Correlation Method," *Strain*, **48**(4), pp. 326-332.

27] Cunningham, B. J., Gagliardi, F. J., and Ferranti, L., 2013, "Low Strain Rate Measurements on Explosives Using DIC," *Proc. of the SEM Annual Conference*, Springer, Indianapolis, IN, pp. 25-31.

28] Jerabek, M., Major, Z., and Lang, R. W., 2010,"Uniaxial compression testing of polymeric materials." *Polymer testing*, 29(3), pp. 302-309.

29] Fairhurst, C., 1964, "On the validity of the 'Brazilian' test for brittle materials, "International *Journal of Rock Mechanics and Mining Sciences,* **1**(4), pp. 535-546.

30] Yong, Y., Zhang, J., and Zhang, J., 2009, "A modified Brazilian disk tension test." *International Journal of Rock Mechanics and Mining Sciences*, **46**(2), pp. 421-425.

31] Huang, B., Shu, X., and Tang, Y., 2005, "Comparison of Semi-Circular Bending and Indirect Tensile Strength Tests for HMA Mixtures." *Advances in Pavement Engineering*, pp. 1-12.doi: 10.1061/40776(155)14

32] Cady, C. M. et al, 1998, "High and Low strain rate compression properties of several energetic material composites as a function of Strain Rate and temperature," C. Of, S. Energetic, M. Composites, vol. 836.

APPENDIX

SANDIA Report Year 1 14-15

SANDIA LDRD ANNUAL REPORT

YEAR 1: 8/31/2014-8/31/2015

NOVEL METHOD TO CHARACTERIZE AND MODEL THE MULTIAXIAL CONSTITUTIVE AND DAMAGE RESPONSE OF ENERGETIC MATERIALS

Carlos A. Catzin

Department of Mechanical Engineering, The University of Texas at El Paso

Calvin M. Stewart

Department of Mechanical Engineering, The University of Texas at El Paso

ABSTRACT

This study aims to create a scientific breakthrough in the ability to predict the mechanical behavior of energetic materials through the design of a new multiaxial testing method using three dimensional (3D) digital image correlation (DIC) and the development of a novel continuum damage mechanics (CDM) based constitutive model for the volumetric and deviatoric response of energetic materials. Traditional methods to elucidate the volumetric and deviatoric response of energetic materials require the use of complex load frame configurations which apply hydrostatic pressure and uniaxial loads independently. This new method will utilize a variation of the Bridgman notched specimen method and through 3D optical strain measurements elucidate the multiaxial constitutive and damage behavior through comparison to the analytical (skeletal stress) or elastic finite element (FE) solution. This work will be extended to deal with effects of strain rate (0.001 to 1 s-1) and temperature (ambient to 75°C). The primary challenge of this effort is transforming the Bridgman method that was originally developed for metals under tension towards energetic materials under compression. An outcome of this novel characterization method is the development of a CDM-based constitutive model for the prediction of the "batch-to-batch" mechanical behavior of energetic materials. This model will be used to simulate the service conditions of mock plastic bonded explosive (PBX) material including uniaxial and multiaxial states of static and dynamic loading.

In this Year 1 annual report, the current results are presented. These results include:

- The development and optimization of a manufacturing process for an heterogeneous particulate composite (HPC)
- The design of experiments for distinct mechanical test such as uniaxial compression, semi-circular bending, indirect tension, and the Bridgman notch for HPC specimen
- The execution of the above mechanical testing
- The analysis and discussion of 3D Digital Image Correlation recordings.

This report represents the completion of the key objectives and milestones outlined for Year 1 of this Sandia LDRD project.

ACKNOWLEDGMENTS

This research was supported by Sandia National Laboratories. We would like to thank Jaime Moya and Michael Kaneshige from Sandia National Laboratories who provided insight and expertise that greatly assisted the research. We thank Dr. David Roberson for his assistance with the pneumatic press training. Thank you for your support.

INTRODUCTION

Polymer bonded explosives (PBXs) are complex particulate composites that are typically comprised of two fundamental materials: micron size energetic crystals and a polymeric binder material [1]. In some cases a small percent of additives like plasticizers, oxidizers, and antioxidants are added to the composition in order to improve the explosive output and decrease the effect of ageing respectively. The particular mechanical behavior of each respective constituent material will develop the mechanical properties of the new formed particulate composite or PBX. Therefore, it is important to consider the individual mechanical properties of each of the constituent materials, their differences, chemical composition, and distribution [2]. For instance, the elastic modulus of the energetic crystals or particles at room and at elevated temperatures, it is frequently much higher than that of the polymeric binder material. Furthermore, the ratio of the explosive component (energetic material) to the polymer binder is dependent on one material to the next depending on the explosive material specifications; but, typically, the energetic material comprises 80-95% of the total mass of the composite [1]. The geometry of the energetic crystals is not homogeneous. Rather, the energetic crystals geometry is a distribution of different sizes, maintained in a similar range, that make up a heterogeneous arrangement [3]. Also, the size of the energetic crystals has a big impact in the overall mechanical strength and ignition mechanism of the particulate composite or PBX. Compositions containing large size energetic crystals tend to be more explosive and provide a weaker structure than compositions containing both large and small size energetic crystals [2]. One of the main reasons that justifies the used of PBX in industry is their ability to be handle, machined, and lightly deformed while avoiding accidental stimuli. Therefore, the used of large size energetic particles in PBX reduces

Figure 1. PBX used as a Solid Rocket Propellant

their mechanical strength and its ability to prevent accidental stimuli. A composition containing relative large and small energetic crystals will be the optimal choice to ensure safety during their application. PBXs are extensively used by engineers, specifically in the aerospace industry for solid rocket propellant and in the military industry for explosive components and applications. Many innovative applications for PBX can be developed, but a lack of research inhibits the innovative applications. The high cost of gathering the constituent materials, expensive testing setups, and the arduous task of following safe handling procedures of explosives are some of the main issues that slow down the research process. Therefore, a precise and well developed method of manufacturing a standard mock PBX specimen that closely resembles the mechanical behavior of PBXs is required in order to safely study their mechanical behavior. Several methods of manufacturing Mock PBXs have been proposed in literature. However, many of the proposed methods lack the high volume fraction of the mock energetic material or details connecting the proper manufacturing process. Contrary to literature, in the current study, a manufacturing process will be carefully described to facilitate the repeatable production of mock PBX. Once the mock PBX has been developed, it will be mechanically tested in order to characterize its mechanical properties and to measure the level or resemblance when compare to a typical PBX used in industry.

Technical Approach

Conventional contact strain measurement devices such as strain gages, extensometers, and linear variable differential transformers (LVDTs) can only measure local or average strain. The heterogeneous composition and consistency of PBXs contribute to slip, interfacial bond issues, and an overall inadequate measure of strain with these devices. Three-dimensional DIC allows for full-field and non-contact shape, displacement, and strain measurement of the surface of materials. This can help mitigate classical problems such as measuring the bulge (due to inadequate lubrication) of PBX subject to compression [4]. Several studies have been conducted by scientists at Los Alamos and Lawrence Livermore National Laboratories to characterize the properties of energetic materials using 2D DIC [5-7]. Most studies have focused on the tensile, compressive,

thermal, fracture, and failure properties of these materials [8]. A particular novel use of 3D DIC is to study the multiaxial (volumetric and deviatoric) constitutive and damage behavior of PBX using a notched specimen under compression. In the past, the skeletal stress and elastic FE solution have been used in conjunction with rupture data of Bridgman notched specimens to elucidate the multiaxial damage and rupture behavior of metal subject to creep under tension [9-11]. The skeletal stress method is based on the observation that a symmetric specimen subject to simple loading conditions (tension, pressure, or bending) has a point at which stress remains unchanged (spatially and with time) and is insensitive to elastic, plastic, and creep phenomena [12, 13]. Rupture data of uniaxial and Bridgman specimens is used to calibrate the Hayhurst triaxial stress that is dependent on the first principal, hydrostatic, and von Mises stresses [14]. Hayhurst stress is then implemented in the equivalent strain rate, damage evolution, and viscous potential function of a constitutive model. Although it has never been attempted, it is technically possible to use 3D DIC to elucidate the multiaxial damage/rupture using a Bridgman notched specimen of PBX under compression. The strain field in the vicinity of the notch can be extracted and used to identify the Hayhurst parameters or develop a PBX specific equation. It is hypothesized that by subjecting a novel Bridgman-type specimen to compression until fracture or buckling a reverse correlation between optical displacement and the analytical skeletal stress (or elastic FE solution) can be used to elucidate the multiaxial constitutive and damage behavior. These tests will be conducted at various strain rates (0.001 to 1 s-1) and temperatures (ambient to 75°C). The primary technical challenge will be to identify the proper specimen geometry that accommodates size, finish, surface quality, heterogeneity, and other specimen design issues. The expected outcome is the development of a new test standard for the volumetric and deviatoric response of energetic materials. The objective of this topic will be achieved using the following general methodology. All mechanical testing will be performed at UTEP utilizing a mock PBX material. Conventional uniaxial specimens will be tested to collect the linear elastic properties of the material. Experiment design will begin with simple linear elastic simulations (in the limit of small deformation) of various Bridgman notched geometries under compression towards mitigating challenges such as buckling, bulging, etc.

Iterative manufacturing and testing will produce an ideal candidate. A test matrix of ideal candidate specimens will be manufactured into mock PBX specimens. Mechanical tests will be performed on both uniaxial and Bridgman specimens with 3D DIC measurements up to failure. A comparison between the finite element solution and DIC measurements of uniaxial and Bridgman specimens will be used to elucidate the multiaxial constitutive and damage response of the material. Once perfected, this technique will be transferred to Sandia for use on real PBX materials.

Relationship to Prior and Other On-going Work

Numerous constitutive models have been developed (or repurposed) to model the rate-dependence of energetic materials under various conditions (low strain rate, high strain rate, cook-off, etc.). A menagerie of phenomenological and mechanistic viscoelastic and viscoplastic models have been used including generalized Maxwell, standard linear solid, Prony series, Johnson-Cook, Campbell, Steinberg–Guinan–Lund, Zerilli–Armstrong, etc. [15]. Schapery and colleagues have made substantial contribution to developing constitutive theory for elastic media and particulate composites with coupled strain rate and damage laws [16, 17]. Extensions of this isotropic theory have been used to model the 3D constitutive response [18], introduce damage-induced anisotropy [19], introduce property degradation due to damage [20], etc. These features are analogous to those used in the CDM theory [21]. The advantage of the CDM theory is that it allows the seeding of an initial damage distribution. This distribution can be heterogeneously distributed throughout the mesh via pseudo-random variable generation. Recently, Stewart developed a pseudo-nonlocal CDM-based damage evolution equation [11]. The advantage of this equation is the ability to control the localization of CDM and produce delocalized damage distributions about flaws in addition to rupture predictions. The volume fraction and surface area of polymeric binder, crystalline energetic, and voids which constitute a PBX have considerable influence on the resulting mechanical properties, explosive performance, sensitivity, and chemical stability. Slight variations in the manufacturing process can contribute to stockpile consistency issues. Considerable testing is required to verify a batch of explosives meets specifications. The ability to rapidly predict the "batch-to-batch" mechanical behavior of PBX through an analysis of

manufacturing parameters such as volume fraction and mean particle size would revolutionize the validation process. Xu and Sofronis have demonstrated that a rigorous homogenization theory based on volume fraction can be used to model the bulk constitutive response of a solid rocket propellant [22]. In this process, the mechanical properties associated with each constituent of the microstructure undergoes a homogenization process via volume fraction to produce composite mechanical properties that can be used within macro constitutive models. It is hypothesized that a CDM-based constitutive law using homogenization theory of composites [22], a pseudo-nonlocal damage evolution equation [11], a heterogeneous initial damage distribution [21], and a triaxial stress [14] can be used to predict the "batch-to-batch" mechanical behavior (compressive and creep) of mock PBX subject to low strain rate and varied temperature. The ability to predict the "batch-to-batch" mechanical behavior is a major breakthrough. The technical challenges are experimentally determining pre-existing defect quantity and intensity, measuring the volume fraction, and dealing with the varying heterogeneity of test specimens. UTEP and Sandia's proximity makes collaboration on this topic complementary. The establishment of a relationship between Sandia and UTEP will facilitate collaboration on future external funding opportunities.

Goals, Objectives, and Project Milestones

The overarching technical goals for this project are

- Conduct 3D DIC on mock PBX to measure the linear elastic and creep properties
- Conduct 3D DIC on Bridgman specimens to measure the multiaxial constitutive and damage behavior at various strain rates and temperatures
- Develop a constitutive model capable of predicting the "batch-to-batch" constitutive behavior including uniaxial and multiaxial states of loading

Concrete evidence of technical success will be shown through the publication of conference and journal articles in conjunction with the submission of yearly and the final SAND reports.

Year 1 Outcomes

The overarching technical goals proposed for year 1 of the project included:

- 3D digital image correlation of mock PBX (uniaxial specimen)
- A CDM-based constitutive model for mock PBX with heterogeneous damage distribution

The 3D DIC of mock PBX goal includes a submission to the 2015 SEM conference and a journal submission. However due to difficulties in gathering or obtaining mock PBX specimens, the technical goals for year 1 suffered a slight change to the following:

- Material Selection and Manufacturing of a Mock PBX (Particulate composite)
- Microstructural characterization of manufactured Mock PBX
- 3D DIC on Manufactured Mock PBX (Mechanical Testing).

In this report we present the outcomes of these goals. These goals include a submission to a conference and a journal paper .A technical presentation of the manufacturing process presented in this report will be presented in IMECE 2015. Several journal papers will be submitted in the near future.

MATERIALS

Several research studies have been performed in the manufacturing process of energetic materials to characterize their explosive sensitivity [23], hot spot generation [24], and deflagration or detonation initiation [25].Only a few research studies have thoroughly covered the manufacturing process of a “simulant energetic material” or “mock” Specimen. In each of the recent research studies below an effort to replicate the constituent materials geometry, morphology, and properties was made in order to accurately simulate the mechanical properties of a PBX; however, some physical characteristics of PBXs are not taken into consideration for the simplification of the micromechanics towards a homogeneous assumption.

An example of the latter is found in Banerjee et al where instead of using energetic crystals, they used micron size soda lime glass beads that possess a similar mechanical behavior and physical properties compared to energetic crystals that are commonly used in the manufacturing process of PBXs [26].The soda lime glass beads provide the high modulus contrast between the energetic particles and the binder material just like the energetic particles do in a typical PBX [26]. Such substitution is justified making glass-polymer mock PBX a reasonable substitute for mechanical testing. But important physical properties that contribute to the mechanical behavior are omitted, such as the high volume fraction of energetic particles to binder material and the particle morphology. Banerjee et al justifies the lack of such high volume fraction and particle morphology by stating that the effects caused by these physical properties are not needed to be considered in the calibration of their computational model of HPC [26]. It is important to remark that in Banerjee et al the diverse sizes of the energetic particles are considered in the development of their mock material. Summarizing, Banerjee et al describes the material selection process for a mock PBX, describes a brief manufacturing process of a glass-polymer mock PBX, and develop FEM simulations for a HPC. Some of the weak points or issues in Banerjee et al is the lack of fundamental physical properties of PBX in their glass-polymer mock and a detailed description of their manufacturing process.

Yeager and collages also conducted a research study on the material selection and manufacturing process for a mock PBX [27]. In Yeager et al, the energetic particles are substituted by acetaminophen that is a crystalline powder typically used in the pharmaceutical industry as a pain reliever to produce different Mock PBXs. The manufacturing process described in Yeager et al closely resembles the typical slurry formulation process used in the explosive industry; however, many details are missing, modified, or not described at all. Overall, Yeager et al provides different compositions of PBXs, a few compositions of Mock PBXs, a brief description of the manufacturing process, measurements of the crystal-binder bond in different PBXs and Mock PBXs, and the different effects of additives like plasticizers and oxidizers to the crystal-binder bond in each composition of PBXs and their mock counterparts. A few important details are

missing in Yeager et al such as the materials specifications, the weigh or volume percentage of each composition, and a detailed description of the manufacturing process and its justification.

In Xu and collages an expensive yet similar effort to the above studies was approached as they used a simulant of the so called octogen explosive or HMX called pentaerythritol or also called pentek, to replace the actual energetic material [22]. No material selection discussion is delivered; however, they mentioned that a molding powder of the mock 900-21 was provided by a national laboratory. This molding powder is commonly used to simulate the mechanical properties of PBX 9501[5]. The composition of the molding powder and the different properties of its components is given in the form of a table. It is important to remark that the high modulus contrast between the energetic particles and the binder material is present in the molding powder as well as the particle morphology. The manufacturing process was a simple high pressure press of the molding powder into their desired geometry for testing, typically a cylindrical geometry. This method of manufacturing mock PBX is very specific and easy to follow, but is expensive for repetitive production. Overall, Xu and colleges provided the properties of a typically used mock PBX and a manufacturing/machining process.

Siviour and collages take a different approach. Since the main objective of Siviour et al is to predict the mechanical behavior of the materials solely from their composition, a relative inexpensive approach was taken as caster sugar crystals were used to simulate the energetic particles [2]. They mentioned that such substitution is commonly used to simulate the mechanical properties of polymer bonded explosives. Special emphasis is given to the material selection particularly in the crystal-binder interaction and the particle size effects in the mechanical strength of the material. For instance, in Siviour et al it is mentioned that the mechanical strength of the material is not only dependent in the binder material that absorbs the mechanical energy and prevents crystal-crystal friction, but also in the crystal size and crystal separation or homogeneity in the crystal distribution [2]. Siviour and collages used hydroxyl terminated polybutadiene (HTPB) as a binder material because several research studies have previously used this material to successfully recreate the mechanical properties of a PBX. Besides, the HTPB is typically used

as binder material in the explosive industry. However, no much information is given about the caste sugar crystals other than a percentage. Siviour et al describes very briefly the manufacturing process used to obtain their polymer bonded sugar (PBS), but most of its results and discussion are based on several research studies making it a reliable source.

In this study the material selection and manufacturing process are based on the above and referenced research studies, with the objective of creating and develop a safe and relative inexpensive method to study energetic particulate composite materials or PBXs. The mock PBX created with the manufacturing process presented in study is expected to closely resemble the mechanical properties of a real PBX. A description of our manufacturing process is included in the manufacturing section of this report.

Material Justification

Since the specific mechanical behavior of each respective constituent material will develop the mechanical properties of the PBX, it is important to consider the material selection in the development of a "mock" PBX, particularly the binder material. The binder material is responsible of coating and creating strong bonds between the energetic particles which will eventually form the mechanical strength of the PBX, and to ensure the safety during the manufacturing process. For instance, a sensitive explosive will required certain properties of the binder material to avoid accidental stimuli by crystal-crystal friction during the manufacturing process. A list of different binder materials used in industry is available in Table 1. In order to adequately select the binder material to accommodate explosive sensitivity, a parameter must exist that eases the selection process. The glass-transition temperature, Tg, is a parameter that among the material properties of the binder material, will determine if it will reduce or increase the sensitivity of the PBX to impact [29]. Tg is the temperature region where the polymer transitions from a hard glassy material to a soft rubbery material. Therefore, Tg is an imperative parameter for the material selection process and the adequate pairing of the binder and energetic material [2]. Even though, Tg is a parameter that helps in the selection of the binder material, it is not considered in many of the previous research study as a parameter during the selection process.

Table 1. Different Polymer Binder Materials used in the manufacturing process of PBX.

Polymer Binder Material	Melting Temperature (°C)	Adhesive Properties
Polyurethane (PUR/PU)/ Estane	240-280	Excellent
Polystyrene (PS)	100-200	Excellent
Polyethylene (PE)	130-137	Good
Fluoroelastomer / Fluoropolymer (Viton, Fluorel)	177-232	Good
Poly(methyl methacrylate) / (PMMA)	160	Excellent
polyisobutylene (PIB)	106.5	Good
Polyvinylpyrrolidone (PVP)	100	Good
Hydroxy-terminated Polybutadiene	Neglible	Good

Another parameter that plays an important role in this selection process is repetition or usability. In several of the research cases mentioned above, the selection of the binder material took place due to their common used in the manufacturing process of real PBX. Since this seems to be the case, the polymeric material selected in this study to act as a binder material is a special form of Polystyrene. This selection for a binder material is reasonable since the first composition of a PBX included polystyrene as a binder agent [28]. The special form of the polystyrene is in fact to reduce the impact or to enhance the properties of the polystyrene to absorb energy, the high impact polystyrene (HIPS).

The energetic crystal or particles possess certain qualities that make them optimal for the polymer binder explosive application. The main qualities that are obvious, yet they have to be mentioned, are the explosive and mechanical properties. However, for the manufacturing of a mock or simulant energetic material the explosive properties are obsolete. Another set of parameters like the particle morphology and the mechanical properties must be taken in consideration for the adequate selection of the simulant. A list of typical energetic crystals and their sizes can be found in Table 2. One of the main parameters that determines the selection of the simulant of the energetic particles or crystals is the high modulus contrast between the energetic particles and the binder material.

Table 2. Energetic materials and their simulant counterpart.

Energetic Material	Size (μm)	Mock Energetic Material	Size (μm)
TATB (1,3,5-triamino-2,4,6-trinitrobensene)	50-70	Spherical Soda Lime glass beads	150-250
HMX (Octahydro-1,3,5,7-tetranitro-1,3,5,7-tetrazocine)	3-100	Acetaminphen (ACM)	12-100
RDX (cyclotrimethylenetrinitramine)	1-124	Pentaerythritol (Pentek)	45-500
HNS(Hexanitrostilbene)	9	Caster Sugar Crystals	2000 coarse
PETN Pentaerythritol tetranitrate	44-850	Barium Nitrate (Ba (NO3)2)	50-200

In another words, the energetic mock or simulant must poses similar mechanical properties when compared to a typical energetic crystal. However, the parameter that eases the material selection in this study is the particle size. As is shown in Table 2, the material that has a similar mechanical properties and size is the soda lime glass beads. Even though the acetaminophen (ACM) are also crystal particles, there exist law restrictions that will create problems in other to obtain them. As well as safety and handling procedures are stricter when handling chemicals. This is the same case of the barium nitrate. The Pentek is not an inexpensive material and there is many restrictions to overcome in order to obtain it making this material not suitable for this study immediate needs. While the soda lime glass beads closely resembles energetic crystals, it does not provide the wanted random geometry of the crystals like the caster sugar crystal do. Still the soda lime beads have a higher modulus and are closer in size, overwhelming the random geometry generated by caster sugar crystals. The soda lime glass beads will provide the necessary high modulus contrast and size distribution necessary to simulate the energetic crystal for this study. The particulate composites explored in this study are composed of Soda lime glass beads contained in a high impact polystyrene polymer binder.

High Impact Polystyrene (HIPS)

The High Impact Polystyrene (HIPS) pellets used in this study were produced by the polymerization of styrene in the presence of butadiene rubber, which is the typical process used to produce this type of polymer. A picture of the actual HIPS pellets used in this study is shown in Figure 2. If an ultra-thin section of the polymer HIPS is cut, it is possible to detect, in a scanning electron microscope (SEM), that the butadiene rubber particles have a circular structure and are

Figure 2. High Impact Polystyrene Pellets

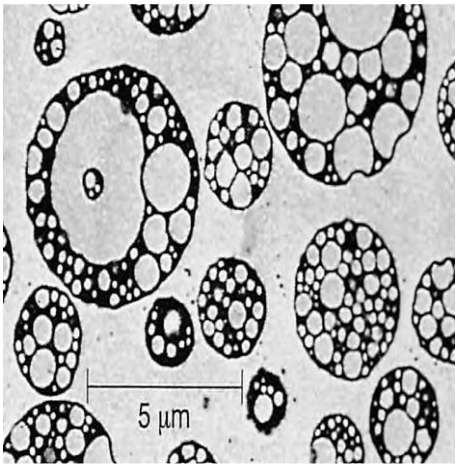

Figure 3. SEM of an ultra-thin section of HIPS

embed in a normal polystyrene matrix as shown in Figure 3. Figure 3 resembles one of the main characteristic of the microstructure of HIPS. The molecular formula of HIPS is present in Figure 4 under this description. The mechanical behavior of HIPS can be considered to be viscoelastic as it is seen in the stress-strain curve in Figure 5. Also, the mechanical behavior of HIPS is characteristic of tough materials such as metals and composite materials like carbon fiber. One explanation for this sort of mechanical behavior in HIPS is the number, size, size distribution and internal structure of these rubber particles which determine the property profile of the HIPS. In another words, the toughness of the high impact polystyrene will increase as the rubber content increases. The commercial grade HIPS used in this study was obtained in pellet form and contained 8.5 wt. % of polybutadiene. It is important to keep in mind that polymers are highly sensitive to the strain rate and temperature. The high impact polystyrene is temperature and Strain rate dependent as shown in Figure 6 at constant strain rate of 2mm/min. At low temperature it will behave like a glass, but above the glass transition temperature it will behave like rubber. The source of the material asked to remain anonymous due to the nature of the project. The HIPS has a melting temperature of 132º C. The room temperature density of HIPS is 1.04 g/cm^3.

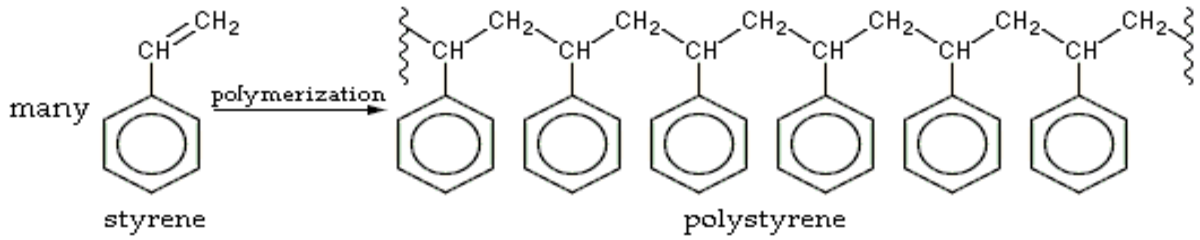

Figure 4. Molecular Structure of HIPS

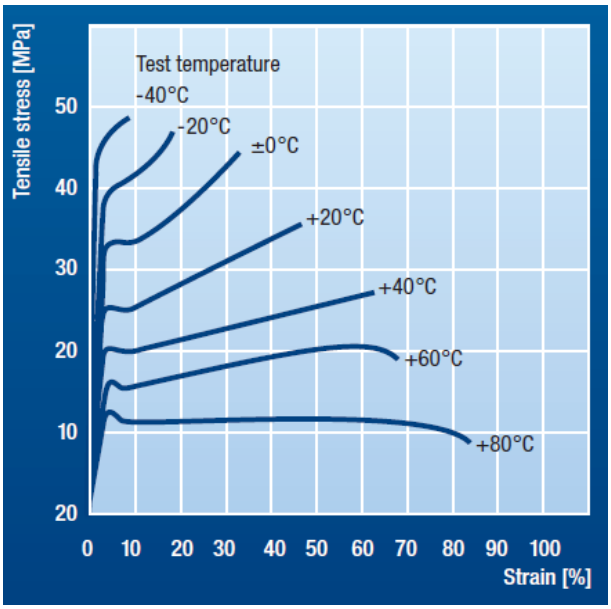

Figure 5. Stress-Strain curve of HIPS at different test temperatures: determined on injection-molded test specimens.

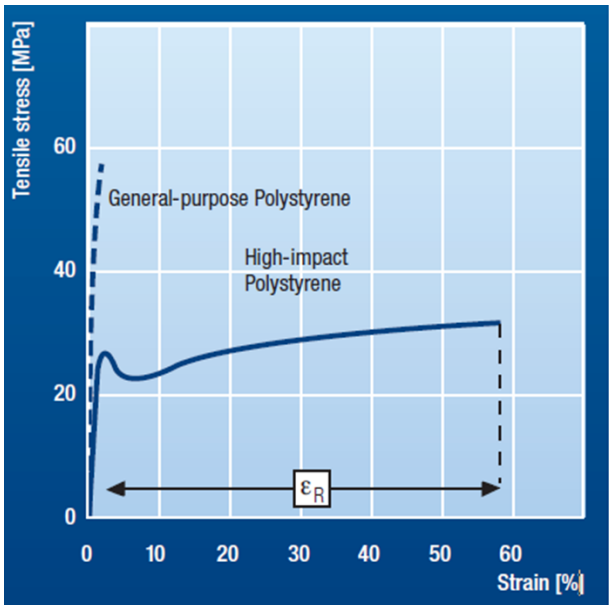

Figure 6. Stress-Strain curve of general purpose polystyrene and HIPS in a tensile test in accordance with ISO 527

Soda Lime Glass Beads

Figure 7. Micron size Soda Lime Glass Beads

The soda lime glass beads used in this study were produced by the typical commercial manufacturing process, but it has a unique washing and polish process free of harmful additives. This gives the soda lime glass beads a pure shiny surface. The glass beads were manufactured by Jaygo Corp as a standard soda lime glass with an average diameter was 200µm ± 50µm. These glass beads are linear elastic in the range of conditions used in the experiments and have a density of 1.02 g/cm^3, a Young's modulus of 63 000 MPa, and a Poisson's ratio of 0.20.

Particulate Composite

A description of the optimized manufacturing process of the glass-HIPS mock PBX is found in the manufacturing section, but the different manufactured compositions are detailed below. Based in literature, several distinct weight compositions where manufactured using the optimized process. A table of the different compositions is shown in Table 3 below. This different compositions are similar to the ones found in literature like Banerjee et al. The glass-HIPS mock PBX specimens started with composition of a high volume fraction of the binder material and concluded with a high volume fraction of the simulant energetic material, however the best composition seem to the composition 2 (50/50). Composition 2 is the selected as the main manufacturing composition for our testing specimens because such composition possess the highest volume of the simulant explosive without affecting the structure of the specimen for machining purposes. Composition 3 seems to be another option for testing specimens as it possess the highest volume of explosive simulant and a relative strong structure for manufacturing purposes. However, as seen in Figure 10, is more probable that during manufacturing big voids will be developed in composition 3 than in composition 2 which could affect machining, polishing, and later on the test. As a results of such voids during manufacturing, composition 3 is not used in this study. Possible

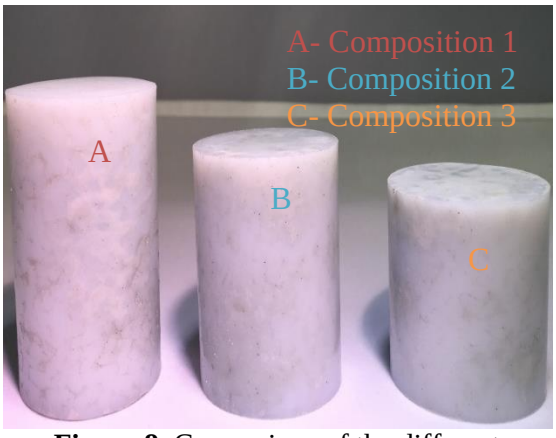

Figure 8. Comparison of the different Compositions

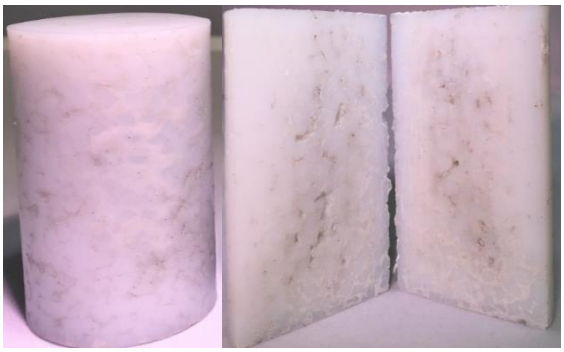

Figure 9. Composition 1 and its internal structure

Figure 10. Composition 3 and its internal structure

solutions to this voids creation will be assess in the near future. Composition 1 was neglected because it did not possessed a high volume of the simulant explosive as seen in Figure 9. No internal structure is found in this study for composition 2, instead an optical microscopy of the optimal composition is found below.

Table 3. Different manufactured compositions of the glass-HIPS mock PBX.

Composition	Energetic Material Simulant (wt.%)	Polymer Binder Material (wt.%)
Composition 1	25	75
Composition 2	50	50
Composition 3	65	35

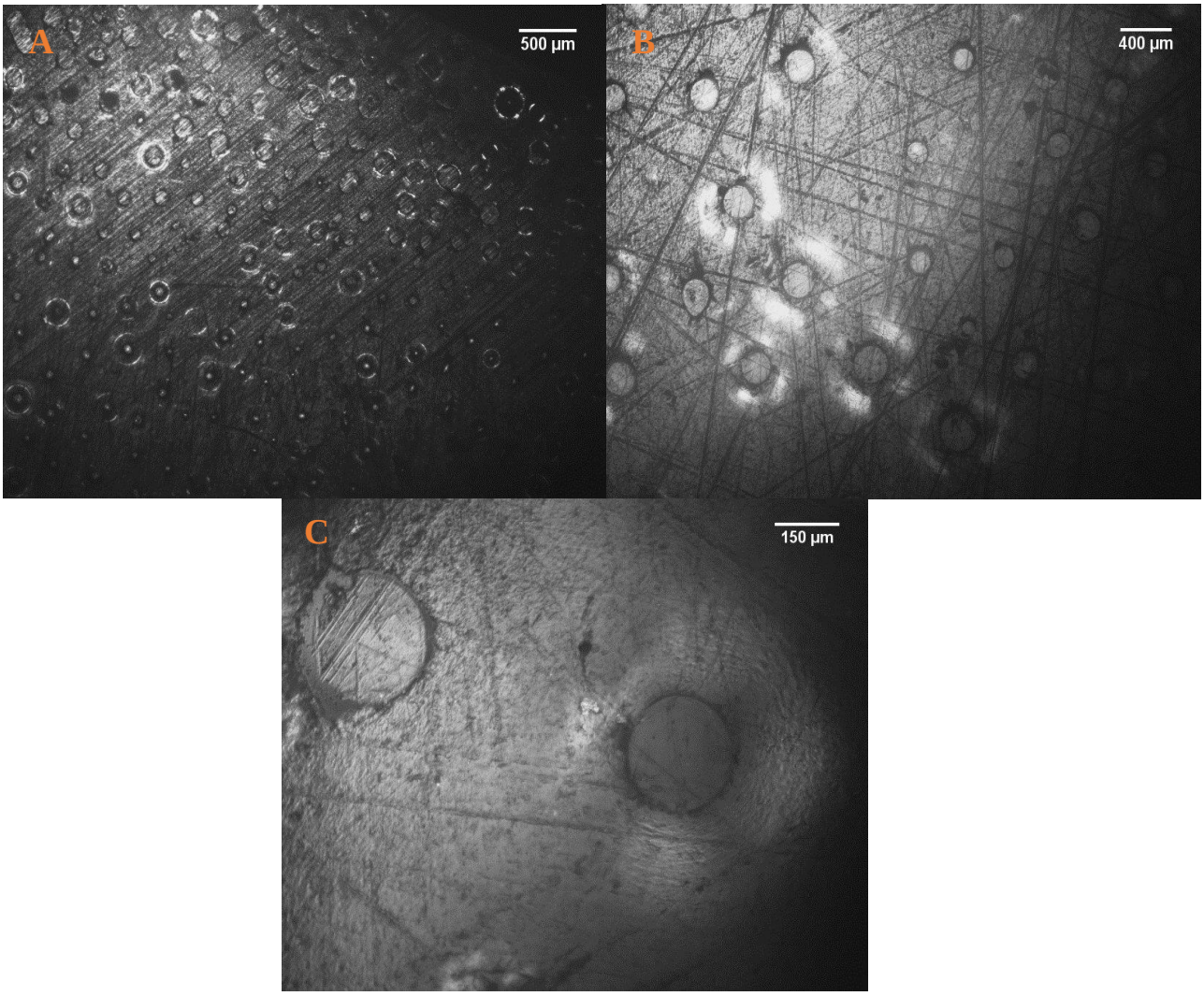

Figure 11. Optical Microscopy of HPC optimal composition (50-50)

Microstructural Characterization

The optical microscopy of composition 2 was the key for the selection of composition 2 as the optimal composition. In Figure 11 part A, is possible to see the different sizes of the soda lime glass beads coated and embedded into the HIPS polymer. The distribution shown in part looks like a normal distribution without agglomeration of the soda lime glass beads. It's also possible to see the effects of polishing in the sample. This is more noticeable in part B of Figure 11. In part B is also possible to see that some of the glass beads are deeply incrusted or coated into the polymer. In part C is possible to see that some of the glass beads were cut in half when machining the sample for the microscopy. The fact that a 50-50 composition has such a good distribution was a strong reason to lean towards selecting the optimal composition.

SPECIMEN MANUFACTURING PROCESS OF MOCK PBX/HPC

Overview and Background Information

The Materials at Extremes Research Group (MERG) at the University of Texas at El Paso (UTEP) has developed and optimized an ingenious manufacturing process of a Heterogeneous Particulate Composite (HPC) for a project concerning the characterization and modeling of the multiaxial constitutive and damage response of energetic materials for Sandia National Laboratories. MERG is creating a mock or simulant of energetic materials using two constituent materials. A polymer, that acts as a binder material, and micron size soda lime glass beads (150-250 micrometers in diameter), to emulate the energetic particles or crystals. These materials are mixed with a very small volume of water to create clusters and make the consistency clumpy, i.e. half a gram in weight. The mixing process involves stirring the two constituent materials during three minutes, and pouring this mixture back and forth between glass beakers at least four times to improve the results of the resulting mock polymer-bonded explosive samples. The mixture is then placed inside a legacy metallographic hot pneumatic press, resulting in a cylindrical coupon 1-1/2" in diameter and up to 2-1/2 inches tall. This coupon is then machined to the desired geometry, using a CNC Lathe to introduce a circular circumferential notch on the specimen, or in a Bluehler abrasive cutter to cut the specimen to the required testing geometry of a shorter, circular "coin", or a semicircular

"coin". After machining, all the specimens are carefully polished in a Buehler Polimet 1000 grinder-polisher to remove any unwanted surface roughness that might affect the results of mechanical tests. A detailed manufacturing process has been developed for this operation and it is available in the Test Procedure and Approach section of this document. It is important to reemphasize that investigators handling these materials are required to wear the appropriate personal protective equipment (PPE), which was selected based on the material safety data sheets (MSDS) of both constituent materials. This is covered more thoroughly in a section by its own later in the report, along with an appendix.

The manufacturing process used in this study was based on the idea of completely coating particles in a binder material or matrix to ensure that the final product will closely resemble the mechanical properties of a mock PBX, and to prevent the segregation of the constituent materials. The idea behind this process consist in the replication of a dry granulation process with obvious alterations. This method, typically used in the pharmaceutical industry for tablets manufacturing. It consist in shredding large materials into smaller particle like geometry, then combining the just shredded particles with a micron geometry material to create the final particulate composite that can be manufactured to a desired geometry. The combination process consist in either using a high compressive force to bond the materials or by using a binding agent. For the purposes of this study, the high pressure idea was preferred over the binding agent. The idea of this process helped the MERG research team to develop a similar yet still effective process to develop a heterogeneous particulate composite (HPC). The details and steps of the manufacturing procedure, along with several images of the key steps of the process are described below in the next section.

Personal Protective Equipment and Safety

In order to be able to create a safe manufacturing and machining process environment, it is critical to understand all possible risks and complications that could arise from using the equipment and then provide solutions. In accordance to the material safety data sheets (MSDS) of the constituent materials of the self-manufactured heterogonous particulate composite, investigators handling these materials are required to wear the following personal protective equipment (PPE): lab coat,

steel toe boots, EN 166 compliant eye protection, welding gloves (for handling of the hot press), 8 ml disposable nitrile gloves, and disposable N95 respirator masks. A detailed description of this equipment is provided in Appendix A.

Manufacturing and Equipment

A detailed description of each piece of equipment required for the manufacturing process of the Heterogeneous Particulate Composite/Mock polymer-bonded explosive is presented in Appendix B. These equipment and machinery served a specific purpose in the manufacturing process; their uses are listed in the manufacturing protocol that the research team followed to effectively produce the samples needed.

Manufacturing Procedure of Heterogeneous Particulate Composite (HPC)

All of the equipment listed on the Test Procedure and Approach section should be gathered as an initial step. Both the PPE (must be worn) and the tools used during the manufacturing process, are listed and described in detail in the Appendix section. The station set up and tools required to manufacture the mock polymer-bonded explosive are presented in Figure 12, with the extra details provided on the respective Appendices of the PPE and the manufacturing equipment.

Figure 12. Station Preparation with Tools for Manufacturing Process.

Stage 1: Preparation and Weigh-In of Constituent Materials

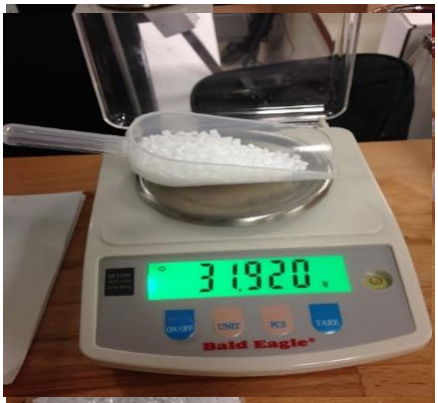

Figure 14. Weighing of Constituent Material.

Figure 13. HIPS (Left) and SLGB (Right).

The dry granulation process begins by plugging in the heating element that is attached to the Leco PR-22 Pneumatic Mounting Press Plug, and turning the switch to 'ON'. The heater requires an approximated time of 30 minutes to reach its maximum temperature of 190°C. Then the scale is turned on and 5 minutes are allowed for the scale to stabilize (indicated on the instructions) and then it is calibrated using the corresponding 100 gram weight. After the calibration, the constituent materials, shown on Figure 13, which will make up the mock PBX sample are collected, and the beakers, flasks, and plastic scoops are checked for complete neatness before the materials are added. Posteriorly, the desired amount of each component material, i.e. 37.5 grams, is measured separately using the plastic scoop that weighs approximately 11.88 grams. This is significant because the weight shown on the electronic balance should be subtracted from the total amount to determine the correct, true mass of anything that is measured. This is illustrated in Figure 14 to the right. The plastic scoops were used because the glass beakers and flasks exceeded the 100 gram weighing capacity of the balance. Then, the balance and plastic scoop should also be used to weigh the proper amount of water (H2O), the used amount is half a gram. All of these different materials should be placed in their respective containers, the polymer and glass beads in a beaker, and the H2O in a flask. The next part of the procedure is to ensure that the metallic cylindrical container (or mold in which the mixture will be placed) ,the moving platform that comes in contact with the mixture, and the upper die that locks the specimen, are free of residues from previous manufacturing sessions. At this point the air pressure valve connected to the pneumatic press is turned on.

Stage 2: Mixing of Constituent Materials

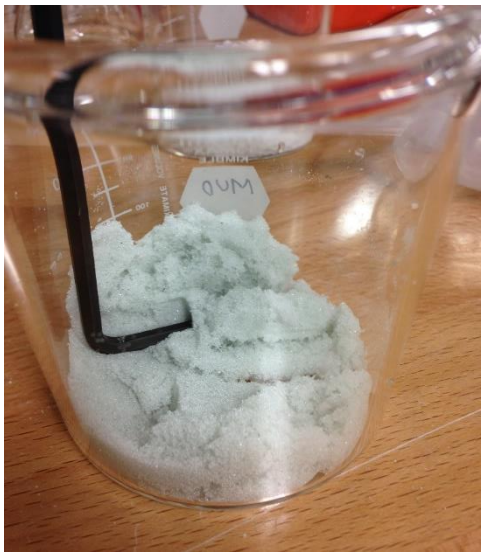

Figure 15. Resulting Desired "Clumpy" Texture of Soda Lime Glass Beads with H_2O.

In the next phase of the manufacturing process, a key step takes place, which is the mixing of the high impact polystyrene pellets and the soda lime glass beads with H2O. The step-by-step procedure with specific chronological order that yielded the highest-quality results is described next. First, the half-gram of H2O is added to beaker containing the soda lime glass beads, and mixed for a minute with a mixing stick, such as a hexagonal key to result in a texture similar to that shown in Figure 15. Then, about 10 grams of polymer, should be put away for the first layer of PBX mixture that will be added to the mold in the pneumatic press. After this, the now lumpy soda lime conglomerate can be added to the beaker of the polymer and mixing with the stick should be done for 3 minutes. An extra measure to ensure the correct mixing of the materials is pouring this mixture from one beaker onto another at least four times. The justification and proof of the added amount of water is described below in the section of manufacturing issues, as it improved the distribution of the glass beads with the binding polymer material in the resulting mock PBX samples.

Stage 3: Preparing Mold in Pneumatic Press

At this point in the manufacturing process, the temperature of the inner part of the heating element should be measured using an appropriate Fluke multimeter, to ensure it is close to its maximum temperature. This in turn means that the heat can be put on the mold and the heat transfer rate will be the highest possible, making the process the most time-efficient it can be. Next, it is necessary to ensure the appropriate dust-proof respirator mask is being worn. Then to apply the silicone spray to the cylindrical metallic tube (in a place with enough ventilation), the surface of the upper locking die, and the moving platform to prevent the sticking of the PBX specimen to these surfaces and thus affect its quality once it's been removed from the mold. It is important to consider that both the silicone release spray and the acetone are highly flammable, and should not be placed near a heat source at any point, as indicated on their Material Safety Data Sheets 30-31].

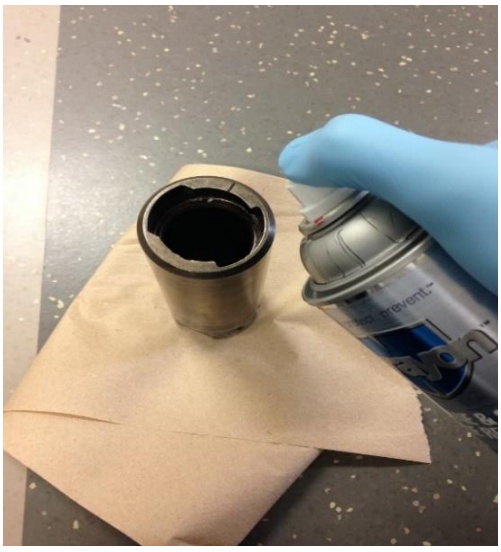

Figure 16. Applying Silicone Release Spray to PBX Mold.

Figure 17. Placing and locking with cylindrical mold in pneumatic press.

The procedure of applying the silicone release spray as lubricant onto the metallic cylindrical container is shown in Figure 16. Next, this previously mentioned mold has to be fit correctly into the respective opening, and tightened securely using the screw. Then, the moving die

Figure 18. RAM control and die moved fully up.

should be moved all the way to the lowest possible point so that it simplifies the process of placing and fixing the cylindrical tube. The placing and locking of the cylindrical, metallic mold onto the pneumatic press using the adjustable screw and a wrench is also depicted in Figure 17.The next step is to raise the moving die to the highest point using the RAM control lever, as shown on Figure 18. This is done in order to posteriorly apply the electric heater around the moving dye to optimize the heating of the polymer and soda lime glass mixture. The resulting PBX specimens, along with the added half gram of water, were consistently the highest quality specimens as opposed to the samples in which these two extra steps were no taken. The electrical heater being applied to the cylindrical mold is depicted as well, in Figure 19 in the next page. The heater should be left fitted onto the cylindrical container with the adjustable die, until the temperature of this aforementioned die reaches 135 ºC. The motivation for this is that at this temperature the polymer pellets that come into the contact with the surface will begin to melt and will stick to the surface more easily, thus enhancing the process of creating a layer of polymer that can encompass the whole cylindrical sample and prevent concentrations of soda lime glass beads, which will inevitably occur, from falling out of the specimen and creating voids on the surface, disabling the PBX specimen for the purpose of testing.

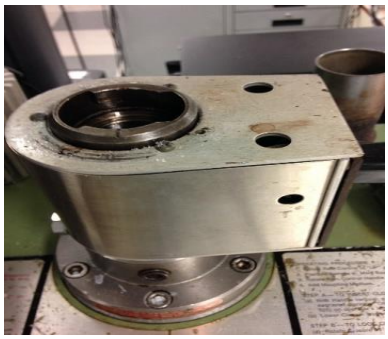

Figure 19. Electrical Heater applied to the cylindrical mold.

Figure 20. Moving die adjusted up to eliminate the space with the mold.

Stage 4: Pouring Mixture into the Cylindrical Mold and Locking It In

After the mold has been fitted in place, and the desired temperature of 135 degrees has been reached (which usually takes an average of 15-20 minutes at a room temperature in the low 20's) the mixture can now be poured in into the mold where it will be heated and compressed to form the desired mock PBX sample. In order to do this, the adjustable, cylindrical die must be raised,

however just enough in order to completely fill the void at the bottom and completely eliminate the space between moving die and the inner wall of the cylindrical mold. This is shown on an image to the left, on Figure 20. Following this, now very carefully the heterogeneous mixture of constituent materials into the cylindrical metallic tube can be poured (See Figure 21-A). This, should be preceded by the pouring of the 10 grams of polymer that were set aside from the mixture with added H2O to it, in order to create a 'floor' on which the mock PBX specimen can be formed. It was discovered that prior to adding this extra step to it, if a significant amount of soda lime glass fell isolated on the bottom layer it would tend to fall off as it would not have a coating of polymer to bond to and remain solid and compact after the solidification and removal process. After all of the mixture has been poured in the cylindrical tube, the external cylindrical dice should be placed into the cylindrical metallic tube (See Figure 21-B) in such a way that the dice should fit inside the tube and leave a small gap for the dice holder. Then the dice holder is placed on top of the external cylindrical dice and inside of the metallic tube. The dice holder must be switched into its locked position by twisting it 90 degrees, as shown in Figure 21-C. The dice holder face reads "Lock" and "Open" for either case, so the user should ensure the former is securely adjusted. Another manner to ensure that the die holder has been placed into its correct position is to gently try to remove the

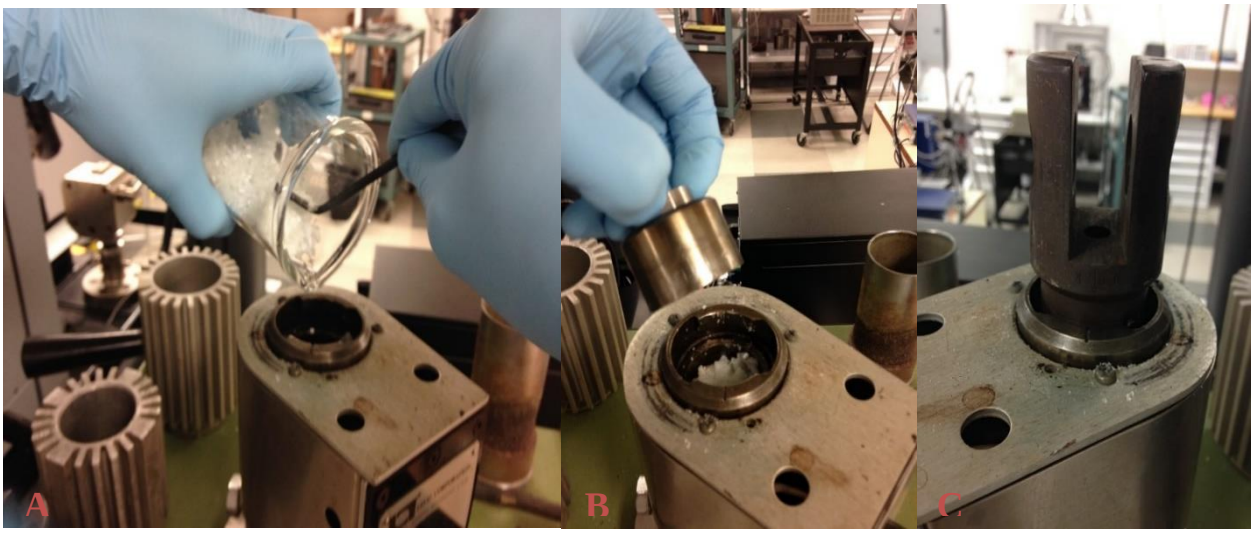

Figure 21. Pouring in of mixture into metallic tube (A). Locking, external die being place on top of cylindrical mixture to compress the mixture (B). Locking die turned to 'locked' position to ensure safe compression of materials (C).

die holder (it should not come out if locked in properly). At this point, the pressure should be raised to its maximum (4,000 psi with the given diameter of the locking die of 1.5 inches), and a crushing sound will be heard representing the densification of the mixed constituent materials with H2O. After this, the pressure and heating element should be maintained at its current position for approximately 180 minutes to ensure adequate heat transfer through the metallic tube and into the mixture to yield the best resulting mock PBX possible.

Stage 5: Solidification and Removal of Mock PBX Sample

The final steps which will be described next involve the solidification or cool down process, and the removal of the cylinder-shaped resulting mock PBX sample that has been manufactured. The first step of the solidification process is to turn off the electric heating element within the pneumatic press. Then the researcher should place the two heat sinks with finned exterior around the metallic cylinder, to increase the surface area and the overall heat transfer rate through natural convection 32]. This can be seen Figure 22. Due to the heat expansion coefficient of the metallic, cylindrical mold in which the mock PBX sample solidifies, the research team used experimental results (i.e., the process of removing the specimen) to conclude that the higher the temperature at which the sample is removed the less mechanical force it is required to remove accomplished, the fastening screw has be loosened in order to remove with the specimen inside using the appropriate wrench. After the mold is removed from the pneumatic press, the final step is to remove the mock PBX specimen from the mold (See Figure 23-A) , and this can be accomplished using a steel rod and a steel hammer to impact the upper, locking die with a downward force repeatedly to push down the mock PBX sample manufactured. The end product should come out of the metallic mold after several impacts (See Figure 23-B), so an absorbing layer of paper or plastic underneath the hammer is recommended to protect the integrity of the PBX sample. In other words, at higher temperatures, the expansion of the metallic mold allowed for a more straightforward removal of the PBX sample

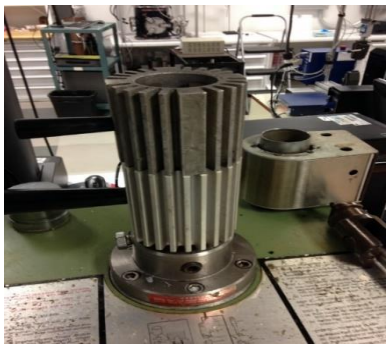

Figure 22. Heat Sinks applied over the metallic mold.

with less force and a reduced number of impacts of the steel rod and hammer that were used to push down the specimen and remove it). As a result, the recommended time to wait after the heater is turned off, is anywhere between 10-15 minutes (with the heat transfer through natural convection occurring between the heat sink and the air a room temperature in the low 20's). This should cool down the temperature of the exterior of the metallic mold to 50ºC- 60ºC, making it manageable with the use of the heat resistant gloves, which should be worn for the process of removal of the mock PBX sample. After this time range, and the user has ensured that the temperature of the mold is not high, the pressure using the RAM lever should be removed. This is in order to remove the die holder that would otherwise be pressed against and would be extremely difficult to remove. Then the die holder has to be turned to its "Open" position. An important note is that if the die holder is tightened very strongly then a metallic rod or wrench can be used in conjunction with the hammer to turn the die hold loose and then to its "Open" position. After this has been sample once it hits the ground. And finally, the locking die is removed using the exact same approach (See Figure 23-C), to prepare for the next manufacturing batch.

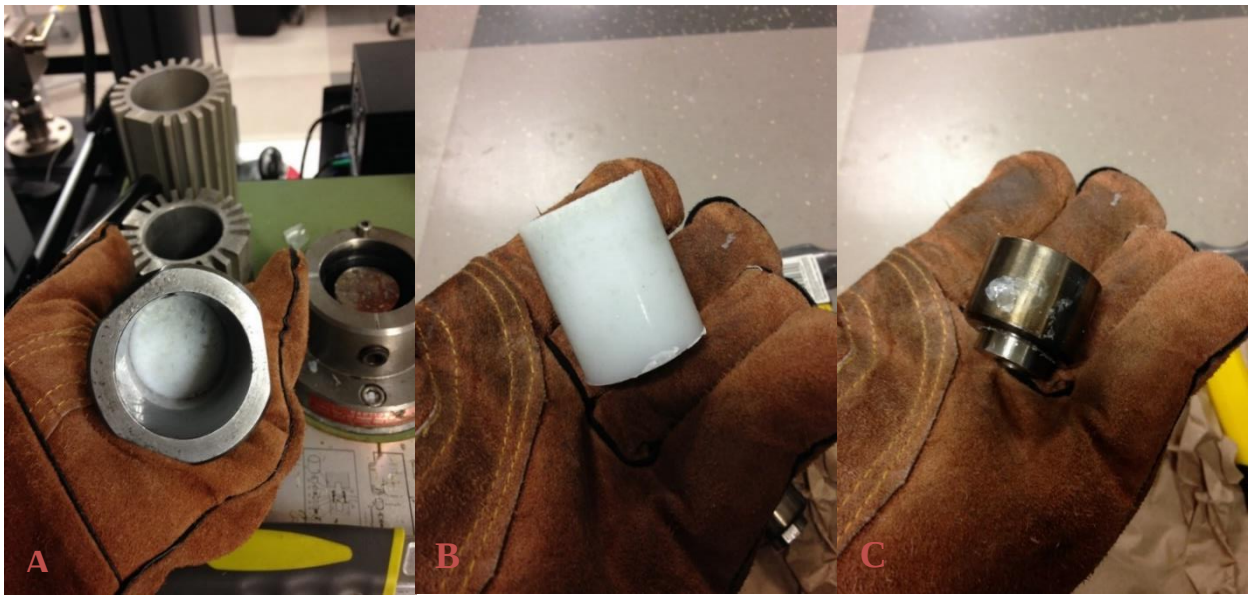

Figure 23. Mock PBX sample within the metallic mold (A). The mock PBX sample after removal from the mold (B), and the locking die as well (C).

Manufacturing Issues

Inadequate Mixing of Constituent Materials

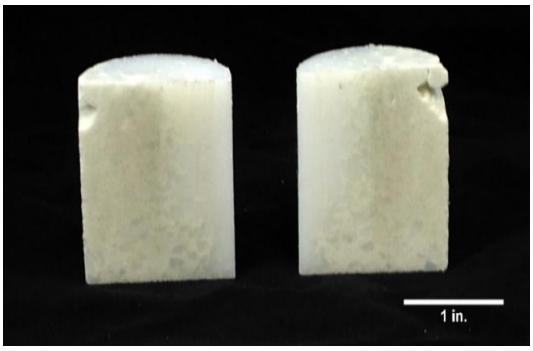

Figure 24. Several Defective PBX Samples Made with no amount of water.

The previously described and finalized novel process for manufacturing mock polymer-bonded explosives or its abbreviation PBX, was the end result of an experimental trial-and-error approach and the analysis of resulting specimens. Since the PBX specimen is supposed to be a heterogeneous particulate composite material, from the initial step of mixing the two constituent materials, High Impact Polystyrene and Soda Limes Glass beads, a great deal of attention was required. This is quite simply because the resulting mixture which would be later added to the cylinder lubricated with silicone release spray within the pneumatic press would largely determine the mixing interaction between the polymer pellets and the glass beads. Several mixing methods of the PBX component materials were at experimented with during the first trials. One method consisted of mixing the two materials in a beaker after being weighed individually and then proceeding to add the resulting mixture to the cylinder in the pneumatic press. Another method was adding each constituent material to the cylinder individually and then using the mixing stick to mix the materials into what should turn into a heterogeneous composite material that should, by definition, not be uniform throughout to resemble more closely an actual polymer-bonded explosive. Both of these mixing methods, however, yielded PBX specimens that revealed a fundamental issue with the process: the glass beads were not adhering to the polymer pellets adequately to stick to them once the polymer was melted. Therefore, the resulting solid specimens had clusters of pure soda limes glass that would not only fall off from the specimen easily and leave large voids on the surface, but were not yielding an acceptable heterogeneous composite material. Further analysis by cutting the PBX specimen revealed that these concentrations of soda lime glass beads were occurring on the inside, and overall these described mixing processes were deemed unsuccessful

in creating the desired heterogeneous composition of the mock PBX. An image of one of the specimens created using this ineffective method is depicted on Figure 24. On this image, it can be appreciated that the glass beads and the polymer are completely apart, and the mock PBX sample is not a good imitation of the actual heterogeneous particulate material, which does not have a definite, repeatable pattern but is instead mixed in a heterogeneous manner. It is also important to note, that the heating time was increased from the original 50 minutes that were calculated (using the arithmetically calculated rate of heat transfer from the metallic mold onto the PBX mixture, assuming a perfectly linear and constant rate of heat transfer for calculation purposes) to 90 minutes because the polymer pellets on the inside of the cut specimens near the center of the specimen were not melted and remained solid.

H2O Excess and Heating Time

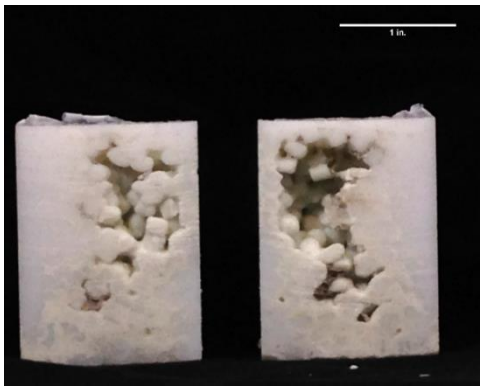

Figure 25. Interior Voids within Defective PBX Samples Made with 2 grams of H_2O.

The next development resorted to in an attempt to fix this issue was the addition of a small amount of water to the mixture of both materials before pouring it in the cylinder within the pneumatic press. At first, the amount of liquid H2O was arbitrarily selected to be 2 grams, resulting in a ratio of approximately one gram per 35 grams of the heterogeneous composite materials for every specimen. The ratio is described as approximately because the mass of the resulting specimens varied slightly from specimen to specimen, even while following the same process identically. this presumably due to losses of the aforementioned materials caused by sticking to the inside of the flasks during the weighing and mixing process, and to the cylinder surface during the heating and pressurization process. After going through the manufacturing process numerous times with the arbitrarily selected amount of H2 O of 2 grams, the resulting specimens showed a great improvement over the previous specimens that had no H2 O added to the mixture, but still had some deformations in the form of air voids on both the outer surface and on the inside of the mock polymer-bonded explosives. At

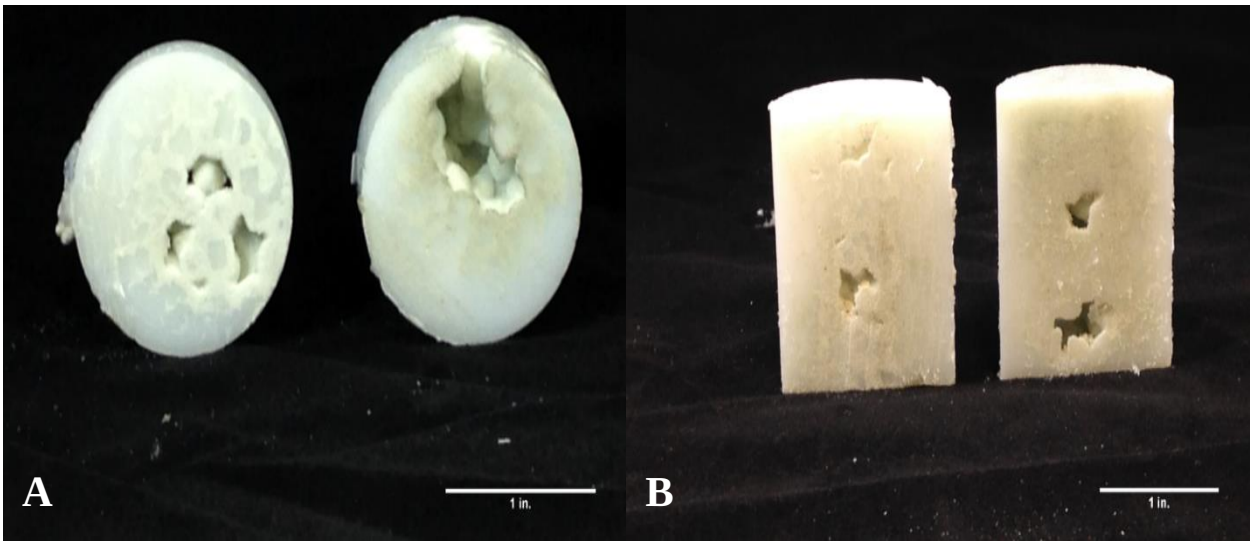

Figure 26. Inner Face (Left) and Top Face (Right) of a PBX Samples Made with 2 grams of H_2O (A) and the Inside of Another PBX Sample Made with 2 grams of H_2O (B).

the bottom of the previous page, on Figure 25, the interior of one of these aforementioned samples is shown. As it can be seen, these large voids make the sample impractical for mechanical testing purposes because the large size of the voids would greatly affect the results, since it would fail faster in any given test due to the lack of material. the heating time at this point of the manufacturing process remained at 90 minutes, since it consistently yielded higher-quality samples than before with only 50 minutes. The images of other samples with defects caused presumably by excessive water in the mixture are presented next, and one that shows the outer part, the top part in fact are presented below in Figure 26.

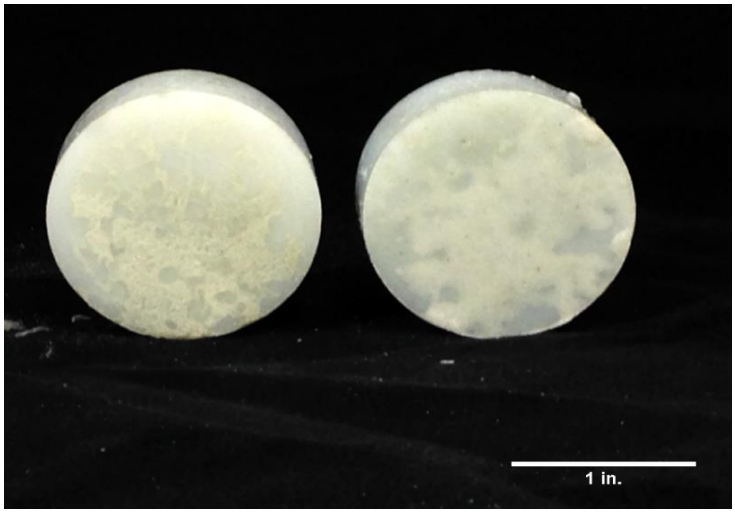

Figure 27. Outer Face (Left) and Inner Face (Right) of PBX Samples Made with .5 grams of water.

The meaningful conclusion from these defective specimens using 2 grams of water, and a heating time of 90 minutes, is that these voids were being caused by the water since the original specimens did not have these defects. The experimental results were analyzed and it was concluded that

there were trade-offs between the amount of water and the heterogeneity of the mixture. In other words, the amount of water improved the mixing of the polymer pellets and the glass beads, but resulted in large voids in the exterior and interior that made the specimens useless for the desired purposes. This could be attributed to a number of factors. Such as improper mixing of the component materials, resulting in clusters of glass beads that could fall off the specimen at the moment of impact when the specimen is removed from the cylinder. By inadequate pressure levels throughout the melting process, resulting in air gaps within the PBX specimen that remain after the cooling and solidification stage. The first parameter to be modified to further increase the quality of the mock polymer-bonded explosives, was the amount of water used due to indicative evidence. The rationale for this was that the amount of water in the mixture could be a factor in creating the air voids since 2 grams in significant enough that it was presumed that the physical change to its gaseous state could be modifying the PBX specimen as it is heated and when it is cooled down and solidifies. This could be explained in an alternative way that the liquid H2O turning into water vapor gains thermal energy and moves within inside the cylinder with the

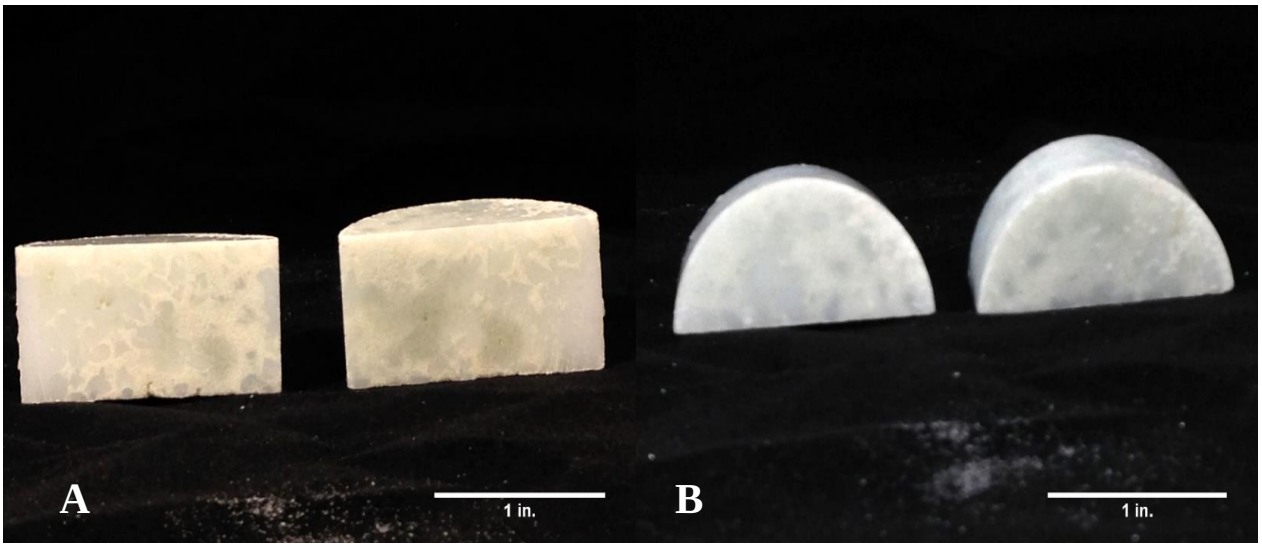

Figure 28. (A) Inner face (left) and top and bottom face (B) of a PBX Specimen manufactured with the finalized manufacturing process.

mixture and could create voids of air and/or H2O within the specimen that remain after the specimen solidifies and the water condenses and turns into liquid droplets.

The next measure taken was to experiment with lesser amounts of H2O to reduce the negative effects it appeared to be having on the quality of the specimens. The practical approach for this was to use the least amount of water possible in order to create the desired 'lumpy' texture of the glass beads in multiples of half a gram. The team discovered that half a gram of H2O was sufficient to create that required texture. Several mock PBX specimens were created with this process, yielding much higher-quality specimens overall. The reduced amount of water and the relationship to the increase of quality of the specimens presumably confirms that the amount of water was the likely responsible for the defects in earlier specimens. An example of this high-quality specimens produced can be seen on Figure 27. On this image, it can be observed how the mixture of the component materials has mixed enough resulting in great quality of heterogeneity of the mock PBX sample. The image also shows the outer face and the interior with a horizontal cut to view its inside. This method of manufacturing with a new fixed amount of water, lead to another parameter to adjust, the heating time. While overall good resulting specimens were manufactured with 0.5 grams of water and with a heating time of 90 minutes (such as the previous figure shown), some polymer pellets that had not melted properly near the center of the specimen (meaning that the heat transfer from the metallic mold was not occurring all the way through the center) and taking advantage of the fact that the heating process does not require any active supervision the heating time was doubled to the current ideal time of 180 minutes. Therefore, all of the specimens that were used for mechanical testing were manufactured and had these two parameters adjusted. Some of these high-quality specimens with the finalized parameters used are shown in Figure 28, in the next page. As it can be appreciated on the images of the same specimen, which were cut for the half-bending mechanical test, these samples are solid throughout

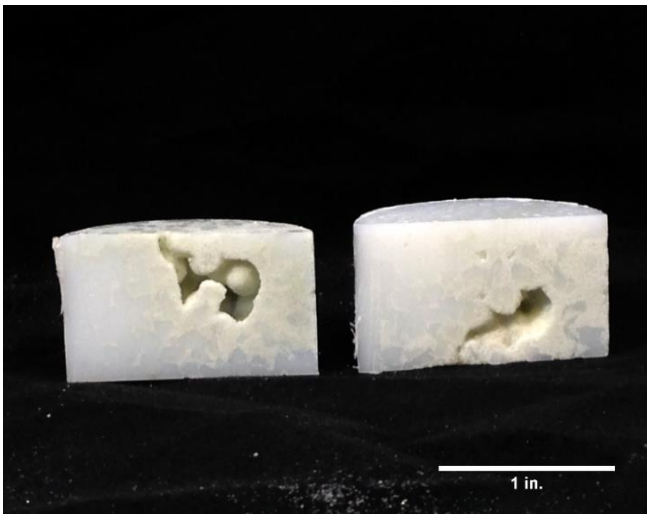

Figure 29. Voids Within Defective PBX Samples Made with Optimized Process.

and show a high-quality mixture of the constituent materials with one another, giving it a more realistic characterization of the real heterogeneous particulate composite energetic material that the research team is attempting to emulate to determine its mechanical behavior. It is important to disclose, that using this final manufacturing procedure with optimized parameters of H2O amount and heating time, some specimens manufactured had some internal vacancies even if the exterior looked neat. This ratio, however, was very small to the number of high-quality mock PBX samples that were produced using this method. A visual reference of such imperfect specimens can be seen to the right, on Figure 29. Another plausible explanation for this voids, is that at the time of using the abrasive cutter there was a concentration of soda lime glass beads in the region that was not coated by the polymer and simply fell off during the process. This theory also provides a possible explanation for the polymer pellets that did not melt, in correlation with the significant discrepancy thermal properties of both component materials. The material data sheets on these material types indicate that the thermal conductivity and specific heat of the polymer and the soda lime glass are quite different. The thermal conductivity of the soda lime glass beads is more than four times larger than that of the polymer, and the specific heat is 59% less than the specific heat of the polymer as well 3334], creating a less than ideal uniform heat transfer situation. In simpler terms, it means that the soda lime glass beads are better conducting the thermal energy while the mixture is being heated, but takes much longer to increase its temperature due to its higher specific heat. This in turn could resulted in polymer pellets that are isolated in clusters of soda lime glass beads and that do not receive enough heat conducted in their direction to melt as desired, explaining the internal voids in the manufactured specimens.

Amount of Component Materials

Another issue that was faced as the development of the novel PBX manufacturing process was the amount of component materials used; first it was opted for a mass-based composition to determine the ratio of each material in the mixture, the total weight had to be calculated based on experimental attempts and observations. For the most part, the problem that would occur would be when the material would overflow from the mold, and the upper locking die and the die holder could not be

properly attached, creating a mechanical hazard. The solution for this that the team figured out was to revise the amount, and after a repetition of attempts, the total mass ideal to yield the desired height (diameter of the specimen was constant) was reached at 70 grams.

Removing Specimen from Cylinder

Perhaps the least straightforward step during the manufacturing process was removing the mock energetic material specimen once it had cooled down and solidified. This step was simplified to the greatest extent possible by applying a lubricant, in this case Silicone Release Spray, to make the task of taking out the manufactured specimen less physically demanding. This step, still involved a significant amount of physical effort since a hammer and a solid, steel tube were used to impact the locking piece of the cylinder until the specimen could be taken out. It also presented unforeseen problems since the strenuous impacting of the cylinder would cause some areas with glass beads on the surface to fall off from the manufactured sample. Thus, rendering the specimen useless as it had too many surface defects and voids to be considered to yield reliable results during the mechanical tests. This problem really stems from the procedure in itself and it was not something that could be altered to improve the manufacturing results, other than ensuring that sufficient time was given to allow the PBX sample to cool down and solidify throughout.

Other Issues

Other non-systematic problems that were faced at least once during the manufacturing process and that were directly related to the equipment and process in itself involved the air pressure hose connected to the pneumatic press. As mentioned, this was not a problem with the procedure in itself but rather of the nature of the equipment being used. For example, the hose was disconnected due to improper moving of the pneumatic press causing it to be in an awkward position. In other cases, the pneumatic press, presumably due its use, did not maintain the maximum pressure required for the specimen to be

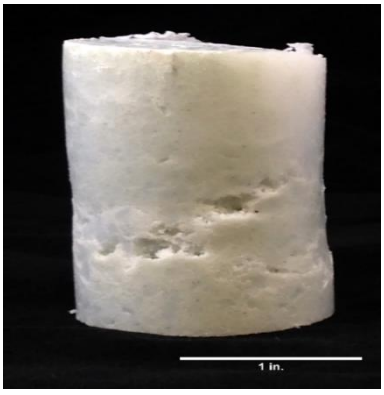

Figure 30. Flawed PBX Due to Pressure Failure.

compressed and yielded very porous specimens, one of which can be viewed on the right, on Figure 30.

SPECIMEN MACHINING

Machining Equipment

The detailed, technical specifications of the equipment utilized for the machining of the manufactured cylindrical-shaped, mock energetic materials into the required geometry required for the mechanical tests is given in Appendix 3.

Machining Process

To obtain the desired geometry on the manufactured PBX samples for the mechanical tests several different machining equipment were necessary. A full description of the machining equipment is found in Appendix C. The compression test did not required any mayor modification because the manufactured product was of a cylindrical nature, resulting in the desired geometry directly from the manufacturing process. The only necessary machining was to polish the specimen. The dimensions are further specified in the mechanical testing section along with its respective figures. Overall, however, the diameter remained constant for all machined specimens, except for the Bridgman Notch sample, which had a circular notch of .3 inch-diameter cut at the center (See Figure 31-Figure 32). For the bending and semi-bending tests, the abrasive cutter simply had to be used with care to make a clean cut, and result in the desired geometry (See Figure 27 for bending test or indirect tensile test geometry, and Figure 28 for semi-bending geometry test) each with its respective required thickness for valid mechanical testing results; and at the end, to remove any unwanted residues that might affect the test results in the form of surface roughness or extra materials that results from the abrasive cutting the polisher was used.

Bridgman Notch Procedure for Mock Polymer-Bonded Explosive

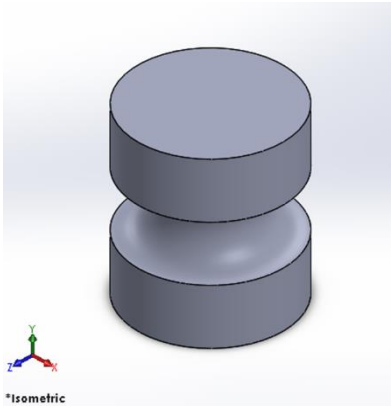

Figure 31.CAD Model of Bridgman Notch

Figure 32. Bridgman Notch Specimen.

The procedure followed to obtain the desired geometry on the polymer-bonded explosive required the use of a CNC lathe, and its software, along with the corresponding CAD drawing done in SolidWorks 2015. The CAD drawing of the model can be seen on Figure 31. Since Computer Numerical-Control (CNC) machines do not require much input during the actual machining process, the only task was to convert the CAD file into 'IGS' format to make it readable for the CNC software to process and perform the desired machining. The resulting and actual mock PBX sample is seen Figure 32, where it can be appreciated the high quality not only of the sample in itself, but of the cut performed by the CNC Lathe. It is important to repeat that the height of this Bridgman Notch Test mock polymer-bonded explosive is the same as the original manufactured cylindrical explosive, and only had a semi-circular notch cut into it with a radius of .30 inches right at the center of the specimen in the vertical direction. More details about the equations utilized for this are given in the mechanical testing section.

MECHNICAL TESTS

MERG performs several distinct mechanical tests on a variety of materials. Currently, the group is conducting tests on HPCs, steels, and additively manufactured polymers. Our mechanical testing involves the use of Universal Testing Machines (UTMs). These machines are designed to measure the mechanical response of diverse materials when subject to mechanical loads. The outcomes are the mechanical properties of materials. They can perform several ASTM International standardized tests including but not limited to: tension wedge, tensile threaded, compression,

spherical seat compression, three- and four-point bending, shear, compact tension, punch, etc. The only limited factors are the availability of appropriate grips, load cells, and displacement measurement devices. All tests must be performed according to ASTM International standard in order to be viable for publication. Tests that are not according to ASTM International standard are not performed by MERG, unless they involve materials and processing yet to be standardized by the relevant ASTM international committee. So far, no test of that nature have been performed or are planned by MERG. Students conducting these tests are required to wear several personal protective equipment including: lab coats, closed toe shoes, EN 166 compliant eye protection, and ear protection (for tests that produce audible acoustic emissions, none so far). A detail description of each UTM and examples of the mechanical testing capabilities of MERG are located below in Table 4. All tests were performed using a universal testing machine, Instron 5969 Tabletop Universal Testing System.

Instron 5969 Tabletop Universal Testing Systems 	5969 Dual Column Tabletop Testing Systems are universal, static testing systems that perform tensile and compression testing; also perform shear, flexure, peel, tear, creep, cyclic, and bend tests.. Typically used for plastics, metals, rubber materials, automotive components, composites, and non-ambient temperature applications. • ±50kN Load Cell • 1/2"-20 Threaded Self-Aligning Tension Grips • 6” compression platens • 3+4 point bending test fixtures • Instron T3119-600 environmental chamber (-150°C to +350°C) • Synchronized with Vic-3D DIC System Product Link: http://www.instron.us/wa/product/5960-Dual-Column-Testing-Systems.aspx

ADMET eXpert 5600 Series UTM 	Highly configurable 5603 Universal Test System with MTESTQuattro Controller. A dual column frame for extended horizontal test space capable of performing tension, compression, and bending tests. While the 5000 series testers are highly configurable, they maintain their rigidity and precision needed for precise control. • ±4.5kN Load Cell • 5kN 10mm Wedge Grips • 5kN 56mm Compression Platens • Detachable Actuator • Synchronized with Vic-3D DIC System Product Link: http://admet.com/products/universal-testing-machines/expert-5000/
Correlated Solutions Vic-3D Digital Image Correlation System 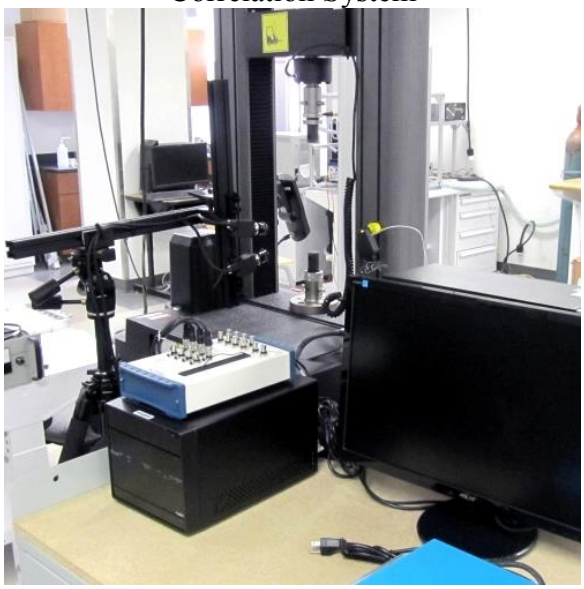	Vic-3D provides full-field, 3-Dimensional measurements of shape, displacement and strain, based on the principle of Digital Image Correlation. Using this method, actual object movement is measured and the Lagrangian strain tensor is available at every point on the specimen's surface. Vic-3D can measure arbitrary displacements and strains from 50 microstrain to 2000% strain and above, for specimen sizes ranging from <1mm to >10m. • Synchronized with UTMs • Two 2.0 Megapixel Digital Cameras (1624 x 1224 @ 30 fps) • Fulcrum Software for vibration or fatigue synchronization Product Link: http://www.correlatedsolutions.com/vic-3d/

Table 4. MERG Testing Equipment

Overview

The mechanical properties of PBX subject to various loading conditions is important to avoid the risk involved in the manufacture, storage and transportation of these energetic materials [35, 8]. Direct tensile test is the most conventional test to measure tensile properties. However, for brittle materials, the direct tensile test is inconvenient due to difficulties in specimen preparation and test operation [36]. Uniaxial compression tests, full-Brazilian tests and semi-circular tests are the common alternatives for measuring tensile properties of brittle materials. Applied load, strain rate, and deformation are the raw data generally collected from experiments for post-processing to characterize the material properties. Optical techniques of measuring deformation during mechanical testing has become popular instead of strain gauge measurement. Strain gauges attached to the specimen and give a measure of the deformation between two points and may provide local reinforcement due to the contact with the specimen. On the other hand, digital image correlation (DIC) compares images captured before and after the test without contact with the specimen [38]. A micro-scale level of deformation analysis can be recorded using DIC [35]. Rae et al. [37] have applied the DIC technique to determine microscopic displacement and strain fields of PBX during Brazilian disc test. Zhou [39] used DIC to calculate strain fields and analyze micro-scale deformation and fracture behavior of a PBX simulant under tensile stress. Zhou and colleagues have applied DIC to study the quasi-static compression deformation and fracture behavior of PBX [39]. Later, Zhou and colleagues applied DIC to obtain dynamic deformation information of Brazilian disc tests (BDT), flattened Brazilian disc (FBD) tests and semicircular bending (SCB) tests [39].

Multiaxial response of material is another important mechanical property. Test under uniaxial loading on Bridgman notch specimen can emulate multiaxial load phenomena [40, 41]. Under uniaxial loading the radial deformation resistant produces by the notched bar develops the state of triaxial stress thus emulates the study of discontinuous shaped components under triaxial stress conditions [42].

The subject material in this study is a complex composite of glass beads in a polymer matrix. Crystal properties such as size, distribution, and weight compositions; and binder property such as elastic-plastic behavior affects the performance of the composite [43]. Interfacial properties such as surface energy, interfacial strength, and glass beads-polymer intermixing control the small scale mechanical behavior influencing the block properties [43, 44]. In this study uniaxial compression test, indirect tension test, semicircle bending test and Bridgman notch specimen test will be performed. In this section, a description of each test will be provided with a discussion of test standards, equations used for analysis, test conditions, the raw data to be collected, and any non-conformity criteria.

Uniaxial Compression Test

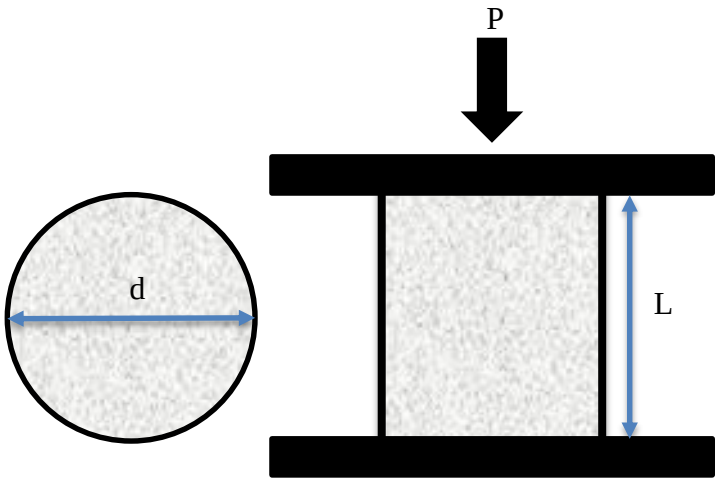

Figure 33. Uniaxial compression test configuration

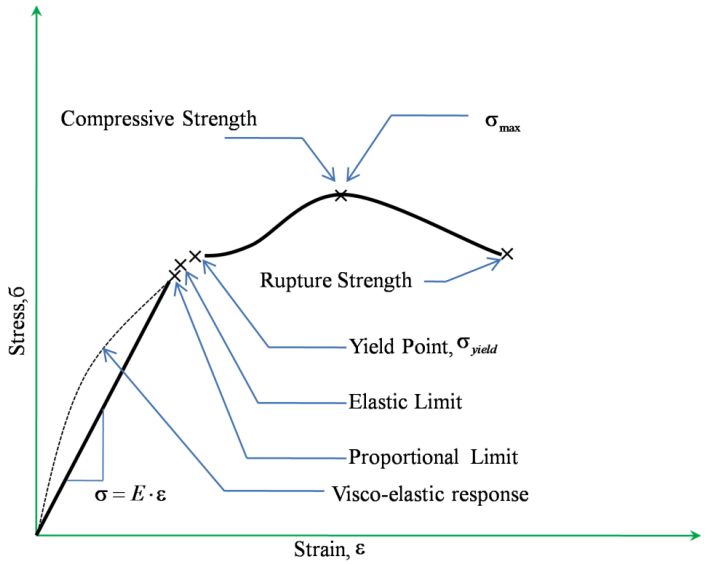

Figure 34. Typical Stress-Strain curve

Glass beads- polymer composite may exhibit viscoplastic behavior. During deformation viscoelastic material undergoes viscous and elastic behavior. Models for viscoelastic materials stress-strain behavior is different than that of elastic material. Maxwell model, Kelvin-Voigt model, and the standard linear solid model are used to predict viscoelastic material response under different loading conditions.

Uniaxial compression is important to study the yield properties of glass beads-polymer matrix. Direct tensile test is not suitable for this type of material. This is due to the comparative high tensile stress of the complex composite such that fracture occurs prior to macroscopic yield [38]. A compressive load is applied along the centerline of the specimen till fracture [Figure 33].

Usually compressive properties are expressed per unit of minimum original cross sectional area [ASTM D695-10]. Most of the compressive properties can be found in typical stress-strain curve [Figure 34]. According to ASTM D695-10, compressive strength is the maximum compressive stress (σ_{max}) carried by the specimen during the compression test,

$$\sigma_{max} = \frac{F_{max}}{A_i} \qquad (1)$$

Where A_i is the initial cross-sectional area and F_{max} is the maximum applied compressive load. The compressive yield strength is the yield load required per unit initial cross sectional area.

The first point on the strain-stress diagram where an increase in strain is visible without an increase in stress is defined as compressive yield point. Brittle material may not exhibit a yield point.

$$\sigma_{com,yield} = \frac{F_{yield}}{A_i}, \quad \frac{\partial \sigma}{\partial \varepsilon} = 0 \qquad (2)$$

Nominal longitudinal strain is a dimensionless parameter defined as the deformation per unit initial length.

$$\varepsilon_{n,l} = \frac{l - l_0}{l_0} \qquad (3)$$

Where, l is the final length and l_0 is the initial length of the specimen.

The relation between true strain and the nominal longitudinal strain is defined as follows

$$\varepsilon_{t,l} = \ln(1 + \varepsilon_{n,l}) \qquad (4)$$

The Poisson ratio is obtained by dividing the nominal longitudinal strain by the true strain.

$$\upsilon_n = -\frac{\varepsilon_{n,l}}{\varepsilon_{t,l}} \qquad (5)$$

Modulus of elasticity is obtained by the ratio of stress to the corresponding strain below the proportional limit of the material.

$$E = \frac{\sigma}{\varepsilon} \qquad (6)$$

Materials may exhibits viscoelastic deformation upon loading. Maxwell, Kelvin-Voigt, standard linear model can be used to accommodate viscoelastic response of the subject material.

To assess the repeatability and reproducibility of the experiment, multiple test must be performed. Standard deviation can be calculated using the following equation

$$s = \sqrt{(\sum X^2 - n\bar{X}^2) / (\mathrm{n}-1)} \qquad (7)$$

Where X is the value of single observation, $\bar{X}$ is the arithmetic mean of all observations, and n is the number of observations.

Test conditions

Load is applied at a constant deformation rate on the specimen. According to ASTM D695-10 the standard speed of the uniaxial compression test shall be (1.3 ± 0.3) mm/min for rigid plastics including high modulus composites. The standard preferred specimen size for a right cylinder is 12.7 mm diameter by 24.5 mm height. Colak has conducted uniaxial compression test on PBXW-128 at a strain rate of 0.01/sec. PBXW-128 is a soft, rubbery solid comprised of approximately 60% by volume HMX powder in a polymer binder. Zhou and colleagues [39] conducted uniaxial compression test on plastic bonded explosive (PBX) samples with aspect ratios of 1.8, 2.0 and 2.3, at a speed of 0.1 mm min^{-1}. Jerabek and colleagues [46] have suggested that for a right cylinder the dimensional ratio should range $1.5 < l/d < 2$ to avoid buckling, barreling, and friction effects. In the current study

- Dimensions, diameter (d) and height (L)
- Specimen Aspect ratio: $1.5 < l/d < 2$
- Test speed: 0.14 mm/min

Raw data collection

Instron 5969 Tabletops Universal Testing System can record load, crosshead displacement and time. The specimen dimension have to be measured before testing. From these data sets the compressive properties can be calculated. Beside this data collection, a 3D DIC analysis will provide the Poisson ratio and better understanding of compression properties.

In the current study the report contains

- Compressive Stress-Strain curve.
    - Compressive strength σ_{max}
    - Compressive yield strength, $\sigma_{com,yield}$
- Poisson ratio, υ_n
    - Nominal longitudinal strain, ε_l
    - Nominal transverse strain, ε_t

Non-conformity criteria

Figure 35. Quasi Static Uniaxial compression

The material may be prepared by compression or injection molding of the material to be tested. Careful machining is required to ensure a smooth surface. The contact between the compression plate and specimen surface is very important. Friction at the contact surface may lead to a multiaxial stress state and specimen barreling. Use of PTFE (poly-tetrafluoro-ethylene) lubricant or tape is common to avoid friction at the contact surface [45, 46]. The specimen center line is aligned with the center line of the compression plate, and the specimen is parallel with the surface of the compression plate. A misaligned specimen surface and compression plate may generate nonlinear force-displacement curves [46].

Indirect Tensile (Brazilian) Test

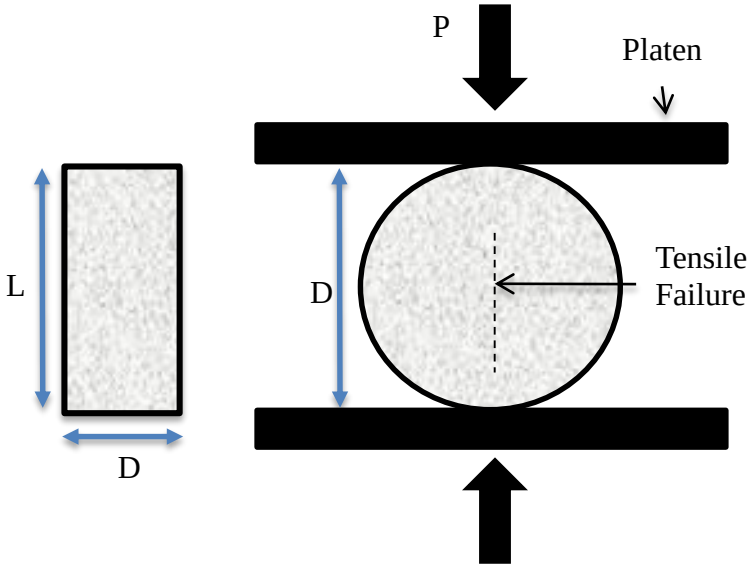

Figure 36. Indirect tension test configuration

In the Brazilian (indirect tensile) test, a disc of material is subjected to two opposing normal strip loads at the disc periphery [Figure 36]. Brazilian test is suggested method for determining the

tensile strength of brittle material like concrete [47]. However, indirect compression test is also a common practice for studying the deformation and fracture behavior PBX simulant material [8]. The analytical solutions to the stress field during Brazilian tests founded [48-52] formulated stress on the axis of the circular cross-section as follows:

$$\sigma_{xx}(x,0)=\frac{2\cdot P}{\pi aL}\left[\frac{(1-\bar{x}^2)\mathrm{Sin}\,2\alpha}{1+2\bar{x}^2\cos 2\alpha+\bar{x}^4}-\tan^{-1}\left(\frac{1-\bar{x}^2}{1+\bar{x}^2}\cdot\tan\alpha\right)\right] \tag{8}$$

$$\sigma_{yy}(x,0)=-\frac{2\cdot P}{\pi aL}\left[\frac{(1-\bar{x}^2)\mathrm{Sin}\,2\alpha}{1+2\bar{x}^2\cos 2\alpha+\bar{x}^4}-\tan^{-1}\left(\frac{1-\bar{x}^2}{1+\bar{x}^2}\cdot\tan\alpha\right)\right] \tag{9}$$

$$\sigma_{xx}(0,\mathrm{y})=\frac{2\cdot P}{\pi aL}\left[\frac{(1-\bar{y}^2)\mathrm{Sin}\,2\alpha}{1+2\bar{y}^2\cos 2\alpha+\bar{y}^4}-\tan^{-1}\left(\frac{1+\bar{y}^2}{1-\bar{y}^2}\cdot\tan\alpha\right)\right] \tag{10}$$

$$\sigma_{yy}(0,\mathrm{y})=-\frac{2\cdot P}{\pi aL}\left[\frac{(1-\bar{y}^2)\mathrm{Sin}\,2\alpha}{1+2\bar{y}^2\cos 2\alpha+\bar{y}^4}-\tan^{-1}\left(\frac{1+\bar{y}^2}{1-\bar{y}^2}\cdot\tan\alpha\right)\right] \tag{11}$$

P is the applied load, L and R is the length and radius of the cylinder, 2α is the radial angel, $\bar{x}=x/R$ and $\bar{y}=y/R$. Stress at any point along the axis can be determined using these aforementioned equations [Figure 37].

Indirect tensile strength can be calculated using following equation

$$\sigma_{in}=\frac{2P_{\max}}{\pi\cdot(\mathrm{D}\cdot L)} \tag{12}$$

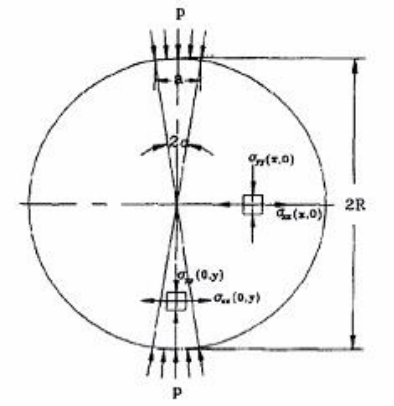

Figure 37. Indirect compression test

Testing conditions

According to TEX-226-F and ASTM D6931 the test deformation rate for bituminous mixture is 50 ± 5 mm/min at temperature of 25°C. Chen and colleagues [8], has conduct indirect tension test on PBX simulant material at 0.05 mm/min. It is suggested that the surface in contact with the specimen needs to be machined to the curvature of the test specimen. Liu [53, 8] has stated that a flat loading surface can be used for indirect tensile test. It is shown that for a contact angle ranging from $0^\circ \le 2\alpha \le 15^\circ$ the displacement profile change is negligible. In this study, a flat loading surface is used.

According to TEX-226, for a specimen of 4 inch diameter the core height should be 1.5 inch and for a specimen of 6 inch diameter the core height of 2 inch is recommended. ASTM D6931 recommended that the minimum height of the specimen should be at least half of the diameter. The length of the loading strip shall exceed the length of the specimen. $D/t \ge 2$. Chen and colleagues [8] has conducted Brazilian test on PBX simulant material of 20 mm diameter and 8 mm thickness of dimension at 0.05 mm/min strain rate.

In this study

- Specimen Aspect ratio:
- Test speed: 0.05 mm/min

Raw data collection

Instron 5969 Tabletops Universal Testing System can record load, crosshead displacement and time. The specimen dimension have to be measured before testing. From these data sets the compressive properties can be calculated. Beside this data collection, a 3D DIC analysis will provide the Poisson ratio and better understanding of compression properties.

Instron 5969 Tabletop Universal Testing System can register load with corresponding time increase. The specimen dimension have to be measured before testing. From these data sets the required indirect tensile strength can be calculated. Beside this data collection, a 3D Digital Image correlation analysis will provide better understanding of this properties.

- Dimensions, Length, and diameter.
- Indirect tensile stress, σ_{in}

- Poisson ratio, υ_n
    - Nominal longitudinal strain, ε_l
    - Nominal transverse strain, ε_t

Non-conformity criteria

Figure 38. Indirect Tensile (Brazilian) Specimen before Speckle pattern.

It has been observed that tensile strength obtained by Brazilian test may be lower than the direct tensile test. Yu and colleagues [47] has suggested that this is due to the compressive stress opening vertical microcracks thus failure occurs at a slightly lower (around 11% reduced) tensile stress.

Semi-Circular Bending (Half Brazilian) Test

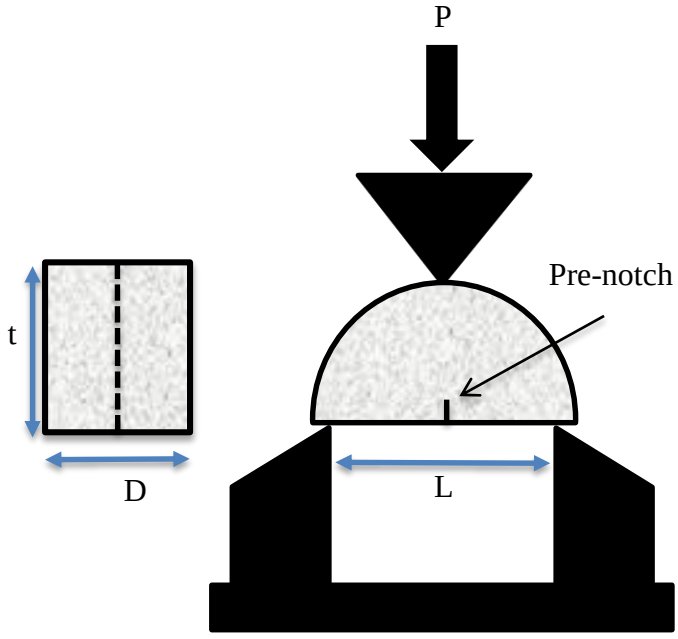

Figure 39. Semi-circular bending test configuration

Materials with weak tensile properties can be tested using the semi-circular bending test [Figure 39] to induce tensile fracture 8]. It is suggested that semi-circular bending test (SCB) can be used as alternative to the Indirect tensile test [54]. SCB tests can also be used to calculate fracture energy, G_f . Fracture energy is defined as the energy required to create a unit surface area of a crack [AASHTO]. The fracture energy can be used as an index parameter to identify mixtures with increased fracture resistance.

The tensile stress at the notch of the lower surface can be calculated as follows [49]

$$\sigma = \frac{3PL}{2th^2} \tag{13}$$

Where, P is the load, L is the spacing between the supports, t is the thickness of the specimen, and $h = D/2$ is the height of specimen.

The fractural resistance, J_c can be calculated from the following equation

$$J_c = -\left(\frac{1}{t}\right)\cdot\frac{dU}{da} \tag{14}$$

Where a is the notch depth, and U is the strain energy to failure. This strain energy can be determined from load versus deformation curve [54].

The fracture toughness can be determined by using following equations [8]

$$K_{IC} = \frac{P_c\sqrt{\pi\cdot a}}{D\delta}Y_k \tag{15}$$

Where, where P is the applied force, D is the diameter of the SCB specimen and δ is the thickness. Y_k is the dimensionless stress intensity factor.

The fracture energy can be calculated by dividing the work of fracture by the ligament area:

$$G_f = \frac{W_f}{A_{lig}} \tag{16}$$

Where G_f is the fracture energy (J/m^2), W_f is the work on fracture defined as the area under the load verses load line displacement curve defined as $W_f = \int P du$. P is the applied load and u is

the load line displacement. A_{lig} is the ligament area defined as $A_{lig} = (r-a)\cdot t \ \ mm^2$ and r is the specimen radius[AASHTO].

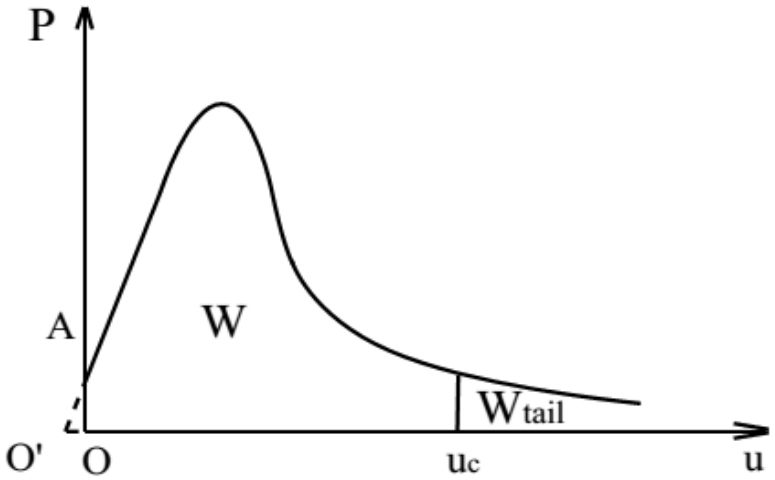

Figure 40. Expected Load versus displacement curve

The work of fracture is the area under the load verses the displacement curve.

Testing conditions

Wu et al has conducted SCB test on asphalt at 25°C at a deformation rate of 0.5 mm/min. AASHTO standard also suggest the same rate of 0.5 mm/min for asphalt mixture. Each semi-circular specimen contains a notch along the symmetrical axis. It is a common practice to use different notch depth with a fixed notch thickness. According to AASHTO/ASTM 1559 the semi-circular specimen is to be 150 mm diameter and 57 mm of height with the notch width of 3.0 mm. It is suggested that three nominal notch depth of 25.4 mm, 31.8 mm, and 38 mm with tolerance of can be used. AASHTO have suggested a different deformation rate of 0.0005 mm/s to calculate fracture energy. And the suggested dimension is 150 mm diameter with thickness. According to AASHTO for an asphalt specimen with diameter of 150 mm the span between the lower supports is 120 mm. In this study the diameter of the specimen is 38 mm and the space between the supports is 30 mm.

In this study

- Specimen is of 38 mm diameter and 19 mm of height.

- Test speed: 0.047 mm/min
- Space between the supports 30 mm.

Raw data collection

Before the test is carried out, is necessary to first measure the room temperature and the dimensions of the specimen. During the test time increase, the corresponding load and the deformation data is collected. Instron 5969 Tabletop Universal Testing System can register this data points automatically given the time step. According to AASHTO the test report should include mainly the fractural resistance, with mean value and standard deviation.

- Dimensions of the specimen, *h* and *t*
- Ligament area, $A_{lig} = (\mathrm{r} - \mathrm{a}) \cdot \mathrm{t} \quad mm^2$
- Spacing between the supports, *L*
- Maximum applied load, *P*
- Notch depth, *a*

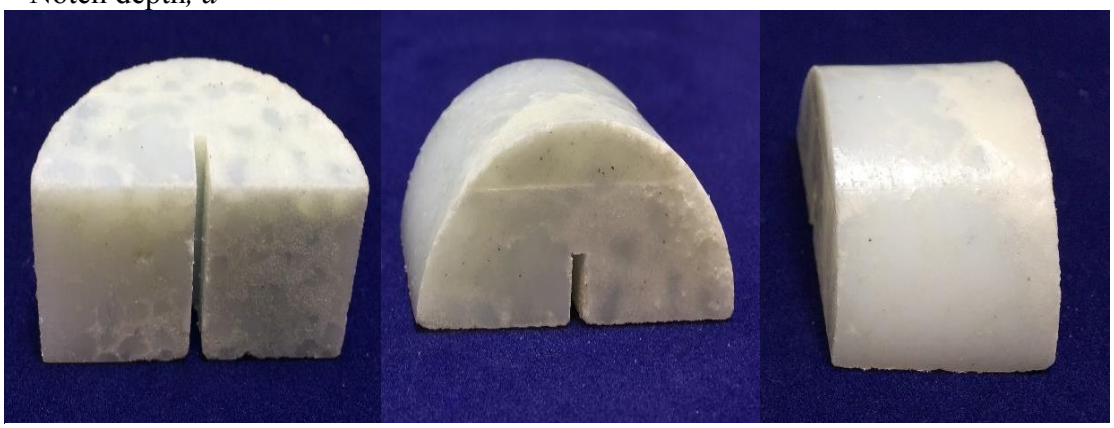

Figure 41. Semi-circular (Half-Brazilian) testing Specimen

Bridgman Notch Test

Bridgeman notched specimen [Figure 42] is used to study triaxial stress condition and damage progression in subject material. Stress triaxiality is a key parameter controlling the fracture strain [55]. The stress and strain distribution of the specimen around the minimum cross-section area is analytically derived by Bridgman [56-58]. This distribution is given as a function of the tensile load acting on the bar, the neck diameter, and the radius of curvature of the neck profile at its root.

Upon uniaxial loading at the remote end, a triaxial state of stress is developed at the notched area. The triaxiality is maximum at the axis of the bar [56]. It is assumed that controlled triaxiality state of stress can be generated by means of artificial neck, and Bridgman notched specimen became popular in fracture mechanism study, determining influence of triaxiality stress on strain and fracture toughness. For the triaxial or 3D conditions the stress state is defined as shown in Figure 43.

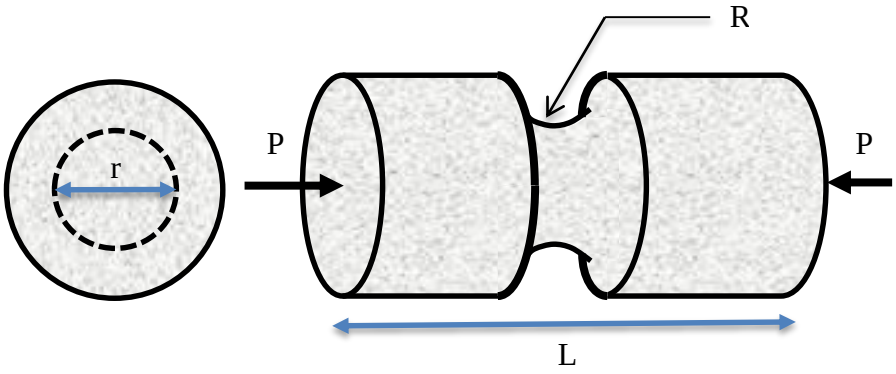

Figure 42. Bridgman notched testing configuration

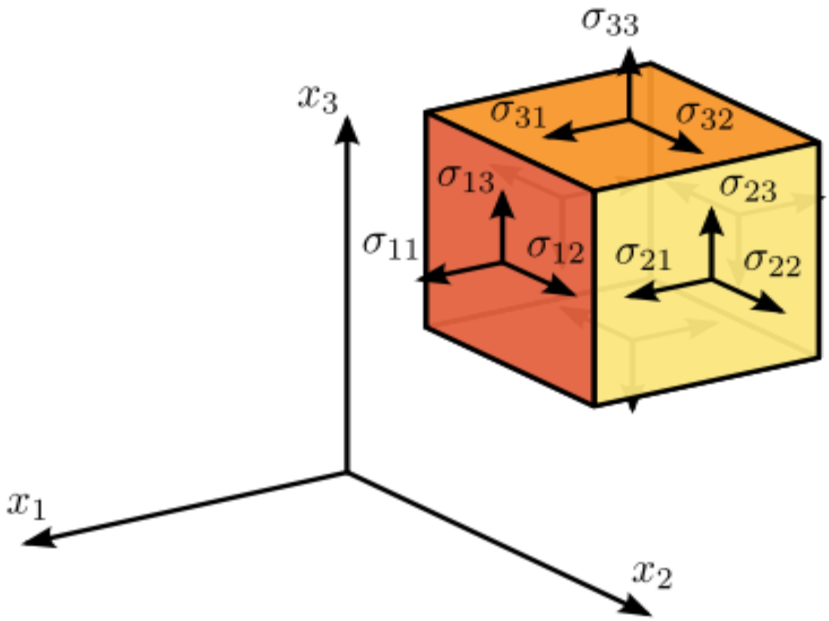

Figure 43. Characterizations of 3D stress state

A stress field in 3D space is defined as [**Figure 43**]

$$\bar{\sigma} = \begin{bmatrix} \sigma_{11} & \sigma_{12} & \sigma_{13} \\ \sigma_{21} & \sigma_{22} & \sigma_{23} \\ \sigma_{31} & \sigma_{32} & \sigma_{33} \end{bmatrix} \tag{17}$$

Assuming material model is isotropic, material model can be formulated in terms of three invariant of stress tensors [55-59]

Hydrostatic stress *p*, and von misses stress *q*

$$p = -\sigma_m = -(\sigma_1 + \sigma_2 + \sigma_3)/3 \tag{18}$$

$$q = \sqrt{(\frac{1}{2}[(\sigma_1 - \sigma_2)^2 + (\sigma_2 - \sigma_3)^2 + (\sigma_3 - \sigma_1)^2])} \tag{19}$$

σ_1 , σ_2 and σ_3 are the principal stress assuming $\sigma_1 \geq \sigma_2 \geq \sigma_3$. A dimensionless hydrostatic pressure/ stress triaxiality parameter (η) has been used in literature [59-61].

$$\eta = \frac{-p}{q} \tag{20}$$

Bai [59] used a third invariant of stress tensor in Bridgman notch specimen as follows

$$r = \left[\frac{27}{2} (\sigma_1 - \sigma_m)(\sigma_2 - \sigma_m)(\sigma_3 - \sigma_m) \right]^{1/3} \tag{21}$$

Using this invariant Bai used another important parameter is Load angel θ which is related to the third deviatoric stress invariant ξ.

$$\xi = \left(\frac{r}{q} \right)^3 = \cos(3\theta) \tag{22}$$

The range of Load angel is $0 \leq \theta \leq \pi/3$, and the range of ξ is $-1 \leq \xi \leq 1$. These parameters can be related through following relation assuming plane stress condition (σ_3) [59,62]

$$\xi = \cos\left[\frac{\pi}{2}(1 - \bar{\theta}) \right] = \frac{27}{2} \cdot \eta \cdot (\eta^2 - \frac{1}{3}) \tag{23}$$

It is suggested that for Bridgman notched specimen the expression for stress triaxiality and Load angel as follows [59,58]

$$\eta = \frac{1}{3} + \ln(1 + \frac{r}{2R}), \quad \theta = 1 \tag{24}$$

R is the radius of the notch and r is the radius of a round bar at the notch. And the equivalent strain to fracture can be calculated as

$$\bar{\varepsilon} = 2\ln\left(\frac{r_0}{r}\right) \tag{25}$$

r_0 is the radius of initial minimum cross-section of r.

Testing condition

In this study

- Specimen is of 38 mm diameter and 45.72 mm of height.
- Test speed: 0.11430 mm/min

Raw data collection

Before the test the room temperature and the dimensions of the specimen is to be measured. During the test time increase, the corresponding load and the deformation data is to be collected. Instron 5969 Tabletop Universal Testing System can register this data points automatically given the time step.

- Force, F
- Stress, σ
- Displacement

Often Bridgman specimen test results are used in finite element calculation to analyze the triaxiality state of stress.

Nonconformity criteria

It is assumed during analytical derivation that the axial strain rate is uniform at the minimum cross-sectional area [56]. A uniform deformation rate during the test will conform to the assumption and derived formulation can be used.

Effect of triaxiality: Due to triaxiality of stress material may go plastic strain before ductile failure occurs

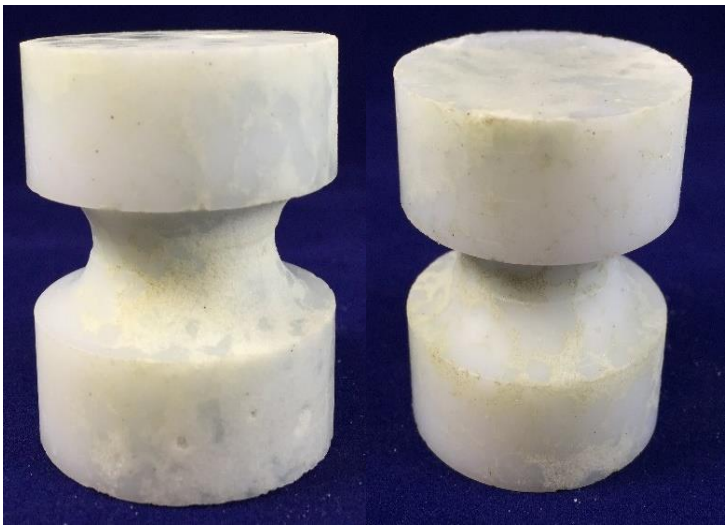

Figure 44. Bridgman Notch Testing Specimen

DIGITAL IMAGE CORRELATION (DIC)

Digital Image Correlation Overview

Digital Image Correlation (DIC) refers to the application of non-contacting two-dimensional and three-dimensional image correlation methods that acquire images of an object or specimen, store images in digital form and perform analysis to extract full-field shape, deformation and/or motion measurements [63]. A digital image correlation technique will be applied to each of the mechanical tests presented in the present work, to measure the out of plane effects, surface displacements, and strain fields on each specimen geometry. The used equipment is a Correlated Solutions VIC-3D DIC system which performs in-site measurement of the surface displacement and strain fields on specimen during mechanical testing using the three-dimensional digital image correlation technique. Three-dimensional digital image correlation is a modern optical measurement technique that allows for full-field and non-contact shape, displacement, and strain measurement of the surface of objects. Two carefully aligned and calibrated cameras allow for in-plane and out-of-plane displacement to be recorded at the micron level. In the DIC technique, displacements are measured by correlating "physical distance" to "pixel distance." A black speckle pattern on a white background is required, this is because the black speckles represent nodes in a mesh used to calculate displacement and strain. The outcome are displacement fields that can be converted though a finite element mesh into contours of surface strain. Such contours include: normal and

shear terms, principal strains, equivalent strains, and Poisson's ratio. Measurements of the surface crack length will be recorded using 3D-DIC (post processing software). As this is a passive system that requires only cameras and appropriate lighting, the Test Procedure and Approval document focuses on speckle pattern disposition, trip hazards, and proper operation to prevent damaging hardware. Examples of the images of DIC results in different materials and geometries are presented in Figure 45.

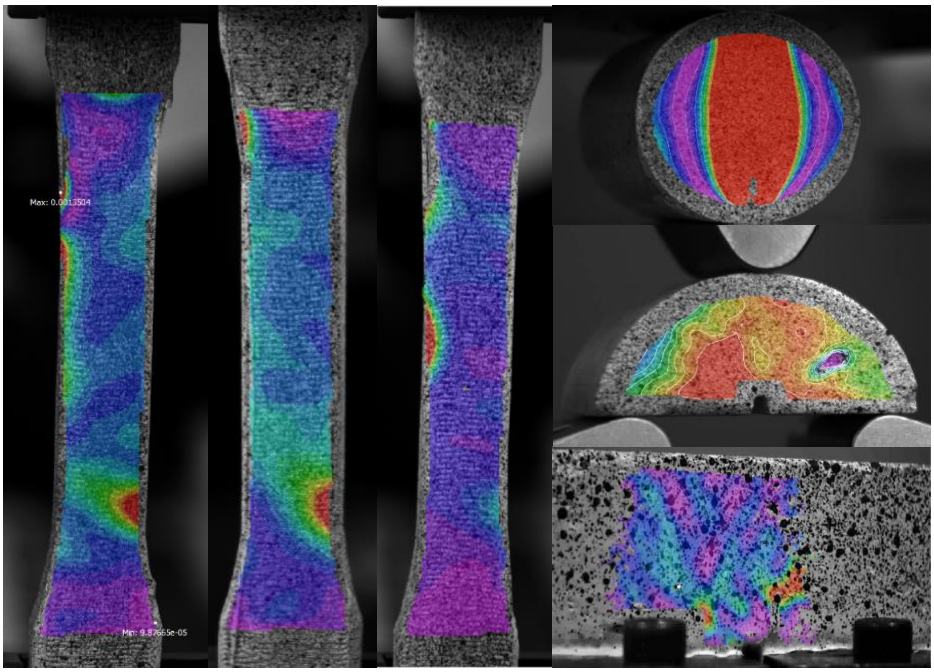

Figure 45. Digital Image Correlation Contours Examples

Introduction

Digital Image Correlation referred to as DIC in this report from this point on, is used among other non-contact methods to measure the mechanical response of a material [64-65]. The DIC method has seen a rise in popularity due to its advantages, which include simple setup and specimen preparation, low requirements in measurement environment, and its ability to measure the strain field over a large area [65-66]. It has particularly gained recognition in the field of experimental mechanics, in which it is used to obtain strain and displacement measurements [66-72], operating under the crucial supposition that no cracks appear in the area analyzed during the deformation process [71]. Studies have further solidified the validity and accuracy of the results produced by

DIC methods when used properly [71-73]. The DIC technique has also previously been applied effectively to particulate composites and used to predict fracture behavior [68]. The DIC operates on basic, theoretical pinhole image equations, and can used for a two-dimensional analysis with a one-camera setup, considering only in-plane deformation, or a three-dimensional examination using two cameras (stereovision) that also accounts for out-of-plane deformation [8]. Therefore, the 3D DIC method (also called digital image stereo-correlation technique (DISC) [74]) holds an important advantage over its 2D counterpart in that it detects and measures planar translation, out-of-plane translation, and out-of-plane rotation [72]. In practice, the investigator is obligated to use the 3D DIC if the test is on a curved surface or if significant 3D deformation occurs [66]. In reality, however, out-of-plane motions are practically unavoidable due to factors such as Poisson's Effect, bending of the specimen, local necking during the loading process, and deviances from the perfect grip conditions [73]. The classic two-camera stereovision system setup that supports three-dimensional digital image correlation is shown in the next page in Figure 46. This technique utilizes a software algorithm that identifies and processes surface and out-of-plane deformations by comparing the set of points in the subset of a given 'Reference Image' to the 'Deformed Image' [75].

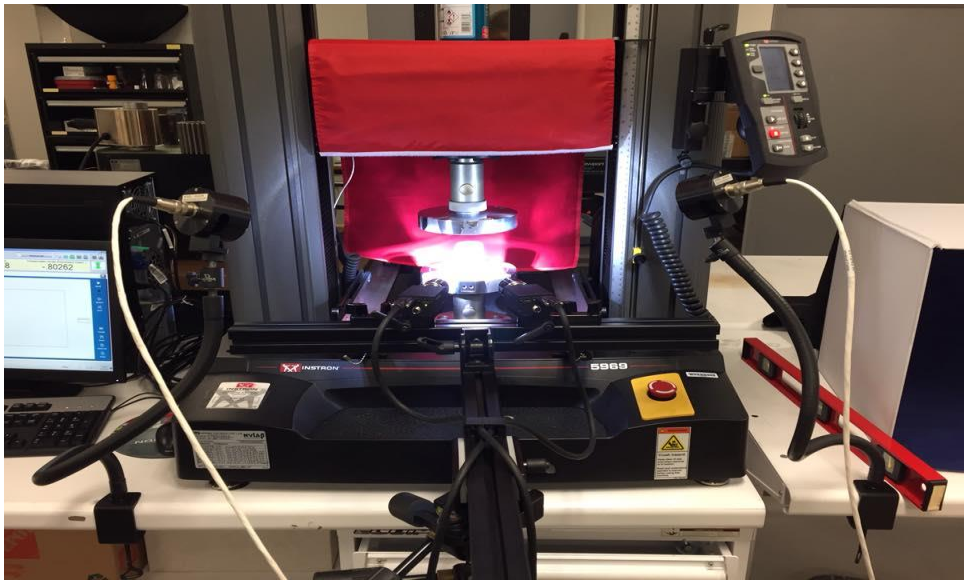

Figure 46. Actual VIC-3D Setup Used During Mechanical Tests

Since it is comparatively new, however, the DIC technique has a significant amount of uncertainty as far as the optimum parameters that should be used for each case, generating an unknown error margin in the results analyzed by the investigator. This has led investigators to study and research the parameters that factor into the results generated by the DIC method, most notably the speckle pattern, subset size, and the correlation algorithm in an attempt to determine the optimal testing conditions [75-79]. Extensive research work has also been done on the errors that affect the quality of results [80-84], which can be systematic errors such as deficient calibration and restricted camera resolution or the inherent uncertainty that derives from the correlation algorithm used by the software. An emerging topic of interest is doing Digital Image Correlation of materials at high temperature, which presents its unique challenges such as the lack of focus by the cameras caused by the flow of hot air around the object being examined and undergoing any type of stress [63].

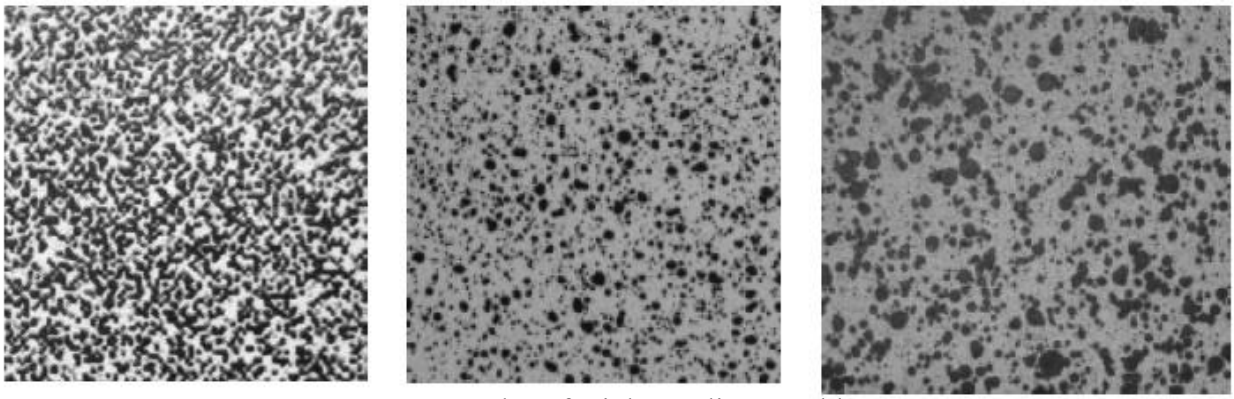

Figure 47. Examples of High-Quality Speckle Patterns.

This is a topic that is soon to be investigated by the research team, as equipment and techniques are being gathered and studied at this present moment. Since the DIC technique relies greatly on the contrasting pattern on the surface of the test specimen, the development of a speckle pattern will be discussed thoroughly. The speckle pattern can be painted, naturally occurring or even projected to the surface. Several techniques to recreate such pattern are available, but in order to provide or achieve an effective correlation several distinct requirements must be fulfilled by such techniques. A good speckle pattern should consist of a layer of speckles sprayed onto a different color surface that results in high contrast between, not necessarily a black on white pattern although it is the popular choice. The speckle pattern should be non-repetitive, isotropic, and high contrast.

The pattern also must be of the adequate size for the subset, or vice versa, since a too large or too small pattern will yield inaccurate results. If a pattern is too large for the subset, it could completely encompass a subset and the matching algorithm done in digital image correlation would not be correct due to the fact that it could match that subset across everywhere on the field. An alternative solution suggested when this occurs is to utilize a larger subset, but it does sacrifice spatial resolution. On the other hand, if the pattern is too fine, the DIC system cameras will not be able to represent the specimen correctly. This image-information issue is called 'aliasing', and a clear sign that this is an issue is a characteristic moiré pattern in the visual data that is generated by the software. In general, speckles should be the size of at least 3-4 speckles in size to avoid image aliasing [85]. In Figure 47 below there are examples of speckle patterns that effectively produce a good correlation, as given in [85]. Overall, any colors that create a high contrast will complete the requirement. There is future possibility of work in the area of speckle patterns application, however, for the relevant DIC tests carried out in this investigation and all of the images shown, the widely accepted technique of spray paint was utilized. One very popular parameter that has been the subject of numerous research studies done by researchers is the speckle pattern, which has been deemed important enough to have studies focus solely on developing quality assessment methods and their effect on the DIC results [76-78]. The VIC 3D apparatus has in its technical specifications for out-of-plane measurements that it offers a resolution of up to $1/50000$ FOV (Field of View), which is the area (m^2) on which the stereovision system is focused. Nevertheless, only one paper presenting work done on actual numerical error estimation using 3D DIC was found in literature [76]. The speckle pattern applied to the testing specimens of this study is shown in Figure 48.

Figure 48. Speckle pattern on Testing Specimens

3-D Digital Image Correlation

Errors in three-dimensional DIC can be classified into two major groups: correlation errors and calibration errors. Correlation errors, as the name suggests, refers to the errors that inevitably result from the nature of the correlation of the subset images can be further divided into two subtypes, systematical and statistical errors. Systematical errors are naturally resulting from subpixel effects, while statistical errors result from the limited correlation of pixels from subset to subset, i.e. the correlation will always introduce some minimal error in the measurements. Calibration errors, on the other hand, impact the 3D reconstruction coordinates directly and can be modified and optimized [72].

DIC Parameters

Several factors affect the results of DIC methods used, and one very important parameter is the stereo angle (also referred to as pan angle), which is the angle between the imaginary lines formed by the position of the cameras relative to the specimen analyzed. Literature recommendations were followed of maintaining the angle between 10° and 30° for 3D DIC for optimal results [63]. The user manual that is included with the DIC System VIC-3D is more specific and suggest 25° as the ideal stereo angle. For all tests, therefore the angle was maintained constant at 25°. It is worth noting, however, that literature also states that a stereo angle of up to 60° can be used for 3D image correlation if needed, with the sacrifice in the loss of accuracy in in-plane measurements.

As mentioned previously on this investigation, the speckle pattern has been the subject of several studies with the aim of more precisely defining a "good" speckle pattern. Some notable studies that covered this matter are mentioned next, along with their important conclusions. One study found that the size of both the subset and the speckles applied have a considerable influence on the accuracy with which heterogeneous and homogenous deformations are calculated in image correlation [76]. Another study found that a high-quality speckle pattern should have a speckle size from two to four pixels and large density, referring to the quantity of speckles applied to the area of interest [77]. And lastly, another study worth mentioning established a parameter called mean intensity gradient as a quality assessment check to evaluate the quality of the complete speckle pattern applied to the area of interest. The mean intensity gradient parameter is calculated using the modulus of local intensity gradient vector and the dimensions of the image in pixels. The investigation concluded that the mean intensity gradient should be large, and coupled with the appropriate subset size, to improve the accuracy of the displacement fields calculated. This practical parameter can be generally used as a guide for surface sample preparation [78]. While no one specific method was followed for the application of the speckle pattern, all of these results and findings were considered and this author judges them noteworthy and relevant to this presented paper. The speckle pattern used however, as mentioned earlier, was applied through the spray painting technique in a random pattern of dark paint over a layer of white paint, since it is considered by literature to be speckle pattern application method that historically yields the most accurate results [63]. One factor that also affects the accuracy of the DIC is the calibration Pad. The knowledge to choose the required calibration pad is a must when doing an accurate DIC. Also, is very important to put attention to the error score given when calibrating. An example of these parameter is shown in Figure 49.

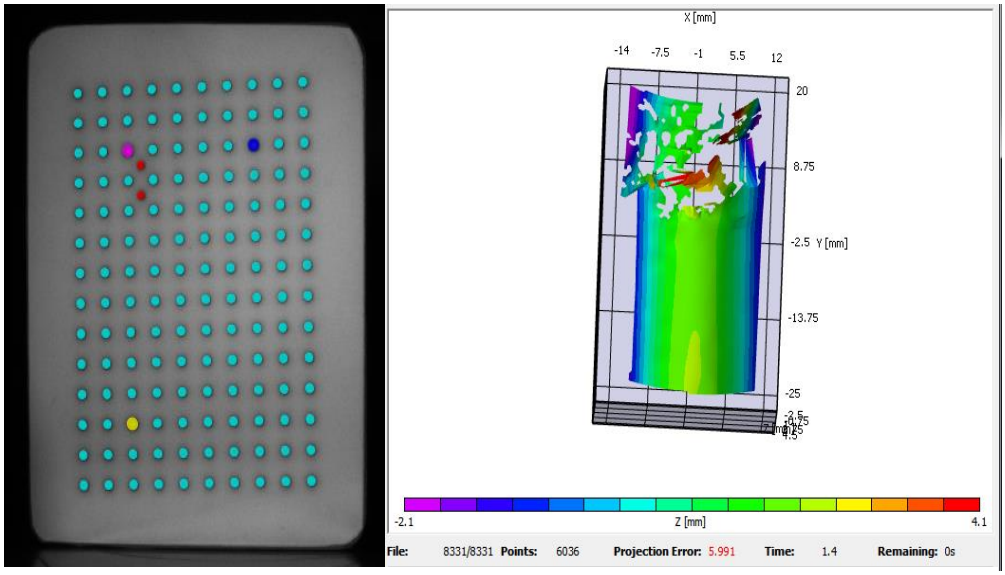

Figure 49. Calibration Pad and post processing images report examples

RESULTS & DISCUSSION

Uniaxial Compression

Quasi-static uniaxial compression loads were applied on the glass-HIPS specimens with the objective of characterizing the particulate composite material in order to develop a valid computational model in the near future. DIC technique was applied during the test in order to determine the full displacement and strain fields. A full description of the DIC method ca be found at the DIC section of this report. The dimensions for the cylindrical uniaxial specimen is 1.5 in. diameter, 2.275 in. of height. Base in the specimen's geometry and Table 5, the specimen is expected to fail by barreling and it will be affected severely by frictional effects.

Table 5. Expected Failure modes table for HPC

Length/Diameter ratio (*l/d*)	Expected Failure Mode	Frictional Effects
≤ 1.5	Barreling	Strong
1.5 - 2	Barreling	Strong
2-2.5	Doble Barreling	Above minimal
2.5-5	Shear	Minimal
5≤	Buckling	Minimal

However, as explain in the testing section of this report some steps are taken in order to reduce or minimalize the frictional effects that are seen during the compression test in between the surface of the compression platen and the specimen. Also, is necessary to take in consideration that such

failure modes belong to pure polymer testing. Yet, they serve as a reference point since it's a possibility that the glass-HIPS specimen might also be affected by those frictional effects.

Experimental results from the quasi-static uniaxial compression test are depicted in Figure 50, which plots the stress with respect to the strain for the glass-HIPS specimen. Since it is known that particulate composites such as the glass-HIPS specimen exhibit a strong dependence on the loading rate, temperature, and pressure, careful consideration was taken in order to take in consideration the strain dependent behavior of the mock PBX. It is difficult to distinguish the yield point. However, the yield point of the specimen is located at 33390 N of load and at 2.7% of strain. The elastic region of the PBX simulant was determine to end at 0.8% of strain. The plastic region seems to be quite extensive as it starts evolving from 0.8% of strain to 2.7% of strain to the rupture point. The maximum stress is determined to 29 MPa. This indicates that the binder material and the micron size soda lime glass beads developed a strong bond during the manufacturing process. In Figure 50 is possible to see the data acquired by the DIC system through the analog system and the data saved by the Instron 5969. The analog signal seems to be a little off, but the data from the DIC is more precise and accurate than the one provide by the load cell displacement.

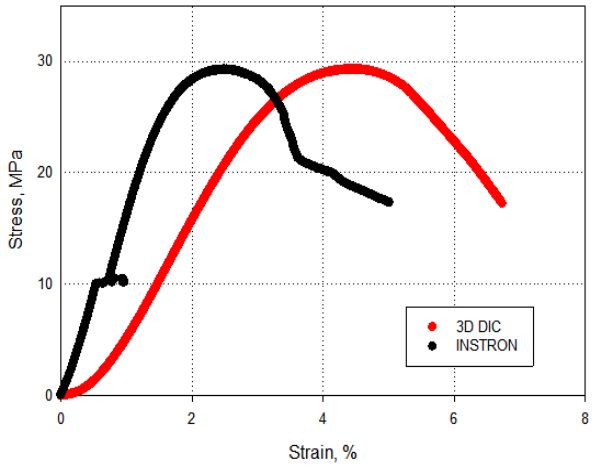

Figure 50. Stress vs Strain curve of glass-HIPS specimen

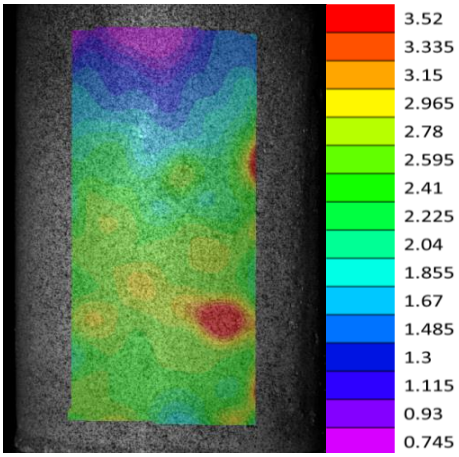

Figure 51. Initial Effective Poisson's Ratio

Since the poison's ratio is the ratio of different measurements (the transverse strain and axial strain), attempts to measure these by the use of extensometers have proven to be too erratic. Also,

is necessary to take in consideration that the glass-HIPS specimen is a composite ergo not a continuous material. The nature of the specimen introduces an error or a variation in behavior utilizing the extensometer method to measure. DIC method has the advantage of averaging strains over large surface areas and of providing the wanted strain data from the same measurement. As shown in Figure 51, the initial poison ratio is of 2.41. However as the test evolve, so does the poison ratio increasing. The poison ratio increases with increasing strain. This sort of behavior makes sense in a particulate composite such as the glass-HIPS specimen. The reason for this sort of behavior lies in the nature of the particulate composite. Voids that could have been introduced during the manufacturing process or develop within the specimen while the material is deforming start to increase in size as the strain increases. These voids, which are caused mainly by the separation of the binder material and the energetic crystal surfaces, have a bulking effect in glass-HIPS specimen. Figure 52 shows the evolution of the poison ratio during testing. It's important to take in consideration that larger strains will cause a large variation or evolution. At point A there is just a slight variation when compared to the initial effective Poisson's ratio because there is not a significant change in time. At B the application of the strain rate to some extent change the initial value of the Poisson's ratio when compared to point A has expected. At B the Poisson's ratio increases from the original initial value, but not an unexpected value. However, at C, the Poisson's ratio increases to a value of 5. After C, the Poisson's ratio continues to increase reaching a significant change to the original value. This is caused by the creation and/or development of the voids. In order to discuss the deformation and fracture behavior of the glass-HIPS specimen under compressive load, different images were captured while performing DIC. Figure 53 shows different contours prior to total failure. In Figure 53 picture A can be easily distinguish that a strain concentration is located in an area that runs along the load axis close to the top center of the specimen. Meanwhile, a localized shear strain band concentrated in the area near the diagonal line, as shown in Figure 53 part C. From these strain maps, it can be seen that the extension strain is larger than the compression and shear strain in the top right, demonstrating that the macroscopic fracture mode of the specimen is dominant caused by extension and shear action when under

external force. The whole vector field of displacement distribution gives an initial impression of the failure mode of the specimen, as shown in Figure 54. First is clearly that the specimen is going to fail by the barreling effect that was previously mentioned. Also, the direction of the vector field gives the impression that the specimen is going to fail by a shear fracture. As shown in Figure 55, the specimen fails by shear. This is consistent with the failure mode and the heterogeneous nature of the HPC or mock PBX.

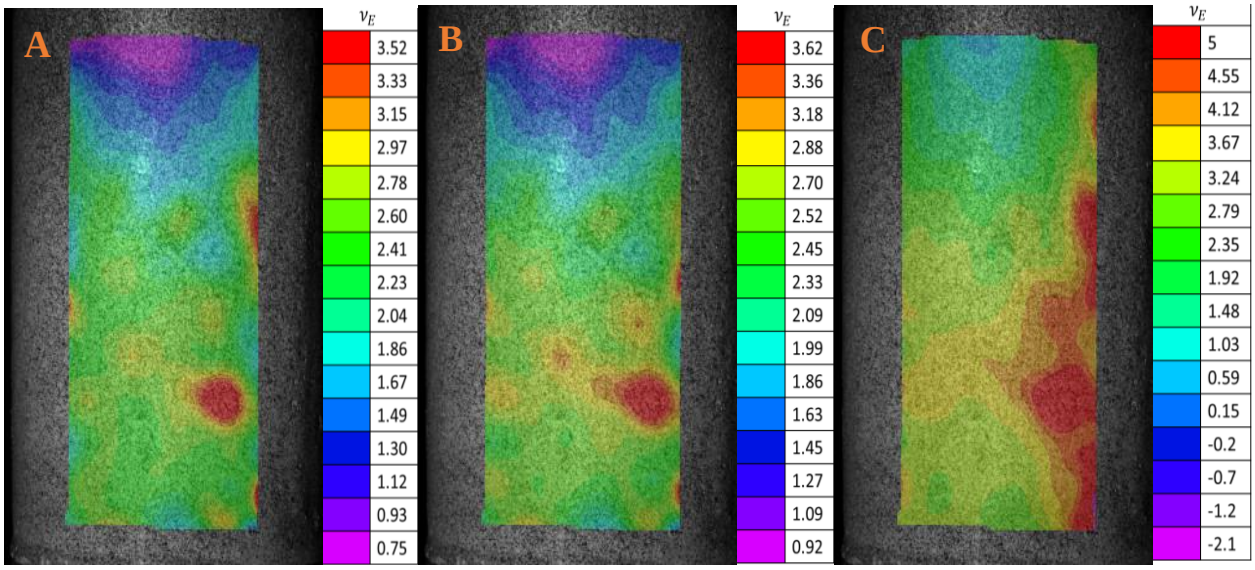

Figure 52. Effective Poisson's Ratio at different applied strain

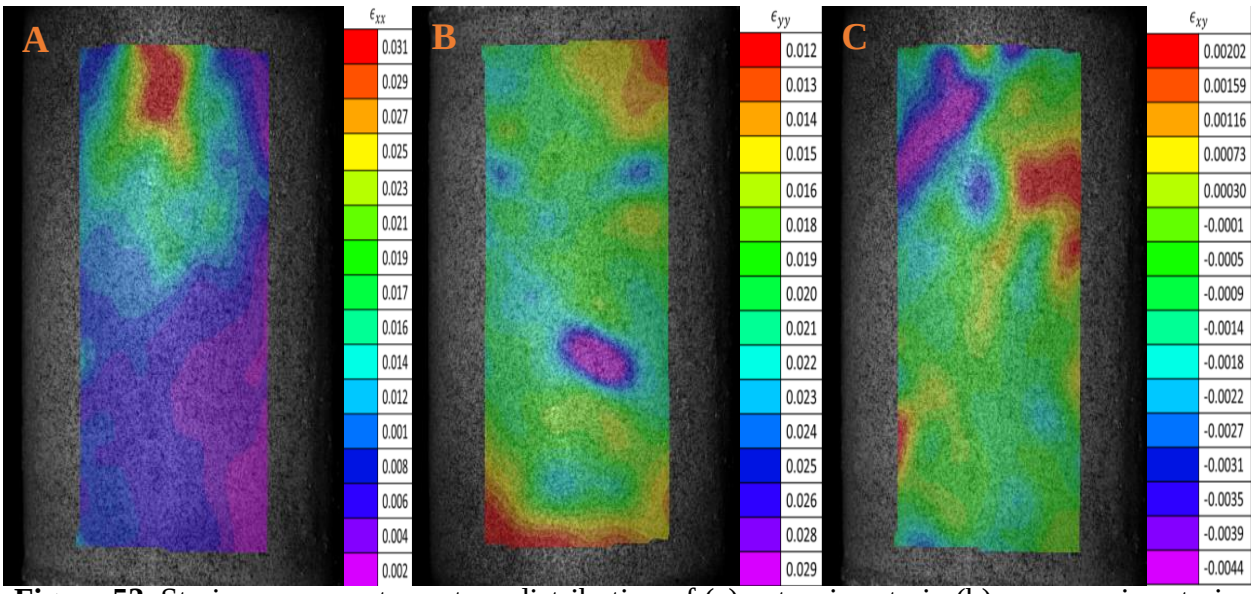

Figure 53. Strain components contour distribution of (a) extensive strain (b) compressive strain and (c) shear strain prior to total failure

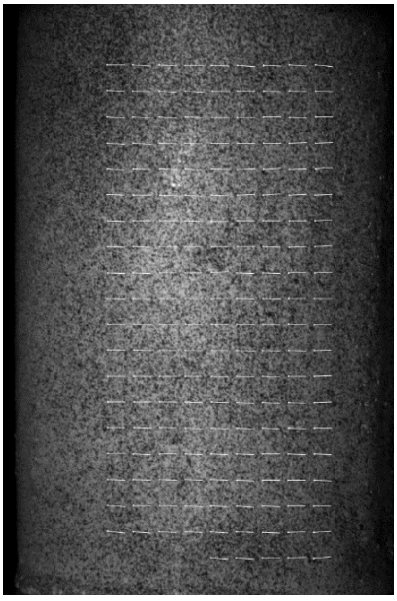

Figure 54. Displacement Vector Prior to total fracture

Figure 55. Fractured Specimen

Indirect Tensile (Brazilian) Test

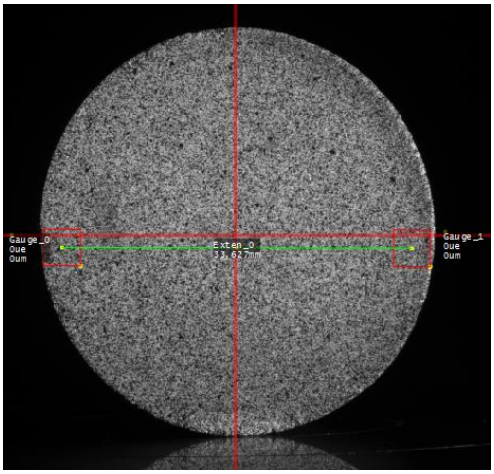

Figure 1. Virtual gauges and extensometer applied to Brazilian Specimen

Indirect Tensile compression loads were applied on the glass-HIPS specimen with the objective of characterizing the particulate composite material in order to develop a valid computational model in the near future. DIC technique was applied during the test in order to determine the full displacement and strain fields. The dimensions for the disc specimen are 38 mm diameter and 22 mm thickness. The Brazilian specimen was diametrically compressive loaded in the Instron 5969 with compression platens. The applied strain rate was 0.05 mm/min. Images of the evolving movement were recorded at frame of 5 frames per second. Two virtual gauges and a virtual extensometer were applied during the test as shown in Figure 56. Similar virtual gauges were applied to all the tested specimens. It is obvious that the applied force will at behave linearly at the earliest moments of the test and that due to the HIPS the specimen will plastically deformed before fracture. In another words the glass-HIPS specimen was never going to fail by a brittle fracture due to the nature of the HIPS. This is because even though the soda lime crystal are brittle, they are completed coated by the polymer. It is possible that the crack developed around the soda lime glass beads that were not completely or partially coated. This can be seen in Figure 57.

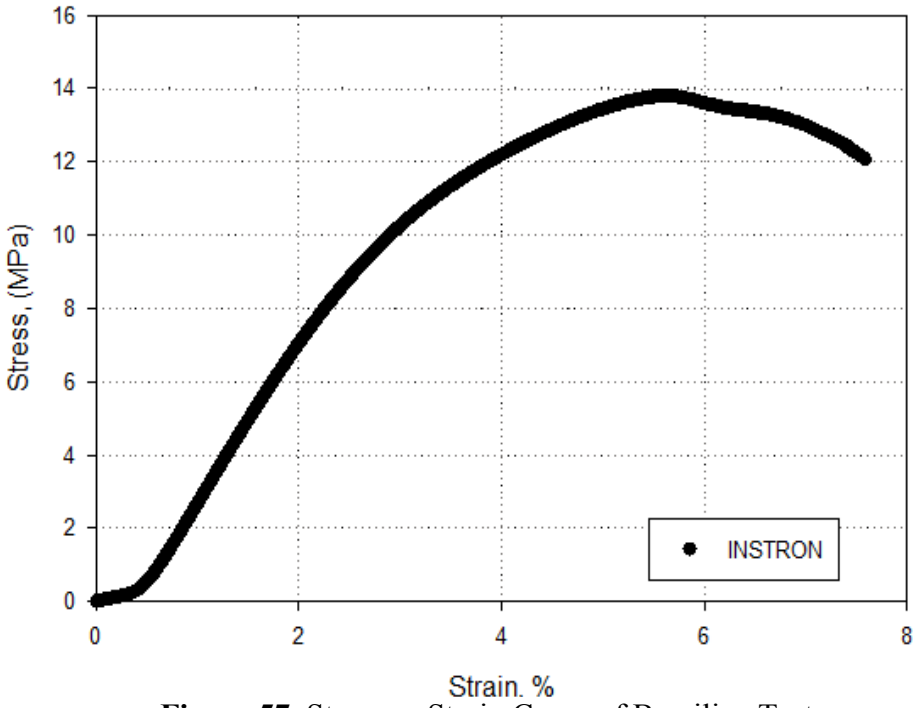

Figure 57. Stress vs Strain Curve of Brazilian Test

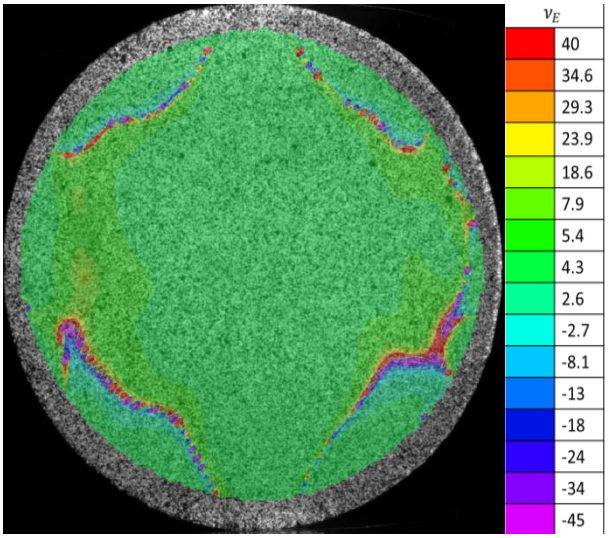

Figure 58. Effective Poisson's ratio of Brazilian Specimen

The maximum load that was reach was 5838 N. Therefore the indirect tensile stress is equal to 4.45 MPa. This seems to contradict Figure 57, however the plot only takes into consideration the compressive strength, ergo these two quantities cannot be compare rationally. Figure 58 shows the

Poisson's ratio corresponding to the Brazilian specimen. It is worth to mention that the Poisson's ratio increases as the strain evolves.

The strain field distribution equivalent to the state where the fracture occurs is shown in Figure 59. The images shows how the strain localizes along the load axis. The high strain spots might indicate the possible crack route and the possible sites for stress concentration. Another contour that proves that the strain field is predicting the crack route is the equivalent strain shown in Figure 60. It's possible that the equivalent strain contour shows the strain field is developed by the load.

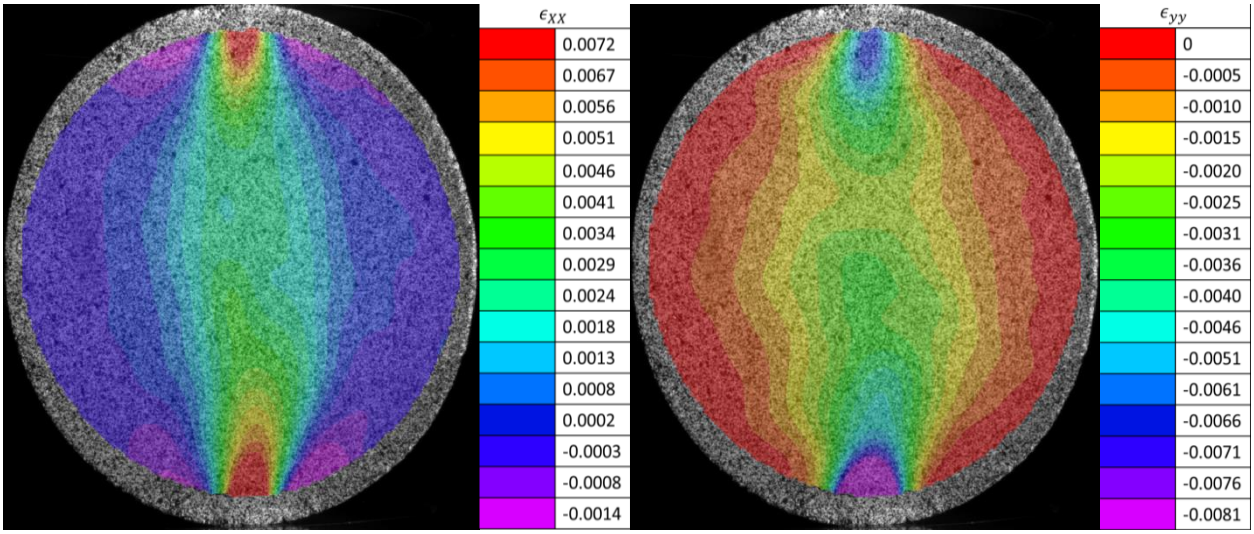

Figure 59. Strain components contour distribution of (a) extensive strain (b) compressive strain

Failure occurs as a crack propagated along the previously designated crack route. Fracture morphology of the specimen is shown in Figure 61.

Based in the results of the test, the strain field calculated from the DIC system can validate the material damage underneath the surface of the specimen. Even though more test are necessary to prove the above validation. The principal crack initiated from the contact surface, but quickly propagated through the center of the specimen. This means that the crack was developed in the center prior to the crack from the contact surface. One of the cracks located at the bottom surface was developed due to shear stress in the specimen, but quickly fuse with the primary crack and followed the crack route.

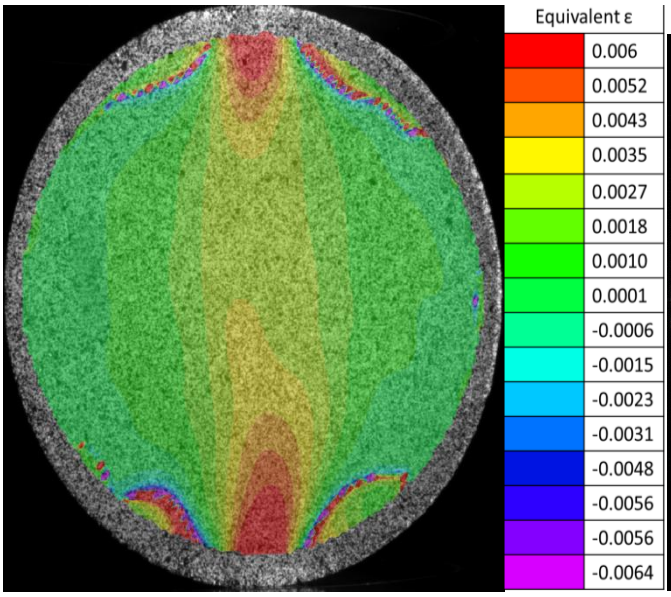

Figure 2. Equivalent Strain Contour

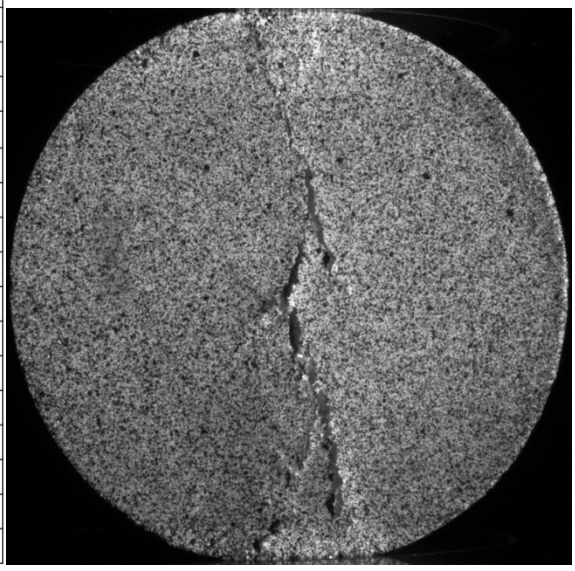

Figure 3. Fracture morphology

Semi-Circular Bending (Half Brazilian) Test

Semi-circular three point bending compression loads were applied on the glass-HIPS specimen with the objective of characterizing the particulate composite material in order to develop a valid computational model in the near future. DIC technique was applied during the test in order to determine the full displacement and strain fields. The dimensions for the semi-circular specimen are 38 mm diameter and 19 mm of height. The notch was machined with a blade of 1.65 mm of thickness. The notch of 6 mm length was along the line of symmetry at the edge of the specimen. The orientation was along the direction of compression. The half Brazilian specimen was uniaxial compressive loaded in the Instron 5969 with a 3 point bending set up. The applied strain

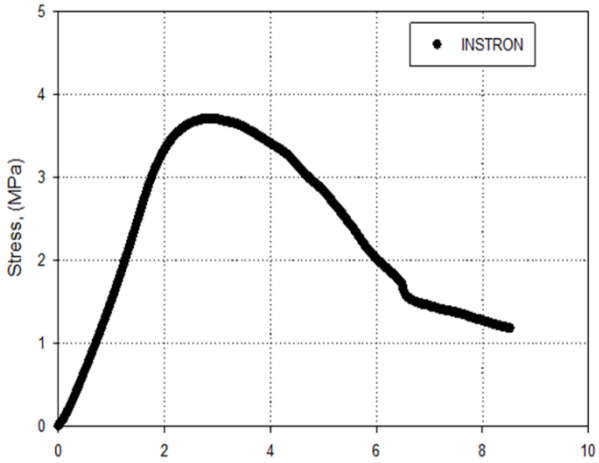

Figure 62. Stress vs Strain curve of SCB specimen

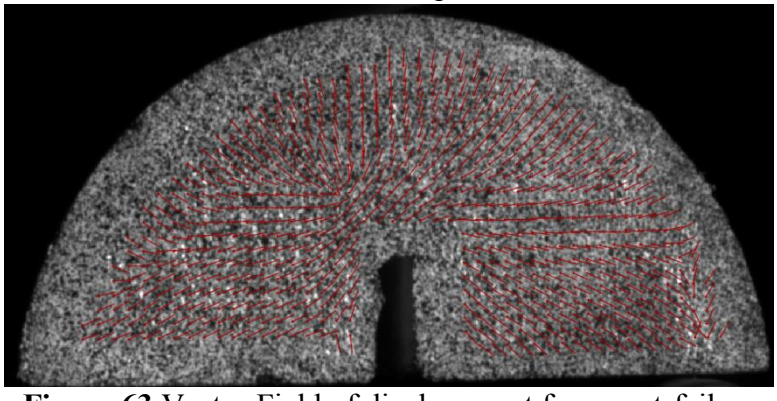

Figure 63. Vector Field of displacement for a post-failure

rate was 0.047 mm/min which was calculated based on literature just like mentioned in the mechanical test section. Detailed description in the mechanical testing section. Images of the evolving movement were recorded at frame of 5 frames per second. The ligament area for the mentioned geometry is 265.18 squared millimeters. Figure 63 shows the vector distribution of displacement under a tensile stress calculated by the DIC system. As is shown in the figure several directions are given by the vector field. This is because of the nature of the mock PBX. It is possible that the location with the most diverse direction is the location of an agglomeration of soda lime glass beads partially coated by the HIPS polymer. The vector field direction and magnitude indicates that the SCB specimen is suffering from a large extension stress under the compressive loading. Even thought is not visible because the occurred in the other side of the specimen, the arrows are pointing towards the crack and predicting its path. The stress vs strain curve shows the viscoelastic behavior of the mock PBX SCB specimen. The curve can be seen in Figure 62. In Figure 64 is possible to see the maximum strain located right at the point were the main crack initiate its route. The DIC calculations provide an excellent starting point for fracture analysis. Fracture analysis can be carried out in order see the relationship between load and the crack propagation. Due to the lack of literature a model will be develop that will reproduce and validate the above relationship.

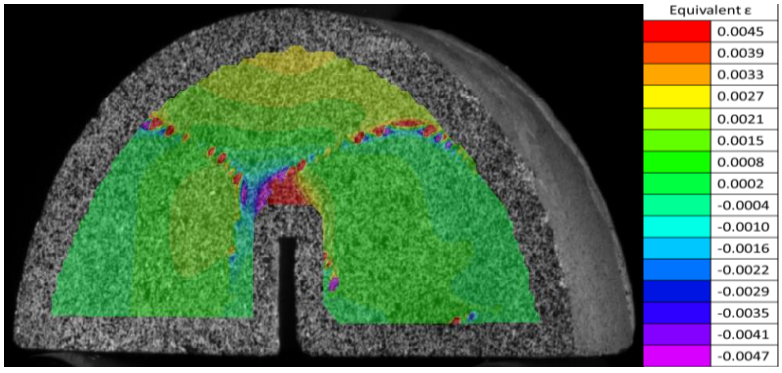

Figure 64. Equivalent Strain of SCB specimen

Bridgman Notch Test

Uniaxial compression loads were applied on the Bridgman notch glass-HIPS specimen with the objective of characterizing the particulate composite material in order to develop a valid computational model in the near future. DIC technique was applied during the test in order to determine the full displacement and strain fields. Images of the evolving movement were recorded at frame of 5 frames per second. The dimensions for the cylindrical Bridgman notch specimen are

38 mm diameter and 46 mm height. The circumferential notch has a diameter of 15 mm. The Bridgman notch specimen was diametrically compressive loaded in the Instron 5969 with compression platens. The applied strain rate was 0.1143 mm/min. Due to the triaxial state of stress induced by the Bridgman notch, Table 5 is not applicable to predict the failure mode. However, the test was run like a typical uniaxial compression. In another words the Teflon tape and grease was utilized during testing.

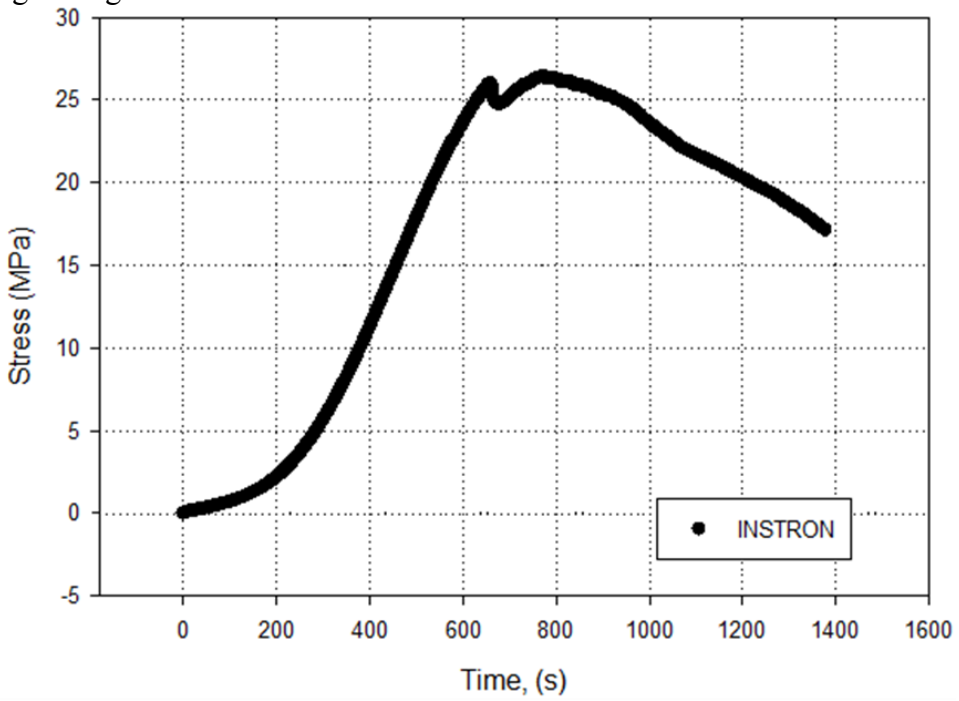

REFERENCES

[1] Cooper, P. W., and Kurowski, S. R., 1996, "Introduction to the Technology of Explosives". New York: Wiley-VCH.

[2] Siviour, C. R., Laity, P. R., Proud, W. G., Field, J. E., Porter, D., Church, P. D., Gould, P., and Huntingdon-Thresher, W., 2008, "High strain rate properties of a polymer-bonded sugar: their dependence on applied and internal constraints," Proc. R. Soc. A Math. Phys. Eng. Sci., 464(2093), pp. 1229–1255.

[3] Dienes, J. K., Zuo, Q. H., and Kershner, J. D., 2006, "Impact initiation of explosives and propellants via statistical crack mechanics," J. Mech. Phys. Solids, 54(6), pp. 1237–1275.

[4] Yeom, K. S., Jeong, S., Huh, H., and Park, J., 2013, "New Pseudo-Elastic Model for Polymer-Bonded Explosive Simulants Considering the Mullins Effect," J. Compos. Mater., 47(27), pp. 3401-3411.

[5] Cady, C. M., Liu, C., Rae, P.J., and Lovato, M. L., 2009, "Thermal and Loading Dynamics of Energetic Materials," Proc. of the SEM Annual Conference, Albuquerque, NM.

[6] Cunningham, B. J., Gagliardi, F. J., and Ferranti, L., 2013, "Low Strain Rate Measurements on Explosives Using DIC," Proc. of the SEM Annual Conference, Springer, Indianapolis, IN, pp. 25-31.

[7] Liu, C., 2010, "Elastic Constants Determination and Deformation Observation Using Brazilian Disk Geometry," Exp. Mech., 50(7), pp. 1025-1039.

[8] Chen, P., Zhou, Z. and Huang, F., 2011, "Macro-Micro Mechanical Behavior of a Highly-Particle-Filled Composite Using Digital Image Correlation Method," InTech, pp. 437-460, Chap. 18.

[9] Bridgman, P. W., 1952, Studies in Large Plastic Flow and Fracture. McGraw Hill, New York.

[10] Kachanov, L. M., 1986, "On Creep Stresses in a Bridgman Notched Bar," Mech. Mater., 5(3), pp. 229-234.

[11] Stewart, C. M., 2013, A Hybrid Constitutive Model for Creep, Fatigue, and Creep-Fatigue Damage, Dissertation, University of Central Florida, Orlando, FL, Dec 2013.

[12] Hyde, T. H., Xia, L., and Becker, A. A., 1996, "Prediction of Creep Failure in Aeroengine Materials under Multi-axial Stress States," Int. J. Mech. Sci., 38(4), pp. 385-403.

[13] Kraus, H., 1980, Creep Analysis, John Wiley, New York

[14] Hayhurst, D. R., 1972, "Creep Rupture Under Multi-Axial States Of Stress," J. Mech. Phys. Solids, 20(6), pp. 381-390.

[15] Zhang, J., Zhang, J., Chen, X., Sun, C., and Xu, J., 2014, "A Thermovisco-Hyperelastic Constitutive Model of NEPE Propellant Over a Large Range of Strain Rates," J. Eng. Mater. Tech., 136(3), pp. 1-8.

[16] Schapery, R.A., 1990, "Theory of mechanical behavior of elastic media with growing damage and other changes in structure," J. Mech. Phys. Solids, 38(2), pp. 215–253.

[17] Schapery, R.A., 1991, "Analysis of damage growth in particulate composites using a work potential," Compos. Eng., 1(3), pp. 167–182.

[18] Ha, K., Schapery, and R. A., 1998, "Three-dimensional viscoelastic constitutive model for particulate composites with growing damage and its experimental validation," Int. J. Solids Struct., 35(26-27), pp. 3497–3517.

[19] Hinterhoelzl, R.M., and Schapery, R.A., 2004, "FEM implementation of a three-dimensional viscoelastic constitutive model for particulate composites with damage growth," Mech. Time-Dependent Mater., 8, pp. 65–94.

[20] Jung, G-D., and Youn, S-K., 1999, "A nonlinear viscoelastic constitutive model of solid propellant," Int. J. Solids Struct., 36, pp. 3755–3777.

[21] Kachanov, L. M., 1986, Introduction to Continuum Damage Mechanics, Springer Science & Business Media.

[22] Xu, F., Aravas, N., Sofronis, P., 2008, "Constitutive Modeling of Solid Propellant Materials with Evolving Microstructural Damage," J. Mech. Phys. Solids, 56, pp. 2050-2073.

[23] Doherty, R. M., and Watt, D. S., 2008, "Relationship Between RDX Properties and Sensitivity, "Propellants, Explosives, Pyrotechnics, 33(1), pp. 4–13.

[24] Compton, D., Hunt, E. and, Jackson, M., 2011, "Coating and Characterization of Energetic Materials," FLIR Syst. Inc., pp. 1–4.

[25] Anderson, E. K., Aslam, T. D., and Jackson, S. I., 2014," Transverse initiation of an insensitive explosive in a layered slab geometry: Front shapes and post-shock flow measurements," Combustion and Flame, 161(7), pp. 1944–1954.

[26] Banerjee, B., Cady, C. M., and Adams, D. O., 2003, "Micromechanics simulations of glass-estane mock polymer bonded explosives," Modelling and Simulation in Materials Science and Engineering, 11(4), pp. 457–475.

[27] Yeager, J. D., Ramos, K. J., Hooks, D. E., Majewski, J., and Singh, S., 2014, "Formulation-Derived Interface Characteristics Contributing to Failure in Plastic-Bonded Explosive Materials," LA-UR-14-24860, Proc. 15th International Detonation Symposium, San Francisco, CA.

[28] Xiao, J. J., Wang, W. R., Chen, J., Ji, G. F., Zhu, W., and Xiao, H. M., 2012," Study on structure, sensitivity and mechanical properties of HMX and HMX-based PBXs with molecular dynamics simulation," Computational and Theoretical Chemistry, 999, pp. 21–27.

[29] Campbell, M. S., Garcia, D., and Idar, D., 2000, "Effects of temperature and pressure on the glass transitions of plastic bonded explosives," Thermochimica Acta, 357–358(836), pp. 89–95.

[30] Sunnyside Corporation, 2009, "Acetone 840 Product Data Sheet".

[31] Sprayon Products, 2014, "Urethane and Styrene Silicone Release Agent Aerosol Material Safety Data Sheet".

[32] Çengel, Yunus, 2007, "Heat and Mass Transfer: A Practical Approach", McGraw-Hill, Boston, MA.

[33] Jaygo Incorporated, 2013, "SiLibeads Glass Beads Type S, Microglassbeads EU Safety Data Sheet According to Attachment II EC Reg. 1907/2006".

[34] Total Petrochemicals & Refining USA, Inc., 2012, "Impact Polystyrene Material Safety Data Sheet".

[35] Zhou, Z., et al., 2012, "Study on Fracture Behaviour of a Polymer-Bonded Explosive Simulant Subjected to Uniaxial Compression Using Digital Image Correlation Method," Strain, 48(4), pp. 326-332.

[36] Zhou, Z., et al. "Dynamic tensile deformation and fracture of a highly particle-filled composite using SHPB and high-speed DIC method." EPJ Web of Conferences. Vol. 26. EDP Sciences, 2012.

[37] Rae, P. J., et al. "Quasi–static studies of the deformation and failure of β–HMX based polymer bonded explosives." Proceedings of the Royal Society of London A: Mathematical, Physical and Engineering Sciences. Vol. 458. No. 2019. The Royal Society, 2002.

[38] Heinz, Stephen R., and Jeffrey S. Wiggins. "Uniaxial compression analysis of glassy polymer networks using digital image correlation." Polymer Testing 29.8 (2010): 925-932.

[39] Zhou, Zhongbin, et al. "Experimental study on the micromechanical behavior of a PBX simulant using SEM and digital image correlation method." Optics and Lasers in Engineering 49.3 (2011): 366-370.

[40] Goodall, I. W., & Skelton, R. P. The importance of multiaxial stress in creep deformation and rupture. Fatigue & Fracture of Engineering Materials & Structures, 2004, 27(4), 267-272.

[41] Ha, J., Tabuchi, M., Hongo, H., Yokobori, A. T., & Fuji, A. Creep crack growth properties for 12CrWCoB rotor steel using circular notched specimens. International journal of pressure vessels and piping, 2004, 81(5), 401-407.

[42] Lukáš, P., Preclík, P., & Čadek, J. Notch effects on creep behaviour of CMSX-4 superalloy single crystals. Materials Science and Engineering, 2001: A,298(1), 84-89.

[43] Yeager, J. D., et al. "Microstructural effects of processing in the plastic-bonded explosive Composition A-3." Materials Chemistry and Physics 139.1 (2013): 305-313.

[44] Martin, E. C., and Rena Y. Yee. Effects of Surface Interactions and Mechanical Properties of PBXs (Plastic Bonded Explosives) on Explosive Sensitivity. No. NWC-TP-6560. NAVAL WEAPONS CENTER CHINA LAKE CA, 1984.

[45] Çolak, Özgen Ü., 2004, "Mechanical Behavior of PBXW-128 and PBXN-110 under Uniaxial and Multiaxial Compression at Different Strain Rates and Temperatures," Turkish J. Eng. Env. Sci, 28, pp. 55-65.

[46] Jerabek, M., Z. Major, and R. W. Lang. "Uniaxial compression testing of polymeric materials." Polymer testing 29.3 (2010): 302-309.

[47] Yu, Yong, Jianxun Zhang, and Jichun Zhang, 2009, "A modified Brazilian disk tension test." International Journal of Rock Mechanics and Mining Sciences 46(2) .pp. 421-425.

[48] Hondros, G. "The evaluation of Poisson's ratio and the modulus of materials of a low tensile resistance by the Brazilian (indirect tensile) test with particular reference to concrete." Australian Journal of Applied Science 10.3 (1959): 243-268.

[49] Huang, Baoshan, Xiang Shu, and Yongjing Tang. "Comparison of semi-circular bending and indirect tensile strength tests for HMA mixtures." Advances in Pavement Engineering 16 (2005): 225-227.

[50] Mellor, Malcolm, and Ivor Hawkes. "Measurement of tensile strength by diametral compression of discs and annuli." Engineering Geology 5.3 (1971): 173-225.

[51] Kim, Y., et al. "Dynamic modulus testing of asphalt concrete in indirect tension mode." Transportation Research Record: Journal of the Transportation Research Board 1891 (2004): 163-173.

[52] Fairhurst, C. "On the validity of the 'Brazilian'test for brittle materials, "International Journal of Rock Mechanics and Mining Sciences & Geomechanics Abstracts. Vol. 1. No. 4. Pergamon, 1964.

[53] Liu, C. "Elastic constants determination and deformation observation using Brazilian disk geometry." Experimental mechanics 50.7 (2010): 1025-1039.

[54] Wu, Zhong, et al. "Fracture resistance characterization of superpave mixtures using the semi-circular bending test." Journal of ASTM International 2.3 (2005): 1-15.

[55] Bai, Yuanli, Xiaoqing Teng, and Tomasz Wierzbicki. "On the application of stress triaxiality formula for plane strain fracture testing." Journal of Engineering Materials and technology 131.2 (2009): 021002.

[56] Valiente, A. "On Bridgman's stress solution for a tensile neck applied to axisymmetrical blunt notched tension bars." Journal of applied mechanics 68.3 (2001): pp. 412-419.

[57] Bridgman, P. W., 1944, "The stress distribution at the neck of a tension specimen, "Trans. ASM 32, pp. 553-574.

[58] Bridgman, P. W., 1964, Studies in Large Plastic Flow and Fracture, Harvard University Press, Cambridge, MA.

[59] Bai, Yuanli, and Tomasz Wierzbicki. "A new model of metal plasticity and fracture with pressure and Lode dependence." International Journal of Plasticity24.6 (2008): 1071-1096.

[60] Bao, Yingbin, and Tomasz Wierzbicki. "On fracture locus in the equivalent strain and stress triaxiality space." International Journal of Mechanical Sciences 46.1 (2004): 81-98.

[61] Deng, Y. C., et al. "Strain limit dependence on stress triaxiality for pressure vessel steel." Journal of Physics: Conference Series. Vol. 181. No. 1. IOP Publishing, 2009.

[62] Wierzbicki, Tomasz, and Liang Xue. "On the effect of the third invariant of the stress deviator on ductile fracture." Impact and Crashworthiness Laboratory, Technical Report 136 (2005).

[63] Sutton, M. A., Orteu, J., and Schreier, H. W, 2009, "Image Correlation for Shape, Motion and Deformation Measurements," Springer, New York, NY.

[64] Peters WH and Ranson WF, 1982, "Digital Imaging Techniques in Experimental Stress Analysis," Optical Engineering, 21(3), pp. 427–431.

[65] Haddadi, H., and Belhabib, S., 2008 "Use of Rigid-body Motion for the Investigation and Estimation of the Measurement Errors Related to Digital Image Correlation Technique," Optics and Lasers in Engineering, 46(2), pp. 185-196.

[66] Pan, B., Qian, K., Xie, H., & Asundi, A., 2009, "Two-dimensional Digital Image Correlation for In-plane Displacement and Strain Measurement: A Review," Measurement Science and Technology, 20(6).

[67] Wang, Z. Y., Li, H. Q., Tong, J. W., & Ruan, J. T. ,2007. "Statistical Analysis of the Effect of Intensity Pattern Noise on the Displacement Measurement Precision of Digital Image Correlation Using Self-correlated Images,'' Experimental Mechanics, 47(5), pp. 701-707.

[68] Li M, Zhang J, Xiong CY, Fang J, Li JM, Hao Y, 2005, "Damage and Fracture Predication of Plastic-bonded Explosive by Digital Image Correlation Processing," Optical Lasers Engineering, 43(8), pp. 856–68.

[69] Sun Z, Lyons JS, McNeil SR, 1997, "Measuring Microscopic Deformations with Digital Image Correlation," Optical Laser Engineering, 27(1), pp. 409–28.

[70] Vogel D, Kuhnert R, Dost M, Michel B., 2002, "Determination of Packaging Material Properties Utilizing Image Correlation Techniques," J Elect Pack, 124, pp. 345–51.

[71] Lava, P., Cooreman, S., Coppieters, S., De Strycker, M., & Debruyne, D., 2009 "Assessment of Measuring Errors in DIC Using Deformation Fields Generated by Plastic FEA," Optics and Lasers in Engineering, 47(7), pp. 747-753.

[72] Becker, T., Splitthof, K., Siebert, T., & Kletting, P., 2006, "Error Estimations of 3D Digital Image Correlation Measurements," International Society for Optics and Photonics, Speckle 6, pp. 63410F-63410F.

[73] Sutton, M. A., Yan, J. H., Tiwari, V., Schreier, H. W., & Orteu, J. J., 2008, "The Effect of Out-of-plane Motion on 2D and 3D Digital Image Correlation Measurements," Optics and Lasers in Engineering, 46(10), pp. 746-757.

[74] Orteu, J. J., 2009, "3-D Computer Vision in Experimental Mechanics," Optics and Lasers in Engineering, 47(3), pp. 282-291.

[75] Yaofeng, S., & Pang, J. H., 2007, "Study of Optimal Subset Size in Digital Image Correlation of Speckle Pattern Images," Optics and Lasers in Engineering, 45(9), pp. 967-974.

[76]Lecompte D, Smits A, Bossuyt S, et al., 2006, "Quality Assessment of Speckle Patterns for Digital Image Correlation," Optical Lasers Engineering, 44(11), pp. 1132–45.

[77] Hua, T., Xie, H., Wang, S., Hu, Z., Chen, P., & Zhang, Q. 2011, "Evaluation of the Quality of a Speckle Pattern in the Digital Image Correlation Method by Mean Subset Fluctuation," Optics & Laser Technology, 43(1), pp. 9-13.

[78] Pan, B., Lu, Z., & Xie, H., 2010, "Mean Intensity Gradient: An Effective Global Parameter for Quality Assessment of the Speckle Patterns Used in Digital Image Correlation," Optics and Lasers in Engineering, 48(4), pp. 469-477.

[79] Triconnet, K., Derrien, K., Hild, F., & Baptiste, D., 2009, "Parameter Choice for Optimized Digital Image Correlation," Optics and Lasers in Engineering, 47(6), pp. 728-737.

[80] Haddadi H, Belhabib S., 2008, "Use of Rigid-body Motion for the Investigation and Estimation of the Measurement Errors Related to Digital Image Correlation Technique," Optics and Lasers Engineering, 46, pp.185–196.

[81] Schreier, H. W., Sutton, M. A., 2002, "Systematic Errors in Digital Image Correlation Due to Undermatched Subset Shape Functions," Experimental Mechanics, 42(3), pp. 303–10.

[82] Schreier HW, Braasch JR, Sutton MA., 2000 "Systematic Errors in Digital Image Correlation Caused by Intensity Interpolation," Optics and Lasers Engineering, 9(11), pp. 2915–21.

[83] Wang ZY, Li HQ, Tong JW, Ruan JT., 2007, "Statistical Analysis of the Effect of Intensity Pattern Noise on the Displacement Measurement Precision of Digital Image Correlation Using Self-correlated Images," Experimental Mechanics, 47, pp. 701–707.

[84] Lava, P., Cooreman, S., Coppieters, S., De Strycker, M., & Debruyne, D., 2009, "Assessment of Measuring Errors in DIC Using Deformation Fields Generated by Plastic FEA," Optics and Lasers in Engineering, 47(7), pp. 747-753.

[85] Correlated Solutions, Vic-3D V7 Testing Guide, pp. 1-22.

APPENDICES

Appendix A- Personal Protective Equipment

Lab Coat 	The Tech Wear 2XL white lapel ESD/anti-static lab coat was used during the manufacturing process. It is made from a carbon nylon monofilament, conductive fiber, and polyester fabric. The main purpose it served was to protect the skin and clothes from the micron-sized, irritable glass beads.
Steel Toe Boots 	Steel toe boots were used in the lab at all times in accordance with the Department of Labor's Code of Federal Regulations (CFR) Title 29. General PPE requirements are given in the Occupational Safety and Health Administration's (OSHA's) standard 1910.132 and Foot Protection requirements are in 1910.136.
EN 166 compliant eye protection 	The eye protection gadgets that were used were in compliance with EN166, which is the core technical standard to which all PPE involved in protecting the eyes or face must be approved.

Welding Gloves 	Blue Hawk™ brown welding gloves were utilized when handling the cylindrical, metallic tube after being heated and when using the heater. The gloves are manufactured of leather construction with gauntlet to ensure heat- and chemical-resistance for the user.
KingSeal™ Nitrile Examination Gloves 	(Powder Free, Medical Grade) were used at the laboratory at all times. These are thicker and higher quality than standard gloves, and mainly provided protection when handling the soda limes glass beads (skin irritant) and the polymer pellets.
Comfort-Fit Cartridge Respirators for Solid Particles 	A half mask face piece, reusable air purifying respirator model with a P100 filter was used throughout the process of handling the constituent materials and sprays and vapor produced by the heater, these respirators resist oil exposure for up to 40 hours and filter out 99.97% of solid particles.

Appendix B-Manufacturing Equipment

Leco PR-22 Pneumatic Mounting Press 	The Leco PR-22 Pneumatic Mounting Press, along with is complementary components such as the heating element, cylindrical dice, dice holder, and heat sinks (shown below), is the single-most important piece of equipment utilized during the manufacturing process. It provided the heating and pressurization required to melt the polymer and glass beads mixture and then compress them together to yield the resulting mock PBX Sample. It indicates a maximum pressure of 4,000 psi.
Heating Element of Leco PR-22 Pneumatic Mounting Press 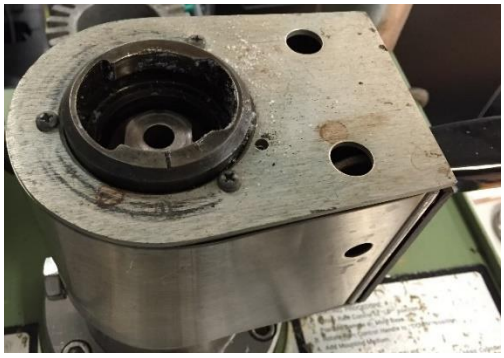	The heating element of the Leco PR-22 Pneumatic Press is an electrical heater with a voltage capacity of 115 V and an amperage capacity of 5.2 Amps. The average maximum temperature capacity experimentally reached was read by the electrical thermostat to be 190°C, and heat the cylindrical metallic tube containing the mixture to a maximum of 155°C, sufficient to melt the polymer pellets.

Glass Beakers and Flasks 	Laboratory grade 400 ml glass beakers, 150 ml glass flasks, and 6 oz. plastic scoops, were used for mixing of the previously weighed high impact polystyrene pellets and the soda lime glass beads.
Acetone Container 	The acetone was used to clean up all the equipment tools that come into contact with the PBX mixture, including the locking dye, moving platform, and the cylindrical, metallic container. According to the technical specifications it is highly flammable, and it can be used to dissolve many natural and synthetic gums, waxes, oils and dyes.
Urethane & Styrene Silicone Release Spray 	The Urethane & Styrene Silicone Release Agent Spray was utilized during the manufacturing process to simplify the process of taking out the PBX sample of the cylindrical container. The spray has a maximum working temperature of 287°C which is under the temperature conditions of the manufacturing process.

BE1188 Bald Eagle Powder Scale  	The BE1188 Bald Eagle Powder Scale was utilized for measuring the mass of the component materials and water before being mixed in the flaks and beakers. The glass scoops were used as a practical way to get around the 100 gram mass limit the scale has, according to the manufacturer website. It also states that it can be used without a power supply nearby, operating either on 120V AC or a 9V DC battery. It possesses a 110 grain capacity that has an accuracy of 0.001g and can measure in grams, carats, grains, pennyweight, and ounces.
Fluke 175 True-RMS Digital Multimeter  	The Fluke 175 True-RMS Digital Multimeter was used during the manufacturing process for measurement of the temperature. According to the manufacturer website, this instrument can measure True RMS voltage and current measurements with a 0.09% basic accuracy. Some other notable features include its digital display with analog bar graph and backlight, and its measuring speed (about twice as fast as other multimeters).

Appendix C-Machining Equipment

Abrasimet 250 Manual Abrasive Cutter 	The Abrasimet 250 Manual Abrasive Cutter is a versatile and easy-to-use cutter ideal for laboratory environments. The company website states that it uses 4Hp of power, and is designed for 10in [254mm] cut-off wheels. It has a 12mm T-Slot stainless steel bed and includes a mechanical brake.
PoliMet 1000 Grinder/Polisher 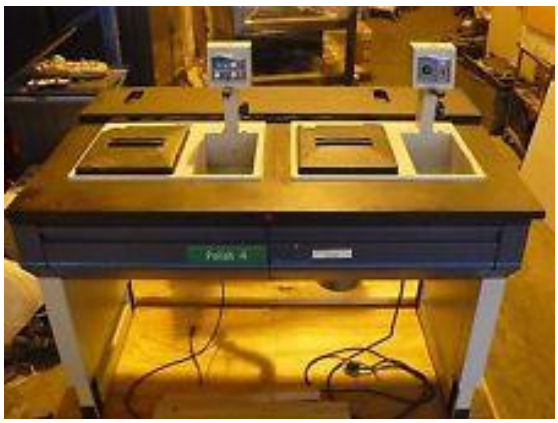	The PoliMet 1000 Grinder is designed for low volume laboratories preparing single specimens. The fully adjustable speed and high pressure capability (2-10 lbs/10-50N) reduces preparation time; it can be used to grind and polish composite materials, and even some harder materials such as aluminum and steel.

KENTOCN KLR-12 CNC Lathe 	KENTOCN KLR-12 CNC Lathe CNC (Computerized Numerical Control) lathe at the facilities was utilized to machine the required Bridgman notch onto the PBX sample to be apt for testing. According to the manufacturer website, it has a 20/25hp Fanuc Spindle Motor and a maximum cutting diameter and length of 17.7”

VITA

Carlos Alberto Catzin was born on august 31st, 1990 in El Paso, Texas. Carlos completed a high school equivalence test (GED) in El Paso in May 2009 in order to enroll in the community college. He graduated from El Paso Community College in 2012 with an associate of Arts. He then enrolled in The University of Texas at El Paso where he completed his undergraduate studies and received his Bachelor of Science in Mechanical Engineering in December 2014. In January 2015, Carlos began his master's degree in Mechanical Engineering under the supervision of Dr. Calvin M. Stewart. Also, he started working as a teacher assistant and as a graduate research assistant. After graduation Carlos will pursue a career in the Mechanical Engineering track in industry.

Permanent address: 3905 Bliss Ave
El Paso, Texas, 79903

This thesis was typed by Carlos Alberto Catzin.